

**A SPECTROSCOPIC STUDY OF THE ELECTRONIC  
EFFECTS ON COPPER(II) AND COPPER(I)  
COMPLEXES OF LIGANDS DERIVED FROM  
VARIOUS SUBSTITUTED BENZYLALDEHYDE- AND  
CINNAMALDEHYDE-BASED SCHIFF BASES**

**SUBMITTED IN FULFILMENT OF THE REQUIREMENTS FOR THE  
DEGREE OF**

**MSc**

**IN THE DEPARTMENT OF CHEMISTRY,  
FACULTY OF SCIENCE,  
RHODES UNIVERSITY**

**By**

**Nomampondo Penelope Magwa**

## ABSTRACT

Several Schiff base ligands, N, N'-(aryl)benzyaldiimine ligands (R-BEN); N, N'-(aryl)benzyaldiamine dihydrochloride ligands (R-BENH•2HCl); N, N'-(aryl)benzyaldiamine ligands (R-BENH); N, N'-*bis*(cinnamaldiimine) ligands (R-CA<sub>2</sub>EN) were synthesized for the investigation of the electronic effect of the substituents at para-position of the Schiff base ligands and their copper complexes.

The synthesis of Schiff bases was carried out by reacting a series of para-substituted benzaldehyde, and para-substituted cinnamaldehyde with ethylenediamine. The imine group of Schiff bases, N, N'-(aryl)benzyaldiimine ligands and N, N'-*bis*(cinnamaldiimine) ligands were reduced to corresponding amines with sodium borohydride in methanol.

These ligands, N, N'-(aryl)benzyaldiamine ligands (H-BENH), N, N'-*bis*(cinnamaldiimine) ligands (CA<sub>2</sub>EN) were reacted with copper(II) dihalide and copper(I) monohalide ions respectively to form complexes. The ligands and their complexes were analysed using elemental analyses, FT-IR spectroscopy (mid-IR), UV/vis in aprotic and protic solvents, while mass spectrometry, <sup>1</sup>H-NMR and <sup>13</sup>C-NMR were used to further analyse the ligands.

By using substituent parameters, both the single and dual substituent parameters with the spectroscopic data obtained from the spectroscopic techniques mentioned above, it was hoped to monitor and determine whether the electronic effects (resonance or inductive effects) was predominantly within the Schiff base ligands and copper complexes.

The NMR studies with dual substituent parameters suggest that the effects of the substituents are transmitted through the ligands, *via* resonance effects and that the phenyl group is non-planar with the azomethine in N, N'-(aryl)benzyaldiimine ligands. The presence of an extra

double bond in Schiff base {(N, N'-*bis*(cinnamaldiimine) ligand)} altered the electron density.

The UV/vis studies showed that the symmetry of the N, N'-*bis*(4-R-benzyl)-1, 2-diaminoethanedihalidecopper(II) complexes were predominantly tetrahedral for both chloro and bromo complexes. The correlation studies from mid-infrared were beneficial in monitoring the effect experienced by N, N'-(aryl)benzaldiimine ligands, the studies suggest that the inductive effect is more pronounced at the  $\nu_{C=N}$ .

## ACKNOWLEDGEMENT

All praise to God, Father of our Lord Jesus Christ for walking with me in this journey.

A very special thank you to my supervisor Professor G. M. Watkins for all his help, expert guidance, his optimism and his method that revolutionises an independent growth and develop critical thinking required by the student in real world.

I also wish to extend my sincere thanks and appreciation to the staff of the chemistry department Dr Edith Antunes for running microanalyses. Mr J. Fourie and Mr A. W. Sonemann for their help in running mass spectroscopy of the Schiff bases.

Special thanks to Dr Rafiu Olarewaju Shaibu from Nigeria for the good time we had together in LAB F5, to all friends at Rhodes University and outside the University.

Sincere gratitude needs to be extended towards my family: my sisters, my brother and my nephews and nieces for their encouragement. Without my family I would not be where and who I am today.

Lastly to my late parents, Lillian Mkasoka and Swelekile Alfred Magwa for their teachings and support given me while they were alive, may God bless their souls.

## CONTENTS

<b>ABSTRACT</b>	<b>i</b>
<b>ACKNOWLEDGEMENT</b>	<b>iii</b>
<b>LIST OF ABBREVIATIONS</b>	<b>ix</b>
<b>LIST OF FORMULAE AND ABBREVIATIONS COMPOUNDS</b>	<b>x</b>
<b>LIST OF SCHEMES</b>	
<b>LIST OF TABLES</b>	
<b>1. INTRODUCTION</b>	<b>1</b>
<b>1.1 Schiff bases</b>	<b>1</b>
1.1.1 Background	1
1.1.2 Applications and properties	2
1.1.3 Synthesis of Schiff bases	5
1.1.4 Spectroscopic properties	6
<b>1.2 Copper</b>	<b>9</b>
1.2.1 The copper(II) ion	11
1.2.2 Electronic properties of copper(II) ion	12
<b>1.3 Metal complexes of Schiff bases</b>	<b>14</b>
<b>1.4 Amine ligands and their metal chelates</b>	<b>15</b>
1.4.1 Spectroscopic properties of amine ligands	16
<b>1.5 Substituent constants</b>	<b>17</b>
<b>1.6 Proposed system of investigation</b>	<b>20</b>
<b>1.7 References</b>	<b>23</b>

<b>2.</b>	<b>EXPERIMENTAL (PHYSICAL AND CHEMICAL METHODS)</b>	<b>35</b>
<b>2.1</b>	<b>Physical methods</b>	<b>35</b>
2.1.1	Mid infrared spectroscopy (MIR)	35
2.1.2	Nuclear magnetic resonance (NMR)	35
2.1.3	Mass spectrometry	35
2.1.3.1	Electrospray ionization mass spectrometry (ESI-MS)	35
2.1.3.1	Atmospheric pressure chemical ionization spectrometry (APCI-MS)	36
2.1.4	Electronic spectra (UV/vis solution)	36
2.1.5	Microanalyses	36
2.1.6	Melting point	36
2.1.7	Thin-layer chromatography (TLC)	36
<b>2.2</b>	<b>Reagents and instrumentation</b>	<b>37</b>
<b>2.3</b>	<b>Synthetic method</b>	<b>37</b>
2.3.1	Synthesis of the N, N'-(aryl)benzaldimine ligands	37
2.3.2	Synthesis of the N, N'-(aryl)benzaldiamine dihydrochloride salts	42
2.3.3	Synthesis of the N, N'-(aryl)benzaldiamine ligands	47
2.3.4	Synthesis of copper(II) halide complexes derived from the N, N'-(aryl)benzaldiamine ligands	48
2.3.5	Synthesis of the N, N'- <i>bis</i> (cinnamaldimine) ligands	53
2.3.6	Synthesis of the N, N'- <i>bis</i> (cinnamaldiamine) ligands	54
2.3.7	Synthesis of the copper(I) complexes derived from N, N'- <i>bis</i> ( <i>trans</i> -cinnamaldehyde)-1,2-diiminoethane	55
2.3.8	Synthesis of the copper(II) complexes derived from	

	N, N'- <i>bis(trans-cinnamaldehyde)</i> -1, 2-diiminoethane	56
2.3.9	Attempted to synthesize copper(II) complexes derived from N, N'- <i>bis(trans-cinnamylbenzyl)ethylethylenediamine</i> ligand	56
2.4	<b>References</b>	<b>58</b>
3.	<b>RESULTS (PHYSICAL AND CHEMICAL STUDY)</b>	<b>59</b>
3.1	<b>Physicochemical data for the ligands and complexes</b>	<b>60</b>
3.2	<b>NMR spectroscopy spectra data for the ligands</b>	<b>69</b>
3.3	<b>Electronic spectra data for the ligands</b>	<b>76</b>
3.4	<b>Electronic spectra data for the N, N'-(aryl)benzaldiaminedihalidecopper(II) complexes</b>	<b>79</b>
3.5	<b>Electronic spectra data for the copper(I) and copper(II) N, N'- <i>bis(cinnamaldehyde)</i>-1, 2-diiminoethane complexes</b>	<b>81</b>
3.6	<b>Mid-infrared spectra data for the N, N'-(aryl)benzaldiimine ligands</b>	<b>82</b>
3.7	<b>Mid-infrared spectra data for the N, N'-(aryl)benzaldiamine dihydrochloride salts</b>	<b>83</b>
3.8	<b>Mid-infrared spectra data for the N, N'-(aryl)benzaldiamine ligands and their copper(II) halide complexes</b>	<b>84</b>
3.9	<b>Mid-infrared spectra data for the N, N'-<i>bis(cinnamaldiimine)</i> ligands and their copper(I) and copper(II) halide complexes</b>	<b>85</b>
3.1	<b>References</b>	<b>86</b>
4	<b>DISCUSSION (PHYSICAL AND CHEMICAL STUDY)</b>	<b>87</b>
4.1	<b>Elemental analyses</b>	<b>87</b>
4.1.1	Micro-analyses of Schiff base ligands and their copper(II) halide complexes	87

4.1.2	Micro-analyses of N, N'- <i>bis</i> (cinnamaldiimine) ligands and their copper(I) halide and copper(II) dihalide complexes	87
<b>4.2</b>	<b>Mass spectrometry studies of the Schiff base ligands</b>	<b>88</b>
4.2.1	APCI-MS studies of the N, N'-(aryl)benzaldiimine ligands	89
4.2.2	APCI-MS studies of the N, N'-(aryl)benzaldiimine dihydrochloride salts	92
4.2.3	ESI-MS studies of the N, N'-(aryl)benzaldiamine ligands	96
4.2.4	Comparison between the mass spectral patterns of the N, N'-(aryl)benzaldiamine ligands and N, N'-(aryl)benzaldiamine dihydrochloride salts	98
4.2.5	Comparison between the mass spectral patterns of the N, N'-(aryl)benzaldiamine dihydrochloride salts analogues	99
<b>4.3</b>	<b><sup>1</sup>H- and <sup>13</sup>C-NMR studies</b>	<b>99</b>
4.3.1	Liner Free Energy Relationships and NMR chemical Shifts	99
4.3.2	<sup>1</sup> H- and <sup>13</sup> C-NMR studies of the N, N'-(aryl)benzaldiimine ligands	101
4.3.3	<sup>1</sup> H-NMR studies of the N, N'-(aryl)benzaldiamine ligands	106
4.3.4	<sup>1</sup> H- and <sup>13</sup> C-NMR studies of the N, N'-(aryl)benzaldiamine dihydrochloride salts	108
4.3.5	<sup>1</sup> H- and <sup>13</sup> C-NMR studies of the N, N'- <i>bis</i> (cinnamaldiimine) ligands	109
4.3.6	Comparison between <sup>13</sup> C-NMR studies of the N, N'- <i>bis</i> ( <i>trans</i> -cinnamaldehyde)-1, 2-diiminoethane and N, N'- <i>bis</i> (benzyl)ethylenediimine	110

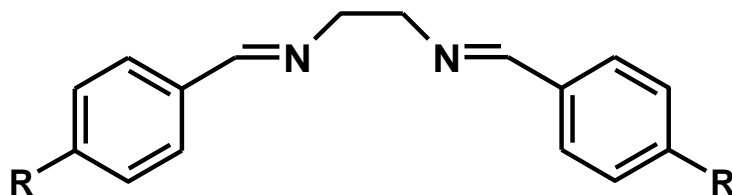
<b>4.4</b>	<b>Electronic spectral studies</b>	<b>111</b>
4.4.1	The electronic spectra of ligands and complexes	112
4.4.1.1	The electronic spectra of the N, N <sup>2</sup> -(aryl)benzaldiimine ligands	113
4.4.1.2	The electronic spectra of the N, N <sup>2</sup> -(aryl)benzaldiamine ligands and their copper(II) halide complexes	120
4.4.1.2.1	Bromo complexes	121
4.4.1.2.2	Chloro complexes	123
4.4.2	Correlation analysis studies for the electronic data of the N, N <sup>2</sup> - (aryl)benzaldiamine ligands and their copper(II) halide complexes	124
4.4.2.1	N, N <sup>2</sup> -(aryl)benzaldiimine ligands	125
4.4.2.2	N, N <sup>2</sup> -(aryl)benzaldiamine ligands	125
4.4.2.3	Bromo complexes	128
4.4.2.4	Chloro complexes	133
4.4.3	The electronic spectra of the N, N <sup>2</sup> - <i>bis(trans-cinnamylbenzyl)</i> ethylenediamine ligand and their copper(I) and copper(II) complexes	136
4.4.3.1	Copper(I)halide complexes of N, N <sup>2</sup> - <i>bis(cinnamaldehyde)-1,</i> 2-diiminoethane ligand	138
<b>4.5</b>	<b>Infrared spectroscopy</b>	<b>140</b>
4.5.1	Infrared spectral studies	140
4.5.2	Group frequencies of the N, N <sup>2</sup> -(aryl)benzaldiimines	142
4.5.3	Group frequencies of the N, N <sup>2</sup> -(aryl)benzaldiamines	144
4.5.4	Group frequencies of the N, N <sup>2</sup> -(aryl)benzaldiamines salts	145

4.5.5	Group frequencies of the N, N'- <i>bis</i> (cinnamaldehyde)1, 2-diiminoethanes and their Cu(I) and Cu(II) complexes	147
<b>4.6</b>	<b>Conclusion</b>	<b>149</b>
<b>4.7</b>	<b>References</b>	<b>151</b>

## LIST OF ABBRIVIATIONS

Abs	absorbance
APCI	atmospheric pressure chemical ionization mass spectrometry
BEN	N, N'- <i>bis</i> (benzyl)-1, 2-diiminoethane
CA <sub>2</sub> EN	N, N'- <i>bis</i> (cinnamaldehyde)-1, 2-diiminoethane
CH <sub>3</sub> CN	acetonitrile
CHCl <sub>3</sub>	chloroform
cm <sup>-1</sup>	wavenumber
<sup>13</sup> C-NMR	carbon nuclear magnetic resonance
DCM	dichloromethane
DSP	dual substituent parameters
ESI	electrospray mass spectrometry
EtOH	ethanol
ε	molar extinction coefficient
g.c.i	grating change in the instrument
<sup>1</sup> H-NMR	proton nuclear magnetic resonance
IR	infrared
I	intensity
kK	kiloKayser
MS	mass spectrometry
mmol	millimole
mid-IR	mid-infrared
nm	nanometres
ppm	part per million
ρ	reaction constant
R	generalized substituent
r	correlation coefficient
SSP	single substituent parametrs
UV/vis	ultraviolet visible spectroscopy

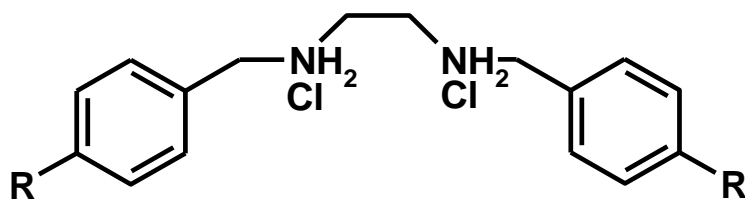
**LIST OF FORMULAE AND ABBREVIATIONS OF LIGANDS AND COMPLEXES APPEARING IN THE TEXT.**



**N, N'-(aryl)benzaldimine ligands**

R = NO <sub>2</sub> ;	N, N'- <i>bis</i> (4-nitrobenzyl)-1, 2-diiminoethane	(NO <sub>2</sub> -BEN)
R = Cl;	N, N'- <i>bis</i> (4-chlorobenzyl)-1, 2-diiminoethane	(Cl-BEN)
R = Br;	N, N'- <i>bis</i> (4-bromobenzyl)-1, 2-diiminoethane	(Br-BEN)
R = H;	N, N'- <i>bis</i> (benzyl)-1, 2-diiminoethane	(H-BEN)
R = CH <sub>3</sub>	N, N'- <i>bis</i> (4-methylbenzyl)-1, 2-diiminoethane	(CH <sub>3</sub> -BEN)
R = OCH <sub>3</sub> ;	N, N'- <i>bis</i> (4-methoxybenzyl)-1, 2-diiminoethane	(OCH <sub>3</sub> -BEN)
R = N(CH <sub>3</sub> ) <sub>2</sub> ;	N, N'- <i>bis</i> (4-dimethylaminobenzyl)-1, 2-diiminoethane	{(N(CH <sub>3</sub> ) <sub>2</sub> -BEN)}

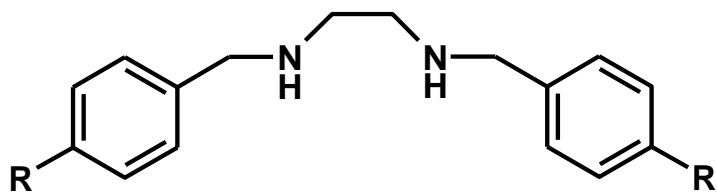
General abbreviation: (R-BEN)



**N, N'-(aryl)benzaldiamine dihydrochloride salts**

- R = NO<sub>2</sub>; N, N'-*bis*(4-nitrobenzyl)-1, 2-diaminoethane dihydrochloride (NO<sub>2</sub>-BENH•2HCl)
- R = Cl; N, N'-*bis*(4-chlorobenzyl)-1, 2-diaminoethane dihydrochloride (Cl-BENH•2HCl)
- R = Br; N, N'-*bis*(4-bromobenzyl)-1, 2-diaminoethane dihydrochloride (Br-BENH•2HCl)
- R = H; N, N'-*bis*(benzyl)-1, 2-diaminoethane dihydrochloride (H-BENH•2HCl)
- R = CH<sub>3</sub>; N, N'-*bis*(4-methylbenzyl)-1, 2-diaminoethane dihydrochloride (CH<sub>3</sub>-BENH•2HCl)
- R = OCH<sub>3</sub>; N, N'-*bis*(4-methoxybenzyl)-1, 2-diaminoethane dihydrochloride (OCH<sub>3</sub>-BENH•2HCl)

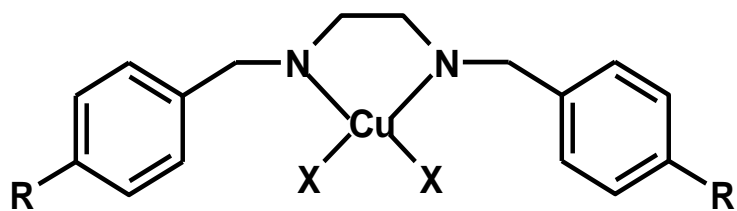
General abbreviation: (R-BENH•2HCl)



**N, N'-(aryl)benzaldiamine ligands**

R	=	NO <sub>2</sub> ;	N, N'-bis(4-nitrobenzyl)-1, 2-diaminoethane	(NO <sub>2</sub> -BENH)
R	=	Cl;	N, N'-bis(4-chlorobenzyl)-1, 2-diaminoethane	(Cl-BENH)
R	=	Br;	N, N'-bis(4-bromobenzyl)-1, 2-diaminoethane	(Br-BENH)
R	=	H;	N, N'-bis(benzyl)-1, 2-diaminoethane	(H-BENH)
R	=	CH <sub>3</sub> ;	N, N'-bis(4-methylbenzyl)-1, 2-diaminoethane	(CH <sub>3</sub> -BENH)
R	=	OCH <sub>3</sub> ;	N, N'-bis(4-methoxybenzyl)-1, 2-diaminoethane	(OCH <sub>3</sub> -BENH)

General abbreviation: (R-BENH)



X = Br

R = NO<sub>2</sub>; N, N'-*bis*(4-nitrobenzyl)-1, 2-diaminoethanedibromocopper(II)  
Cu(II)(NO<sub>2</sub>-BENH)Br<sub>2</sub>

R = Cl; N, N'-*bis*(4-chlorobenzyl)-1, 2-diaminoethanedibromocopper(II)  
Cu(II)(Cl-BENH)Br<sub>2</sub>

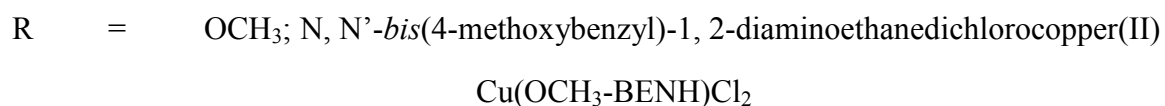
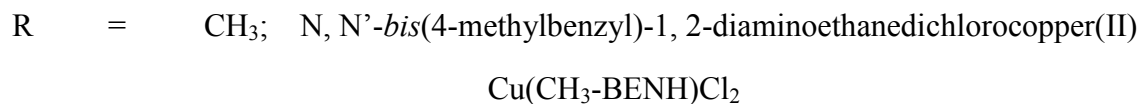
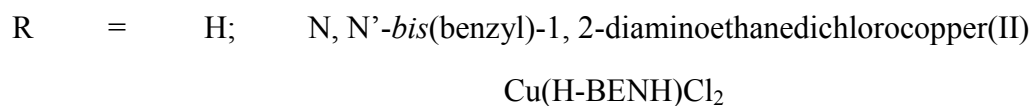
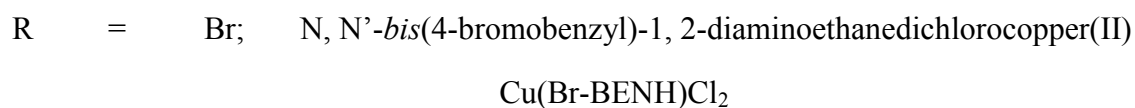
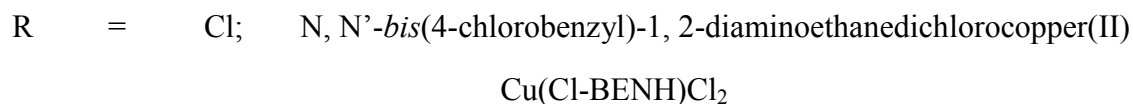
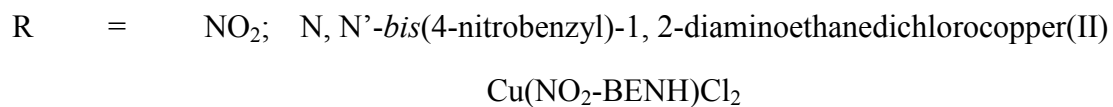
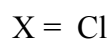
R = Br; N, N'-*bis*(4-bromobenzyl)-1, 2-diaminoethanedibromocopper(II)  
Cu(II)(Br-BENH)Br<sub>2</sub>

R = H; N, N'-*bis*(benzyl)-1, 2-diaminoethanedibromocopper(II)  
Cu(II)(H-BENH)Br<sub>2</sub>

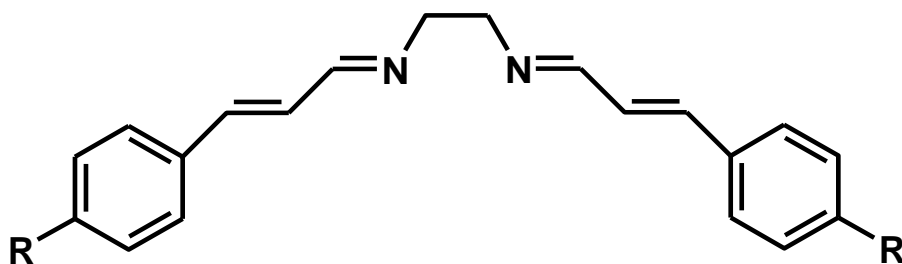
R = CH<sub>3</sub>; N, N'-*bis*(4-methylbenzyl)-1, 2-diaminoethanedibromocopper(II)  
Cu(II)(CH<sub>3</sub>-BENH)Br<sub>2</sub>

R = OCH<sub>3</sub>; N, N'-*bis*(4-methoxybenzyl)-1, 2-diaminoethanedibromocopper(II)  
Cu(II)(OCH<sub>3</sub>-BENH)Br<sub>2</sub>

General abbreviation: Cu(R-BENH)Br<sub>2</sub>



General abbreviation:  $\text{Cu}(\text{R-BENH})\text{Cl}_2$

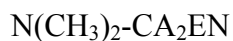


**N, N'-bis(cinnamaldiimine) ligands**

R=H; N, N'-bis(cinnamaldehyde)-1, 2-diiminoethane

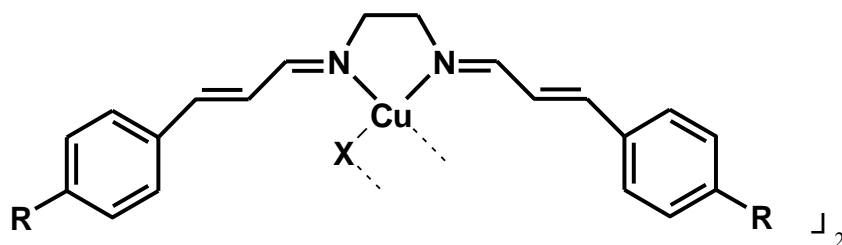


R=N(CH<sub>3</sub>)<sub>2</sub>; N, N'-bis(4-dimethylaminocinnamaldehyde)-1, 2-diiminoethane



General abbreviation: R-CA<sub>2</sub>EN

Γ



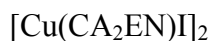
R = H, X = Br; N, N'-bis(cinnamaldehyde)-1, 2-diiminoethane copper(I)bromo



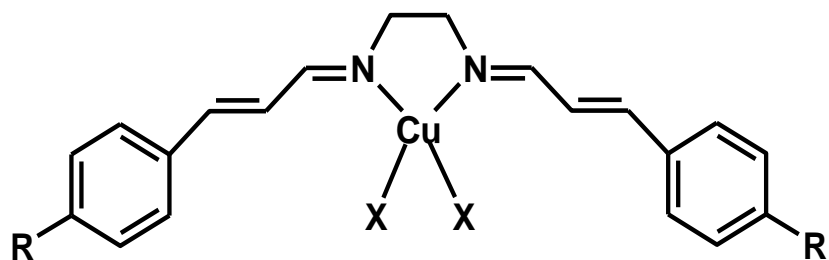
R = H, X = Cl; N, N'-bis(cinnamaldehyde)-1, 2-diiminoethane copper(I)chloro



R = H, X = I; N, N'-bis(cinnamaldehyde)-1, 2-diiminoethane copper(I)iiodo



General abbreviation: [Cu(CA<sub>2</sub>EN)X]<sub>2</sub>



R = H, X = Br; N, N'-*bis*(cinnamaldehyde)-1, 2-diiminoethanedibromocopper(II)

R = H, X = Cl; N, N'-*bis*(cinnamaldehyde)-1, 2-diiminoethanedichlorocopper(II)

General abbreviation: [Cu(CA<sub>2</sub>EN)X<sub>2</sub>]

## LIST OF FIGURES

Figure 1.1	The representative structure of Schiff base.	1
Figure 1.2	The sensory rhodopsin embedded in a lipid bilayer: Red and purple ribbons represent rhodopsin, white ribbon represents fluid lipid bilayer.	3
Figure 1.3	Cis and trans conformation of rhodospin.	4
Figure 3.1	Numbering system used for the Schiff bases.	
Figure 3.2	Numbering system used for the N, N'-bis(cinnamaldiimine) ligands.	
Figure 4.2.1	APCI-MS spectrum obtained for N(CH <sub>3</sub> ) <sub>2</sub> -BEN in chloroform solution.	90
Figure 4.2.2	APCI-MS spectrum obtained for Cl-BEN in chloroform solution.	91
Figure 4.2.3	APCI-MS spectrum obtained for Br-BEN in chloroform solution.	92
Figure 4.2.4	APCI spectrum obtained for (CH <sub>3</sub> )-BENH•2HCl in water.	93
Figure 4.2.5	ESI spectrum obtained for Cl-BENH•2HCl in water.	94
Figure 4.2.6	ESI spectrum obtained for Br-BENH•2HCl in water.	95
Figure 4.2.7	ESI spectrum obtained for Cl-BENH in methanol.	97
Figure 4.2.8	ESI spectrum obtained for Br-BENH in methanol.	98
Figure 4.3.1	Numbering system used for the Schiff bases.	102
Figure 4.3.2	The delocalisation of electrons to the imine nitrogen.	103
Figure 4.3.3	The rotation of the imine ligand about the methylene.	105
Figure 4.3.4	Numbering system used for the N, N'-bis(cinnamaldiimine) ligand.	110
Figure 4.4.1	The Ultraviolet-visible-NIR spectrum.	112

Figure 4.4.2	Ultraviolet absorption spectra of ligands, (a) Cl-BEN, (b) H-BEN and (c) CH <sub>3</sub> -BEN in EtOH.	115
Figure 4.4.3	Ultraviolet absorption spectrum of NO <sub>2</sub> -BEN in EtOH.	116
Figure 4.4.4	Ultraviolet absorption spectra of ligands of CH <sub>3</sub> -BEN, OCH <sub>3</sub> -BEN and N(CH <sub>3</sub> ) <sub>2</sub> -BEN in EtOH.	117
Figure 4.4.5	Plot of wavelength (nm) versus Hammett $\zeta$ values for $\pi \rightarrow \pi^*$ transition of benzene ring for Schiff bases in EtOH.	118
Figure 4.4.6	Plot of wavelength (nm) versus Hammett $\zeta$ values for charge transfer transition for Schiff bases in EtOH.	119
Figure 4.4.7	Plot of wavelength (nm) versus Hammett $\zeta$ values for $n \rightarrow \pi^*$ transition for Schiff bases in EtOH.	119
Figure 4.4.8	Uv-vis spectra of Cu(II)(CH <sub>3</sub> -BENH)Br <sub>2</sub> and Cu(II)(Br-BENH)Br <sub>2</sub> in EtOH.	123
Figure 4.4.9	Uv-vis spectra of complexes, Cu(II)(CH <sub>3</sub> -BENH)Br <sub>2</sub> & Cu(II)(Br-BEN)Br <sub>2</sub> in CHCl <sub>3</sub> .	123
Figure 4.4.10	Uv-vis spectra of Cu(II)(OCH <sub>3</sub> -BENH)Cl <sub>2</sub> in EtOH and CHCl <sub>3</sub> .	124
Figure 4.4.11	Plot of wavelength (nm) versus Hammett $\zeta$ values for $\pi \rightarrow \pi^*$ transition of N, N'-(aryl)benzyaldiamine ligands in EtOH solution.	126
Figure 4.4.12	Plot of wavelength (nm) versus Hammett $\zeta$ values for $\pi \rightarrow \pi^*$ transition of N, N'-(aryl)benzyaldiamine ligands in CHCl <sub>3</sub> solution.	127
Figure 4.4.13	Plot of wavelength (nm) versus Hammett $\zeta$ values for $\pi \rightarrow \pi^*$ transition of Cu(R-BENH)Br <sub>2</sub> in EtOH solution.	129
Figure 4.4.14	Plot of wavelength (nm) versus Hammett $\zeta$ values for $\pi \rightarrow \pi^*$ transition of Cu(R-BENH)Br <sub>2</sub> in CHCl <sub>3</sub> solution.	130

Figure 4.4.15	Plot of wavelength (nm) versus Hammett $\zeta$ values for $\pi \rightarrow \pi^*$ transition of Cu(R-BENH)Br <sub>2</sub> and of the free ligand in EtOH solution.	131
Figure 4.4.16	Plot of wavelength (nm) versus Hammett $\zeta$ values for $\pi \rightarrow \pi^*$ transition of Cu(R-BENH)Br <sub>2</sub> and of the free ligand in CHCl <sub>3</sub> solution.	131
Figure 4.4.17	Plot of wavelength (nm) versus Hammett $\zeta$ values for d $\rightarrow$ d transition of Cu(R-BENH)Br <sub>2</sub> in EtOH solution.	132
Figure 4.4.18	Plot of wavelength (nm) versus Hammett $\zeta$ values for d $\rightarrow$ d transition of Cu(R-BENH)Br <sub>2</sub> in CHCl <sub>3</sub> solution.	133
Figure 4.4.19	Plot of wavelength (nm) versus Hammett $\zeta$ values for $\pi \rightarrow \pi^*$ transition of Cu(R-BENH)Cl <sub>2</sub> and of the free ligand in EtOH solution.	133
Figure 4.4.20	Plot of wavelength (nm) versus Hammett $\zeta$ values for $\pi \rightarrow \pi^*$ transition of Cu(R-BENH)Cl <sub>2</sub> and of the free ligand in CHCl <sub>3</sub> solution.	134
Figure 4.4.21	Plot of wavelength (nm) versus Hammett $\zeta$ values for d $\rightarrow$ d transition of Cu(R-BENH)Cl <sub>2</sub> in EtOH solution.	135
Figure 4.4.22	Plot of wavelength (nm) versus Hammett $\zeta$ values for d $\rightarrow$ d transition of Cu(R-BENH)Cl <sub>2</sub> in CHCl <sub>3</sub> solution.	135
Figure 4.4.23	Ultraviolet spectrum of CA <sub>2</sub> EN ligand in DCM.	137
Figure 4.4.24	Ultraviolet spectra of CA <sub>2</sub> EN and N(CH <sub>3</sub> ) <sub>2</sub> -CA <sub>2</sub> EN ligand in DCM.	138
Figure 4.4.25	UV-vis spectra of [Cu(CA <sub>2</sub> EN)X] <sub>2</sub> complexes in DCM.	138
Figure 4.4.26	UV-vis spectra of [Cu(I)(CA <sub>2</sub> EN)Cl] <sub>2</sub> , [Cu(II)(CA <sub>2</sub> EN)Cl] <sub>2</sub> and CA <sub>2</sub> EN in DCM.	139
Figure 4.5.1	Mid-infrared spectra of 4-CH <sub>3</sub> analogues.	147

## LIST OF SCHEMES

Scheme 1.1	Synthesis of a Schiff base from carbonyl compound with primary amine.	5
Scheme 1.2	Enol and keto tautomers.	8
Scheme 1.3	Biological conversion of dioxygen species into water.	9
Scheme 2.1	The <i>para</i> -substituted benzylideneethylenediamine ligands (R-BEN) employed in the study.	38

## LIST OF TABLES

Table 1.1	Hammett substituent parameters, $\zeta$ .	21
Table 1.2	Values of DSP's for the study.	22
Table 3.1	Microanalysis and analytical data for the N, N'-(aryl)benzaldimine ligands.	60
Table 3.2	Microanalysis and analytical data for the N, N'-(aryl)benzaldiamine dihydrochloride salts.	62
Table 3.3	Microanalysis and analytical data for the N, N'-(aryl)benzaldiamine ligands.	63
Table 3.4	Microanalysis and analytical data for the N, N-(aryl)benzaldiaminedibromidecopper(II) complexes.	64
Table 3.5	Microanalysis and analytical data for the N, N-(aryl)benzaldiaminedichloridecopper(II) complexes.	65
Table 3.6	Microanalysis and analytical data for the N, N'-bis(cinnamaldiimine) ligands.	67
Table 3.7	Microanalysis and analytical data for the N, N'-bis(cinnamaldehyde)-1, 2-diiminoethane copper(I)halide.	68
Table 3.8	Microanalysis and analytical data for the N, N'-bis(cinnamaldehyde)-1, 2-diiminoethane copper(II)halide.	68
Table 3.9	Proton nuclear magnetic resonance data for the N, N'-(aryl)benzaldimine ligands.	69
Table 3.10	Carbon nuclear magnetic resonance data for N, N'-(aryl)benzaldimine ligands.	71
Table 3.11	Proton nuclear magnetic resonance data for N, N'-(aryl)benzaldiamine dihydrochloride salts	72
Table 3.12	Proton nuclear magnetic resonance data for the N, N'-(aryl)benzaldiamine ligands.	73
Table 3.13	Carbon nuclear magnetic resonance data for the N, N'-(aryl)benzaldiamine ligands.	74
Table 3.14	Proton and carbon nuclear magnetic resonance data for the N, N'-bis(cinnamaldiimine) ligands.	75
Table 3.15	UV/vis spectral data for the N, N'-(aryl)benzaldimine ligands.	76
Table 3.16	UV/vis spectral data for the N, N'-(aryl)benzaldiamine ligands.	77

Table 3.17	UV/vis spectral data for the N, N'-(aryl)benzaldiaminedibromide complexes.	79
Table 3.18	UV/vis spectral data for the N, N'-(aryl)benzaldiaminedichloride complexes.	80
Table 3.19	UV/visible spectral data for the N, N'-bis(cinnamaldehyde)-1, 2-diiminoethanecopper(I)halide and copper(II) dihalide.	81
Table 3.20	The mid-infrared spectral data for the N, N'-(aryl)benzaldiamine dihydrochloride salts.	82
Table 3.21	The mid-infrared spectral data for the copper(II) N, N'-(aryl)benzaldiaminebromide and chloride complexes.	83
Table 3.22	The mid-infrared spectra data for the copper(II) N, N'-(aryl)benzaldiaminebromide and chloride complexes.	84
Table 3:23	The mid-infrared spectra data for the N, N'-bis(cinnamaldiimine) ligands and their copper(I) and copper(II) halide complexes.	85
Table 4.1	Trends of the electron donor substituents on the N, N'-(aryl)benzaldiimine ligands.	102
Table 4.2	Correlation coefficients for protons delivered from the H-NMR data of N, N'-(aryl)benzaldiimine ligands and various substituents parameters.	104
Table 4.3	Correlation coefficients for carbons delivered from the <sup>13</sup> C-NMR data of N, N'-(aryl)benzaldiimine ligands and various substituents parameters.	104
Table 4.4	Correlation coefficients for protons delivered from the	

	<sup>1</sup> H-NMR data of N, N'-(aryl)benzaldiamine dihydrochloride salts and various substituents parameters.	106
Table 4.5	Correlation coefficients for protons delivered from the <sup>1</sup> H-NMR data of N, N'-(aryl)benzaldiamine ligands and various substituents parameters.	108
Table 4.6	Correlation coefficients for protons delivered from the <sup>13</sup> C NMR data of N, N'-(aryl)benzaldiamine ligands and various substituents parameters.	108
Table 4.7	Trends of of the electron donor substituent on the N, N'-bis(4-dimethylaminocinnamaldehyde)-1, 2-diiminoethane.	110
Table 4.8	Change in substituent chemical shift values for CA <sub>2</sub> EN and BEN ligands.	111
Table 4.9	Correlation of $\pi \rightarrow \pi^*$ transition for N, N'-(aryl)benzaldimine ligands with various substituent parameters in EtOH solutions.	125
Table 4.10	Correlation of $\pi \rightarrow \pi^*$ transition for N, N'-(aryl)benzaldiamine ligands with various substituent parameters in EtOH and CHCl <sub>3</sub> solutions.	128
Table 4.11	Correlation of $\nu_{C=N}$ for N, N'-(aryl)benzaldimine ligands with various substituent parameters.	142
Table 4.12	Correlation of $\nu_{N-H}$ for N, N'-(aryl)benzaldiamine ligands with various substituent parameters.	144
Table 4.13	Correlation of $\nu_{NH_2^+}$ and $\delta_{NH_2^+}$ for N, N'-(aryl)benzaldiamine dihydrochloride salts with various substituent parameters.	146

Table 4.14 Comparison between the  $\nu\text{C}=\text{N}$  stretches of the BEN and  $\text{CA}_2\text{EN}$  ligands. 147

Table 4.15 Comparison between the  $\nu\text{C}=\text{N}$  stretches of the  $\text{CA}_2\text{EN}$  ligand and their copper complexes. 148

## 1. INTRODUCTION

This study is concerned with the synthesis, characterization and the investigation of the transmission of electronic effects of substituents in Schiff bases and their copper(II) halide complexes, for structural elucidation of the compounds. Accordingly, this chapter covers a brief overview of Schiff bases and their amine ligands with respect to this work, a literature review of Schiff bases, amine ligands and their copper(II) or copper(I) complexes that are relevant to this study. More information will be given later when discussing the substituent parameters with respect to spectroscopic properties.

### 1.1 Schiff bases

#### 1.1.1 Background

A Schiff base is a neutral molecule with an electron pair and contains a carbon-nitrogen double bond. This class of compound was discovered in 1864 by Hugo Schiff, when he reacted an aldehyde and amine, leading to a Schiff base<sup>1</sup>. The compound, an azomethine was named after him in reference to the condensation reaction products he obtained.

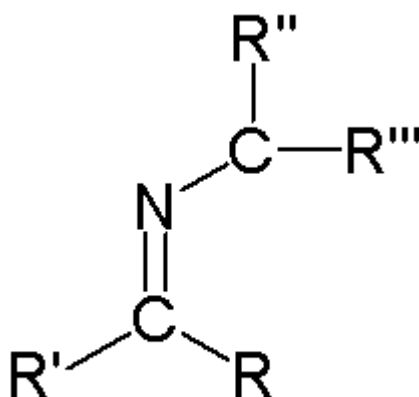


Figure 1.1 The representative structure of Schiff base

Schiff bases are classified according to the number of electrons that the molecule has or to the type of atoms or donor atom groups that the molecule contains. The donor atom can be nitrogen, oxygen, phosphorous or a sulphur. It is these donor atoms that stabilize the structure of Schiff base ligands and that determine the ligand's bioactivity. In the nitrogen compound the presence of a  $\text{-C=N-}$  group in Schiff bases enhances bioactivity<sup>2-3</sup>, and most of the nitrogen donor ligand complexes have been used as precursors in different homogeneous catalytic reactions<sup>4-7</sup>.

Schiff base ligands are capable of stabilizing many different metals in various oxidation states to form complexes using their lone paired electrons. The complex formation occurs through coordination of the metal via the azomethine nitrogen. Schiff base ligands have played an integral role in the development of coordination chemistry since the late nineteenth century. In fact, most of Schiff base ligands require a metal ion for activity<sup>8</sup>.

### **1.1.2 Applications and properties of Schiff bases**

Schiff bases are part of very popular class of compounds in coordination chemistry, particularly in bioinorganic chemistry. They are easily formed and easily broken; their synthesis is a reversible acid catalyzed reaction. These materials are considered special due to their facile synthesis and the flexible skeleton structure that makes it possible to access diverse structural modification by introducing different substituents.

Schiff bases have played an important role in the development of the chemical industry and biochemistry owing to their applications and their biological activities and they played a major role in organic synthesis.

Generally Schiff bases are well known due to their applications as intermediates in the synthesis of medicinal products such as aminoalkylpyridine<sup>9-11</sup> and hydrozone<sup>12</sup>. Schiff bases derived from primary amine and substituted benzaldehyde are known to have antibacterial<sup>2, 13-14</sup>, antitumor<sup>15-16</sup>, anticonvulsant<sup>17</sup> and anti-HIV<sup>18</sup> activities. In addition to

their biological properties Schiff bases play other biological roles <sup>19</sup>, for example in vision, in determining the flexibility of the wall of the veins.

These compounds are not only important intermediates in the synthesis of medicinal products. Schiff bases of pyrazolone have played a crucial role in the petrochemical industry <sup>20</sup> and they are useful reagents for the extraction and separation of various metal ions <sup>21</sup>.

In industry the imines, Retinyl Schiff base salts (ATRSBS) are known to have similar properties to rhodopsin, and they have been used in the military industry as anti-radar shield for aircraft <sup>22</sup>. Rhodopsin (visual purple or light sensitive protein) is a chemical substance that is found in the retina at the back of the eye and it belong to the G-protein receptor family and it appears as redish-purple. The diagram of rhodopsin is given in figure 1.2. This chemical molecule, rhodopsin is very sensitive to photons of light and it transforms the absorbed light (green-blue light) into an image signal, in which these signals are transferred to the brain. This process allows the rhodopsin to go through conformational change, from *cis* to *trans*-conformation as shown in figure 1.3.

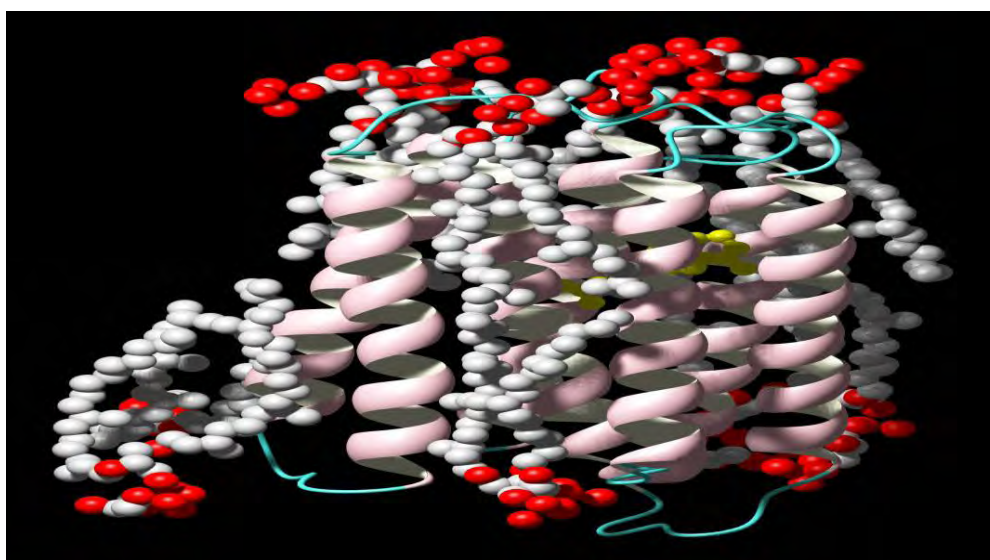


**Figure 1.2 The sensory rhodopsin embedded in a lipid bilayer. Red and purple ribbons represent rhodopsin, white ribbon represents fluid lipid bilayer**

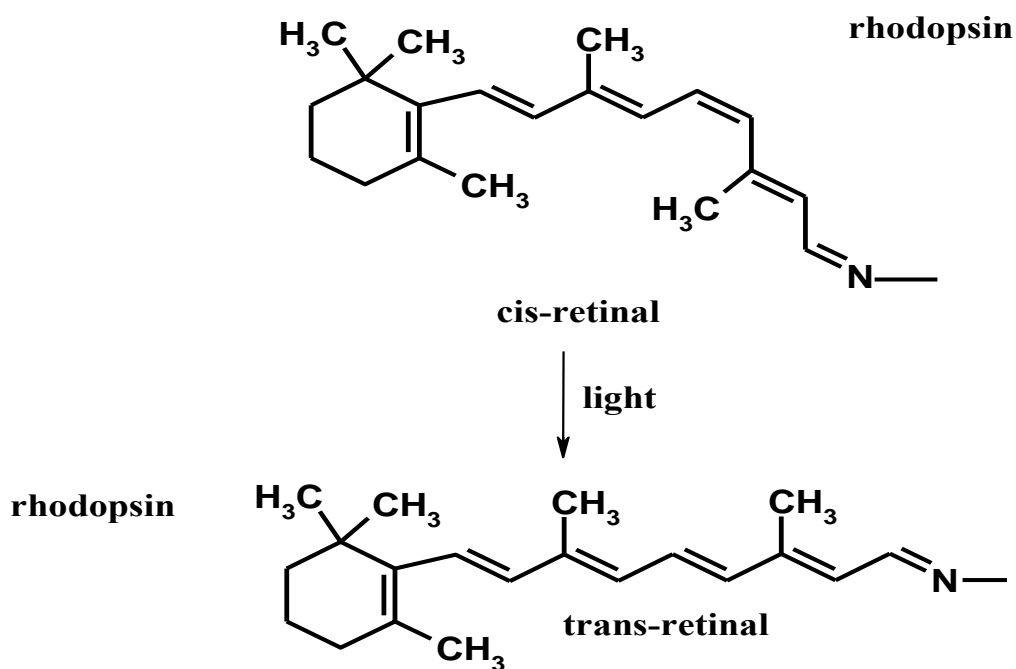


**Figure 1.3 Cis and trans conformation of rhodopsin**

Biological studies of the Schiff bases of the structural formula of ligand, N, N'-bis(benzyl)ethylenediimine and their analogous unconjugated diimine has not been covered comprehensively previously<sup>23</sup>. This may largely be attributed due to the instability of their coordination compounds with most transitional metals, as the result of the hydrolysis of the ligand upon complexation. It has been observed that these Schiff base complexes hydrolysed in the presence of copper(II) giving mixed products<sup>24</sup>.

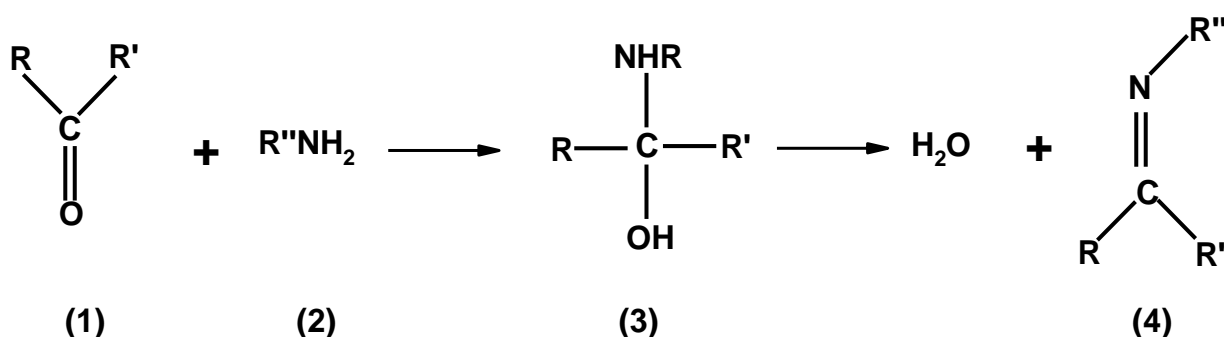
However, Schiff base N, N'-bis(benzyl)ethylenediimine have been used as anticorrosion inhibitors of zinc in sulphuric acid<sup>25-26</sup> and in hydrochloric acid<sup>27</sup>. In addition to their applications these materials have also been used as modulators of structural and electronic properties of transition metal centre for nickel metal<sup>27</sup>. In electrochemistry their nickel complexes have been exploited as a catalyst in the detection of organochlorinated pollutants<sup>28</sup>. In addition to the properties mentioned above, Schiff bases have been investigated for their interesting electronic and structural features.

Salicylidene type Schiff bases (or 2-hydroxybenzaldimine compounds) exhibit thermochromic or photochromic properties. They have been used as modulators of both structural and electronic properties of the transition metal centre, because of their ability to bind with metal ions. The stability of the complexes is enhanced by chelation due to the presence of the o-hydroxyl groups.

### 1.1.3 Synthesis of Schiff bases

Schiff bases are often referred to as imines, azomethines or anils. They are indicated structurally as  $RR'C=NR''$ . The nature of the R groups bonded to the nitrogen or to the carbon atom are limited to alkyl or aryl substituents, because these imines rapidly decompose or polymerize if a hydrogen atom is attached to the imino (C=N) carbon or nitrogen atom.

The most common method for the preparation of Schiff base is the reaction of an aldehyde and ketone with primary amines. It involves a condensation reaction between the carbonyl compound (1) and the primary amine (2). The condensation product, the Schiff base (4) is known to be formed by way of nucleophilic attack by the primary amine on the carbonyl carbon, to yield first a tetrahedral carbinolamine intermediate known<sup>28</sup> as a hemiaminol (3). This intermediate is very unstable, which is followed by elimination of water to generate the imine functional group characteristic of the Schiff base.



Scheme 1.1 Synthesis of a Schiff base from carbonyl compound with primary amine

It has been reported that the nature of the carbonyl compounds as well as that of the amines determines the position of the equilibrium and the reaction mechanism. For example, tertiary aliphatic and aromatic aldehydes react readily with amines to give the corresponding imines even at room temperature<sup>29</sup>. Aromatic aldehydes are so reactive that the product is formed even without the removal of the water formed during the reaction<sup>1</sup>. Para-substituted benzaldehyde with electron-donating groups decrease the reaction rate, while the reverse is true for similar para-substituted anilines<sup>29</sup>. In contrast, aliphatic ketones react with amines more slowly than aldehydes to form imines; the reaction requires a higher reaction temperature and longer reaction time. If the ketone is sterically hindered the reaction becomes slower than an unhindered ketone<sup>30</sup>.

Normally the condensation reaction is acid catalyzed but this role may be often be taken by a metal ion. In this case the imine product is isolated as the metal complex. The product, a Schiff base metal complex, is obtained directly by the reaction between the metal ion, the aldehyde and the amine. The choice of metal ion is crucial in this method, because if there is a strong interaction between the primary amine and the metal ion, it may hinder or prevent the amine from engaging in nucleophilic attack at the carbonyl carbon atom. For example Ni(II) is a good choice for the synthesis of a ligand having a planar tetradentate mode of binding, rather than synthesis of a ligand having pentagonal or hexagonal planar donor atoms<sup>31</sup>.

Schiff bases can also be synthesised through a reaction of nitriles with organometallic compounds. Moureau and Mignonac<sup>32</sup> were the first to obtain imine (ketimine), using an alkyl Grignard, aryl cyanide at 15 °C, treated with hydrogen chloride and with ammonia.

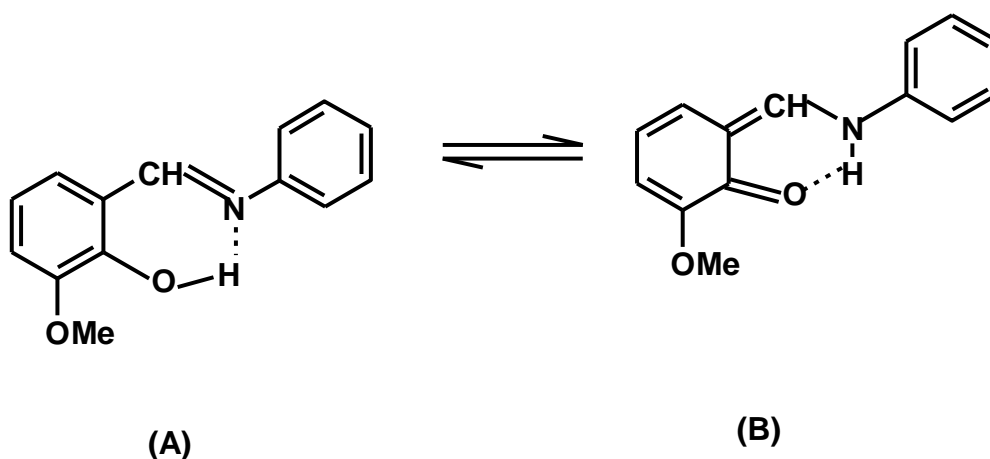
#### 1.1.4 Spectroscopic properties

The most characteristic group frequency of Schiff bases employed in literature is  $\nu_{\text{C=N}}$ . The infrared spectra of imines shows that the C=N stretching frequency absorbs in the region between 1680 and 1603  $\text{cm}^{-1}$  when H, alkyl or phenyl groups are bonded to carbon and nitrogen atoms<sup>33</sup>. The region where the C=N stretch absorbs is guided by a number of

factors, the nature of the substituent groups and the physical state of the compound. In a conjugated system on the carbon and nitrogen atoms for the compound of the type  $R_2C=NR$  the C=N bond absorbs at the lower wavenumber ( $1631-1613\text{ cm}^{-1}$ ), while the unconjugated system absorbs at higher wavenumbers ( $1657-1631\text{ cm}^{-1}$ )<sup>32</sup>. The presence of a substituent in the phenyl ring such as halogen is known to decrease the conjugation which raises the absorption to a frequency range of  $1656-1631\text{ cm}^{-1}$ <sup>34</sup>.

Extensive studies on the Schiff bases have been done using electronic spectroscopy<sup>35-38</sup>. Ultraviolet and visible spectrophotometry has been used for the analysis of the chromophore of Schiff bases. The characterization of Schiff base compounds depends on the chromophores of the molecules. For compounds containing an unconjugated chromophore these groups are characterized by bands due to  $n \rightarrow \pi^*$  transitions in the range 234-272 nm, while the conjugated chromophores, such as those with an alkene group, cause a strong band in the range 180-250 nm due to  $\pi \rightarrow \pi^*$  transitions. The  $n \rightarrow \pi^*$  transitions are very weak absorptions which can be covered (or masked) by  $\pi \rightarrow \pi^*$  transitions.

It has been reported that the electronic spectra of Schiff base compounds derived from 2-hydroxybenzaldimine compounds are solvent dependent. The electronic spectra of these materials have been studied in both polar and non-polar solvents<sup>39-44</sup>. It has been observed that a band above 400 nm, which is associated with a tautomerization effect, is more intense in polar solvents and in acidic media, while it disappears in non-polar solvents<sup>39-44</sup>. This tautomerisation involves a formal migration of a hydrogen atom or proton, accompanied by a switch of a single bond and adjacent double bond, as shown in scheme 1.1. The tautomer equilibrium is widely observed in Schiff bases derived from 2-hydroxynaphthaldehyde and aniline, while in Schiff bases derived from salicylaldehyde and aniline the band at  $> 400\text{nm}$  is only observed in acidic media. For the Schiff base, N, N'-bis(benzyl)ethylenediimine and its analogues the tautomerisation is not expected.



**Scheme 1.2 Enol and keto tautomers**

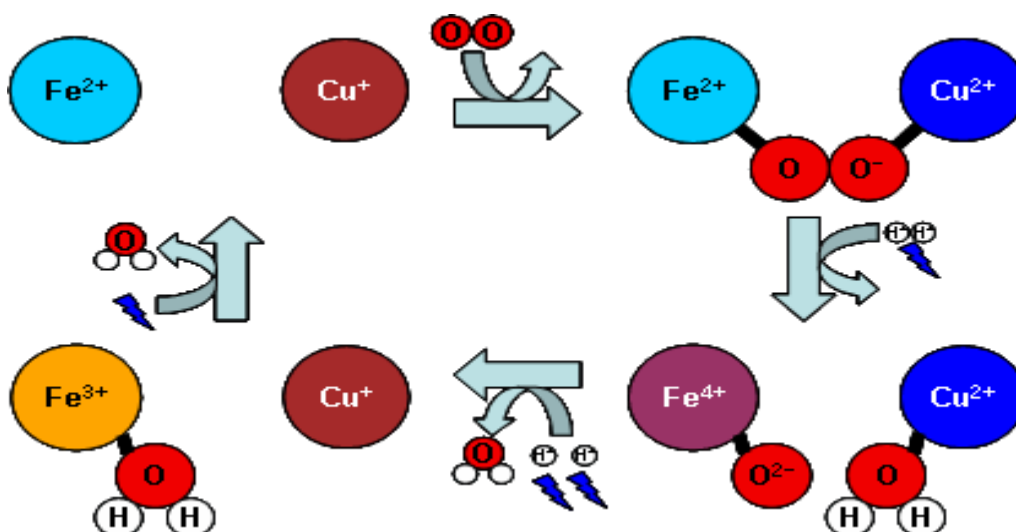
Nuclear magnetic resonance spectroscopy has been used to investigate the chemistry of Schiff bases in solution, this includes the study of intramolecular hydrogen bonding in Schiff bases<sup>45</sup> and the electronic effects produce by the substituents in substituted Schiff bases<sup>46-48</sup>. Schiff base ligands in solution may have two types of intramolecular hydrogen bonds, namely phenol-imine or keto-amine (N-H---O or N---H-O) and the predominance of both types depending on the conditions and have been confirmed by NMR<sup>45</sup>.

Furthermore NMR chemical shifts are sensitive probes of electron-density distributions and have been found useful for the study of the transmission of electronic effects in organic molecules. The <sup>1</sup>H- and <sup>13</sup>C-NMR spectra of these materials have been reported and their data fit the Hammett relationship. The Hammett relationship is based on the principles of linear free energy relationships (LFER)<sup>46-48</sup>.

## 1.2 Copper

Copper is a trace metal which is found in many foods such as liver and shellfish. And it is one of the six metals that are essential in living organisms<sup>49</sup>. In blood plasma copper is part of a number of key proteins, including many vital enzymes. The function<sup>50</sup> of copper in biological systems is primarily in redox reactions associated with the reduction of oxygen to water, meaning the transfer of oxygen to a substrate. This involves the abstraction of the dangerous by-product, such as the superoxide ion, through oxygenation reactions in the system (or blood plasma) and which results in the removal of highly reactive superoxide anion as shown in scheme 1.3.

The superoxide ion is the anion  $O_2^-$  and it is the product of the one-electron reduction of dioxygen, which occurs widely in nature. In living organisms the superoxide ion is a toxic oxygen species that has a high energy. It is formed through uncontrolled autoxidation of low-potential cytochromes, iron-sulphur proteins and flavoproteins, as well as by the decomposition of complexes such as oxyhaemoglobin and it is capable of forming hydrogen peroxide or oxygen either through reduction or oxidation. It is widely deployed by the immune system to kill invading microorganisms<sup>51</sup>.



Scheme 1.3 Biological conversion of dioxygen species into water

The production of superoxide is quite dangerous and it can induce the bacteriostatic action of milk xanthine oxidase and it is implicated in bacteriocidal activity of granular leucocytes.<sup>49</sup>

For the functions mentioned above, copper is tightly bound to enzymes (copper-containing proteins) such as phenolase, or hemocyanin  $\{\text{Cu(I)}\}$  and ceruloplasmin in blood plasma. These enzymes regulate the level of oxygen and normalises the metabolic process<sup>49</sup>.

In addition to the biological functions of the copper binding components, the enzymes control the transportation of copper in the human body, the intake and excretion of copper around the human body. This manages the level of copper and is essential in controlling disease caused by copper deficiency such as Menkes<sup>52</sup> and Wilson's<sup>53</sup> diseases.

Copper salts (e.g.  $\text{CuCl}_2$ ) have been found to be very useful in prevention of fungal growth and killing algae<sup>54</sup>. On the other hand an excess concentration of copper can be dangerous, causing a number of toxic cellular effects.

The element copper has the electronic configuration (argon)  $4s^23d^9$  and it has one *s* electron outside a completed *d* shell. Copper occurs in different oxidation states and this yields a variety of coordination compounds. The oxidation states include copper(0) in the metal, copper(I) in cuprous compounds, copper(II) in cupric compounds and the copper(III) and (IV) oxidation states. Copper(I) and copper(II) are the most common oxidation states but Cu(II) is the most stable state and is the more prolific in the formation of complexes and in the formation of good crystals<sup>55-57</sup>. The copper(I) oxidation state is obtained from the loss of the single *s* electron in the outermost shell and its chemistry is very much less extensive than that of copper(II)<sup>55,56,58-60</sup>. In addition to the properties of the copper(I) ion, the metal ion is very unstable in aqueous solution. This is the result of the disproportion process. The disproportion process of the copper(I) ion involves the exchange of electrons with one another to form copper(0) and copper(II) within the solution medium. While the (III) oxidation state occurs by extensive oxidation of Cu(II).

It is worthy to mention that the copper(III) ion is known to be much less electropositive; this means that the possibility to react by loss of electron is relatively smaller than copper(II), that is why Cu(II) is more stable than the rest of other oxidation states.

### 1.2.1 The copper(II) ion

Copper(II) ion is a borderline hard acid, it is stabilized by complex formation, and nitrogen is the best donor to copper(II) ion, while fluoride is known to be the best halide ligand towards the formation of copper(II) complex. The copper(II) ion is best known in four-coordinate square planar, tetrahedral, five-coordinate square pyramidal or five-coordinate trigonal bipyramidal and six-coordination octahedral stereochemistries and it is one of the transitional metal(II) cations that undergo a variety of distortions such as Jahn Teller distortion<sup>61</sup>.

The distortion of geometries in copper(II) ion complexes is most common in a tetrahedral and in an octahedral environment. The distortion is due to the splitting of the d orbitals of the metal ion into energy levels of certain magnitude in order to remove degeneracy and it can be explained through the Jahn-Teller theorem<sup>56</sup>.

The distorted geometry is influenced by a variety of contributions such as the coordination number of the ligands, the size and nature of the ligand coordinated to the metal centre and they determine the value of  $10Dq$ . For example oxygen and nitrogen are larger donor atoms and they are capable of forming a short distance bond, that is between 1.9-2.1 Å. Halide ligands such as  $Cl^-$  and  $Br^-$  result in intermediate and long distance bonds which lie between 2.29-2.45 Å.

### 1.2.2 Electronic properties of the copper(II) ion

Complexes of copper(II) ion are generally blue or green<sup>57, 59, 62</sup>. The origin of the colour is due to the maximum of up to four electronic transitions: d-d transitions; charge transfer transitions (both metal to ligand and ligand to metal); internal ligand transitions. These electronic transitions occur between the ground state and the excited states of the crystal field levels, and are observed within the range 4.0-30.0 kK (kK = 1000 cm<sup>-1</sup>). In this range the electronic transitions described above, plus combination and overtone vibrations of ligands occur<sup>63</sup>.

The pure d-d transitions in copper(II) complexes tend to occur below 20 kK and their spectra most commonly show only a single broad band (half-width *ca.* 5000 cm<sup>-1</sup>), while the charge transfer and internal ligand transitions are observed above 20-30 kK and the combination and overtone vibrations of ligands occur below 10 kK.

The d<sup>9</sup> ion is characterized by large distortions making it difficult to use electronic spectroscopy alone as a tool for identification of structure. However there is an enormous body of copper(II) electronic spectra in the literature, where the structure is known but the assignment is less certain.

For example, in regular octahedral copper(II) complexes for the  ${}^2T_{2g} \rightarrow {}^2E_g$  transition, the  $t_{2g} - e_g$  separation varies from about 13,000 cm<sup>-1</sup> for CuO<sub>6</sub> to about 18,000 cm<sup>-1</sup> for CuN<sub>6</sub>. But in a tetragonally distorted octahedral copper(II) complexes several absorption bands may be expected in this region, corresponding to the transitions from components of  $t_{2g}$  to  $dx^2-y^2$  and  $dz^2$ ; this is due to the splitting of the  ${}^2E_g$  ground terms of an octahedron as the result of Jahn Teller distortion and it results in the overlapping of bands and a slightly more complex spectrum, with the appearance of a low energy shoulder.

For the tetrahedrally coordinated copper(II) complex, distorted square planar geometry is strongly favoured for the  $d^9$  configuration. The distortion of this system lowers the symmetry from  $T_d$  to  $D_{2d}$  which retains the degeneracy of the  $d_{xz}$  and  $d_{yz}$ . This leads to three possible transitions, namely from the ground state  $^2B_2$  to  $^2E$ , to  $^2B_1$  and to  $^2A_1$ <sup>64</sup>. But commonly, four transitions may be observed, this reflects further distortion to  $D_2$  symmetry due to the splitting of the E-level in  $D_{2d}$  by spin orbit coupling. The distorted tetrahedrally square planar coordinated copper(II) ion complexes with the halogen ligands  $[CuBr_4]^{2-}$  and  $[CuCl_4]^{2-}$  have been studied extensively<sup>65-70</sup>, and they exhibit absorptions below 20kK, while tetra-coordination of the copper(II) ion with stronger field ligands such as imines will naturally appear blue shifted. For example the absorption of the distorted tetrahedral  $CuN_4$  chromophore occurs near 7000–8000, 10,000-11,000, 13,000 to 15,000 or even to 16,000  $cm^{-1}$ <sup>71-73</sup> and these spectra are due to transitions within the spin orbital coupling components of  $^2D$  in a  $D_{2d}$  field<sup>73</sup>.

The spectra of copper(II) ion complexes may be measured in solution<sup>74</sup>, as reflectance spectra<sup>75</sup> and as polarized single-crystal spectra<sup>76,77</sup>. In solution spectra accurate extinction coefficient data may be obtained. But with copper(II) complexes there is a high chance of ligand-solvent exchange or the possibility of more than one species in equilibrium, depending on the coordination number. While the reflectance and single-crystal spectra clearly relate to the crystal structure in solid state, neither yields accurate extinction coefficients<sup>76,77</sup>.

To identify the transitions within copper(II) ion complexes is difficult due to the large half-widths of the copper(II) spectra. In many cases the interpretation and resolution for a copper(II) spectrum has been obtained using software such as Gaussian analysis for the solution spectra, while for the solid spectra Kortuum-type analysis has been used<sup>75</sup>.

### 1.3 Metal complexes of Schiff bases

There has been a great interest in the chemistry of metal complexes of Schiff bases with a large body of information confirming biological activities and stereochemistry of metal complexes of Schiff bases. The data resulting from the spectral analysis of these coordination complexes have been used in understanding the structure of the complexes and their various properties<sup>76-79</sup>.

The interest in these materials is due to their applications in catalysis for various processes<sup>80-83</sup>, in electrochemistry<sup>84-85</sup> and in their biological activities, (eg. some of the metal complexes have anticancer activities)<sup>76</sup>.

Recently there has been a huge interest in the chemistry of metal complexes with tetradentate Schiff base ligands containing oxygen and nitrogen donors due to the structural features. The nickel(II) complex of a symmetric tetradentate Schiff base has been investigated because it has shown structural similarities to phthalocyanines, and it has been used as a modifying agent to produce chemically modified electrodes<sup>28</sup>.

Coordination compounds of copper(II) ions have presented a great variety of biological activities ranging from suppression of inflammation to antimicrobial activity and other pathological process, including destroying cancer cells<sup>86-87</sup>.

It has been observed that some drugs show increased activity when administered as metal complexes rather than as the free organic compounds<sup>8,88</sup>. For example, the antimitotic drug, Taxol is one drug that has a remarkable activity against drug-resistant human ovarian and breast tumours, but the detriments in the application of this drug in cancer chemotherapy are its limited bio-availability and poor water solubility. Test results from the active analogs of taxol, 10-deacetylbaaccatinthiosemicarbazone (DABTSC), against human breast cancer cells line MCF-7, show that the compound is highly effective as an anti-proliferative compound when it is administered as copper(II) complex (Cu-DABTSC)<sup>8</sup>.

In addition to the outstanding properties of the metal(II) complexes, coordination compounds of copper(I) ion and azomethine compounds have been extensively studied because of their instability and unusual structure features for use in solar energy and catalytic activity in photoredox reactions<sup>89-93</sup>.

#### **1.4 Amine ligands and their metal chelates**

For years transitional metal complexes of inorganic amines have been extensively studied because of their interesting chemical properties<sup>94</sup>, their contribution to chemotherapy and their structural resemblance with natural proteins and enzymes.

The first publication on a clinical application of metal inorganic complexes with an amine ligand, Cisplatin, as chemotherapeutic agent for ovarian cancer is date back in early 1974, by Wiltshaw and Cart<sup>95</sup>. Cisplatin was originally discovered by Michele Peyrone in 1844<sup>96</sup>, and is used as an antitumor agent. It currently is still considered as one of the most successful cancer chemotherapeutics. In addition to its application, Cisplatin is known to be more efficient for the inhibiting of a secondary tumour when is combined with ruthenium drugs<sup>97</sup>.

Inorganic amines are compounds that may be synthesized through reduction of the corresponding compound that has the azomethine functional group. The literature is replete with the publications that document the applications of amine. Their applications are very different from those of the Schiff base ligand and they have been utilised in the pharmaceutical industry as an important intermediate for synthesis of leading drugs.

Amine ligands such as polyamine are found in all cells; they regulate and control cancer cellular growth<sup>98-99</sup>. They play an important role in transportation of drugs such as polyamine-drug conjugates to cancer cells<sup>100-103</sup>. Polyamine-drug conjugates, such as bleomycin A5 and peplomycin are clinically employed antitumor agents<sup>104-105</sup> and they have been investigated as an efficient drug-carrier<sup>106</sup>.

Because of their basicity and the fact that they possess both lipophilic and hydrophilic moieties, and they have high binding constants for iron metal, amine ligands, and polydentate amines have been used for mobilization and excretion of excess iron in living organisms<sup>94</sup> and for the treatment of iron overload diseases such as Cooley's anaemia<sup>107</sup>. They have also been used to improve the antiarthritic properties of copper<sup>108</sup>.

Again the structural feature of the amine group ( $N-H_x$ ) has been found to be very useful as an active site in many leading compounds, such as chloroquine for treatment or prevention of malaria<sup>109-110</sup>, nevirapine for the treatment of HIV-1 infection and AIDS<sup>111-112</sup>, in pyrazinamide to treat tuberculosis<sup>113</sup>. For the antimalaria compounds such as primaquine and quinacrine it is known that the amine group on the side chain is essential for the effectiveness of the compound, with an amine containing a four carbon atom chain linked to an aromatic ring being a good pharmacophore for anti-malaria agents<sup>114,115</sup>.

Furthermore amine ligands that contain the benzylamine group have been widely used as an important intermediate for the synthesis of antitumor drugs<sup>116,117</sup>.

#### **1.4.1 Spectroscopic properties of amine ligands**

The characterization of amine ligands using infrared spectroscopy has been found to be a very useful approach for analysis and interpretation of coordination compounds for many years<sup>118-122</sup>. The infrared spectra of amines are characterized by the NH absorption band and the position of the absorption band depends on nature of group attached on the nitrogen atom. The secondary amine exhibits an absorption band due to the N-H stretching vibrational mode near  $3420\text{ cm}^{-1}$  and a weak bending absorption at  $1500\text{ to }1600\text{ cm}^{-1}$ . An infrared spectrum of a primary amine is characterized by four absorption bands, two NH stretching (both the asymmetric and symmetric stretches), a NH bending and a rock of the  $NH_2$  group. Two of these absorption bands are found in the region  $3500 - 3300\text{ cm}^{-1}$  and are due to the asymmetric and symmetric stretches. The third absorption band is due to the  $NH_2$  bending and is observed at  $1600\text{ cm}^{-1}$ <sup>123</sup>. The NH rock is found near  $800\text{ cm}^{-1}$ .

The presence of a substituent on the amine ligands may shift the absorption frequency. It has been found that electron-withdrawing groups shift absorption bands to higher frequency while electron donating groups shift the absorption band to the lower frequency region <sup>124-126</sup>.

The electronic spectra of free aromatic amine ligands is characterized by one electronic transition,  $n \rightarrow \sigma^*$  transition. This transition appears in the far ultraviolet region. In most cases this transition may be submerged (or masked) by stronger absorption associated with  $\pi \rightarrow \pi^*$  transitions <sup>129</sup>.

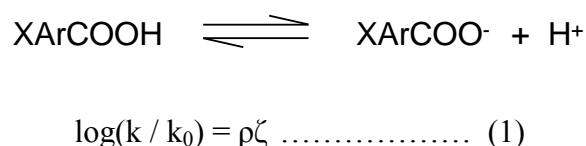
Studies on free amine ligands using <sup>1</sup>H-NMR are of interest, because of the influence of the substituents on the stability and the configuration of these ligands and their complexes. Although the amine ligands are very useful, less attention has been given on the <sup>1</sup>H-NMR chemical shifts of the amino group <sup>130-132</sup>. The <sup>1</sup>H-NMR spectra of amine ligands exhibit a signal due to the chemical shift of NH hydrogen. The signal appears upfield in chloroform solution and the signal of the NH hydrogen varies depending to the solvent used.

## 1.5 Substituent constants

For many years, studies in physical organic chemistry have shown that there are quantitative relationships that exist between the structure of the compounds and their reactivity. It is known that before the 1930s, organic chemists were highly dependent on empirical and qualitative rules, rather than on models to understand these relationships. The earliest, successful and intensively investigated model for the study of these relationships are Linear Free Energy Relationships, which are reported first by Brønsted and Pedersen in 1924 <sup>134</sup>. Linear Free Energy Relationships are a concept that uses mathematic equations to relate observations of one system to observations on other similar systems.

Even though this concept was the first empirical model applicable to study the quantitative relationships, it was not widely recognised until January 1937 when the American Chemical Society published a short paper entitled, “The Effect of Structure upon the Reactions of Organic Compounds”, the author was the physical chemist Louis P. Hammett <sup>135</sup>.

In the paper, Hammett presented equation 1, which describes the influence of the *meta*- or *para*-substituents on the rate constants or equilibrium constants of the side-chain reactions of benzene derivatives, as determined by the ionization of benzoic acid derivatives.



Where symbol  $k$  is a rate or equilibrium constant of ionization for a *meta* or *para* substituted benzoic acid, and  $k_0$  is a rate or equilibrium constant of ionization for unsubstituted benzoic acid in water at 25 °C;  $\zeta$  is the Hammett substituent constant that measures the electronic effect of replacing H by a given substituent in the *meta* or *para* position of the benzoic acid, and it also depends solely on the nature and position of substituent. The reaction constant,  $\rho$  depends on the nature of the reaction, including conditions such as temperature, and it measures the sensitivity of the reaction to the electronic effects of the substituents<sup>136-139</sup>. The ionization of substituted benzoic acid in water at 25 °C was chosen as a standard reaction type for which  $\rho$  is fixed at unity while  $\zeta$  has its value set to zero.

With all these conditions Hammett was able to tabulate positive and negative  $\zeta$  values. A positive  $\zeta$  value for a substituent indicates that the substituent withdraws electrons relative to hydrogen; while substituents with negative  $\zeta$  value repel electrons relative to hydrogen. The Hammett equation is limited only to the *meta* or *para* substituted benzene derivatives, since the *ortho* substituents can give rise to steric interactions which may make the quantitative relationships unreliable. The Hammett  $\zeta$  values indicate the combination of inductive (field) and mesomeric (resonance) effects produced by the withdrawing or donating substituent.

The Hammett methodology was a success in studying and describing the influence of structure on chemical behaviour, but failed in tabulating  $\zeta$  values for some substituents that show a strong interaction between the substituent and the reaction site, such as NO<sub>2</sub> or OH. This has led to the reviewing of the Hammett's equation by severally theoreticians. Jaffe<sup>140</sup>

successfully re-examined Hammett's substituent constants, he recalculated  $\zeta$  values from more recent values of ionization and rate or equilibrium constants obtained for a wide series of reactions. McDaniel and Brown<sup>141</sup> redefined  $\zeta_m$  and  $\zeta_p$  values for the ionization of substituted benzoic acids and suggested that these values be used for substituent constants rather than the mean values derived from all available reactions.

Taft and Lewis<sup>142,143</sup> suggested that the resultant polar effects of substituents on chemical reactivities and physical properties should be quantitatively separated into inductive and resonance effects. Taft's equation is an extension of the Hammett equation, as shown in equation 2.

$$\text{Log}(k / k_0) = \rho_I \zeta_I + \rho_R \zeta_R \dots\dots\dots (2)$$

Here the inductive effect, denoted by  $\zeta_I$ , is assumed to contribute a similar effect for the *meta*- and the *para*-position. The resonance effect is given by  $\zeta_R$  and the contribution for *meta* is different to that of *para*-position. The  $\rho_I$  and  $\rho_R$  are the contribution to the reaction constant due to the substituents.

Swain-Lupton<sup>144</sup> and Yukawa-Tsuno<sup>145</sup> proposed assumptions that were closely related to Taft's. Robert and Moreland<sup>146</sup> extended the approach of Hammett in order to evaluate inductive effects in aliphatic, as oppose in aromatic systems.

The Hammett's structure-reactivity parameters and analogous parameters developed by others have been applied extensively to spectroscopy. Correlation analysis in NMR spectroscopy involves the exploration of the interrelationships between NMR data and molecular parameters, such as transmission of electronic effects of substituents in organic molecules. W. F. Reynolds and his workers were the first people to successfully study electronic effects in conjugated aromatic system using both <sup>1</sup>H- and <sup>13</sup>C-NMR chemical shifts<sup>147,148</sup>. Proton magnetic resonance (PMR or <sup>1</sup>H-NMR) has also been used to show

correlation between substituent constants and the PMR chemical shifts of various protons in organic molecules; for example in the ring protons of substituted phenols <sup>149</sup>, the amino protons of anilines <sup>150</sup>, the carboxylic protons of mono substituted benzoic acids <sup>151</sup> and the ring protons of various pyridines <sup>152</sup>.

Infrared spectroscopy has been applied to substituted aromatic, heterocyclic and aliphatic compounds and correlation made between the frequencies of various ligand vibrations and substituent constants. Correlation analysis studies have shown that there is a linear correlation that exists in the symmetric and asymmetric  $\nu$ N-H of anilines <sup>153</sup> and amines <sup>154</sup>,  $\nu$ C=O of aliphatic ketones <sup>155</sup> and  $\nu$ O-H of phenols <sup>156</sup>, with substituent parameters  $\zeta$  or  $\zeta^*$ .

In coordination chemistry correlation analysis has been used to explore the relationships between  $\nu$ M-L and substituent constants  $\zeta$  or  $\zeta^*$  in metal salicylaldimine complexes <sup>157-159</sup>.

## 1.6 The proposed system of investigation

In an effort to evaluate and identify the electronic effect produced by the substituents within the *para*-substituted Schiff bases and their copper(I)/(II) halide complexes linear correlation analyses were conducted based on Linear Free Energy Relationships. The linear analyses were accomplished by varying the electron donating or withdrawing properties of the substituents and by plotting the experimental spectroscopic data of the *para*-substituted Schiff bases against substituent parameters using *Microsoft Excel*. The experimental data were collected from different spectroscopic techniques including nuclear magnetic resonance, infrared and ultraviolet/visible spectroscopy.

The substituent parameters were chosen in a manner so that overall the electronic effects at *para*-position of the substituted Schiff bases may be monitored. The overall electronic effects of the substituents collectively are composed of both an inductive/field and resonance effect <sup>160, 161</sup>. Inductive effect (I) is an effect that depends only on the nature of the bonds and

the field effect describes a through-space transmission effect, and is denoted by (F).<sup>160</sup> Resonance effects (R), also known as the mesomeric effect, involves the distribution of unshared paired electrons either from or to the substituent<sup>162</sup>.

The electronic effects were expressed in numerical form by calculating correlation coefficients and fitting trend lines using Linear Free Energy Relationships principles, and the classical example is the Hammett equation. The equation describes the combination of inductive and resonance effect produced by the substituent in a benzene ring on the equilibrium constant as described in section 1. To further analyse the effects dual substituent parameters were used. Dual substituent parameter relationships are known to be more beneficial than single substituent parameter relationships, because they offer information on both inductive and resonance effects separately and they are the extension of Hammett equation. For this study the Hammett<sup>163-165</sup>, Swain<sup>166</sup> and Williams & Norrington<sup>167</sup> substituent parameters were used for the investigation of the electronic effects of substituents on Schiff bases, their amine derivatives and their copper complexes.

Table 1.1: Hammett substituent parameters,  $\zeta$

R	Hammett substituent parameter, $\zeta$ <sup>163-165</sup>
4-NO <sub>2</sub>	+0.78
4-Cl	+0.23
4-Br	+0.23
-H	0.00
4-CH <sub>3</sub>	-0.17
4-OCH <sub>3</sub>	-0.27
4-N(CH <sub>3</sub> ) <sub>2</sub>	-0.60

Table 1:2 Values of DSP's for the study

Substituent	Swain <sup>166</sup>		Williams and Norrington <sup>167</sup>	
	S $\zeta_F$	S $\zeta_R$	WN $\zeta_F$	WN $\zeta_R$
R				
4-NO <sub>2</sub>	1.00	1.00	1.109	0.155
4-Cl	0.72	-0.24	0.690	-0.161
4-Br	0.72	-0.24	0.727	-0.176
H	0.00	0.00	0.00	0.00
4-CH <sub>3</sub>	-0.01	-0.41	-0.052	-0.141
4-OCH <sub>3</sub>	0.54	-1.68	0.413	-0.500
4-N(CH <sub>3</sub> ) <sub>2</sub>	0.69	-3.81	0.032	-0.863

The correlation coefficient (r) is a value that provides information on the type of electronic effect produced by the substituent in terms of percentages and it indicates the extent to which the spectroscopic property is influenced by the substituent. It can be equal to or less than one, and can be positive or negative.

The value of r (r =1) implies that a large inductive or resonance effect is more dominating between the substituent and the interaction site or between the substituent and the position of interest within the structure. This also indicates an excellent correlation between substituent parameters and spectroscopic data. A negative correlation (r = -1) indicate a negative correlation between the substituent and the interaction site.

Fitting trend-lines to the resulting data series using *Excel* functions results to a linear plot. The slope of the resultant trend-line is an indication of the extent to which the spectroscopic properties is influenced by the substituent.

## 1.7 References

1. H. Schiff, *Ann. Suppl.*, 1864, **3**, 343-345.
2. X. Zhao, D. K. Song, A. B. Radbil, B. A. Radbil, *Russian J. Appl. Chem.*, 2007, **80**, 1373-1375.
3. Y. K. Agrawal, J. D. Talati, M. D. Shah, M. N. Desai, N. K. Shah, *Corrosion Science*, 2004, **46**, 633-651.
4. P. G. Gozzi, *J. Chem. Soc.*, 2004, **33**, 410-421.
5. R. M. Cender, G. Muller, M. Ordinas, M. A. Maestro, J. Mahia, M. F. Bardia, X. Solans, *J. Chem. Soc., Dalton Trans.*, 2001, 977-985.
6. S. D. Ittel, L. K. Johnson, M. Brookhart, *Chem. Rev.*, 2000, **100**, 1169-1204.
7. B. Milani, G. Mestroni, *Comments Inorg. Chem.*, 1999, **20**, 301-326.
8. A. Murugkar, S. Padhye, S. Guha-Roy, U. Wagh, *Inorg. Chem. Commun.*, 1999, **2**, 545-458.
9. B. Z. Jovanovic, M. Mistic-Vukovic, A.D. Marinkovic, V. Vajs, *J. Mol. Struct.*, 2002, **646**, 113-118.
10. J. E. Robertson, H. J. Biel, T. F. Mitchell, *J. Med. Chem.*, 1963, **6**, 805-807.
11. H. J. Biel, W. K. Hoya, H. A. Leiser, *J. Am. Chem. Soc.*, 1959, **81**, 2527-2532.
12. K. Neuvonen, F. Fulop, H. Neuvonen, A. Koch, E. Kleinpeter, K. Pihlaja, *J. Org. Chem.*, 2002, **68**, 2151-2160.
13. S. V. More, D. V. Dongarkhadekar, R. N. Chavan, W. N. Jadhav, S. R. Bhusare, R. P. Pawar, *J. Indian Chem. Soc.* 2002, **79**, 768-769.
14. K. Vashi, H. B. Naik, *Eur. J. Chem.*, 2004, **1**, 272-276.
15. R. W. Brockman, J. R. Thomson, M. J. Bell, H. E. Skipper, *Cancer Res.*, 1956, **16**,

- 167-170.
16. E. M. Hodnett, W. Willie, *Proc. Okla. Acad. Sci.*, 1966, **46**, 107-111.
  17. A. Iqbal, H. L. Siddiqui, C. M. Ashraf, M. H. Bukhari, C. M. Akram, *Chem. Pharm. Bull.*, 2007, **55**, 1070-1072.
  18. D. Sriram, T. R. Bal, P. Yogeeswari, *J. Pharm. Pharmaceut. Sci.*, 2005, **8**, 565-577.
  19. D. Voet, J. G. Voet, *Biochemistry*, Wiley, New York, 1995.
  20. R. G. Charles, E. P. Riedel, *J. Inorg. Nucl. Chem.*, 1966, **28**, 3005-3018.
  21. B. A. Uzoukwu, P.U. Adiukwu, *Spectrochim. Acta*, 1995, **51**, 2589-2590.
  22. „Vision for the invisible air-craft’, (Science news), August 29, 1987, 1-2.
  23. E. J. Derrah, H. Zhang, L. G. Nikolcheva, S. A. Westcott, *Inorg. Chem. Commun.*, 2003, **6**, 1086-1090.
  24. T. Millward, Honours Project, Rhodes University, 2005.
  25. M.N. Desai, J.D. Talati, N.K. Shah, *Anti-Corrosion Methods and Materials*, 2008, **55**, 27-37.
  26. M.N. Desai, J.D. Talati, N.K. Shah, *Corrosion Science*, 2004, **46**, 633-651.
  27. G. K. Gomma, M. H. Wahdan, *Materials Chemistry and Physics*, 1995, **39**, 209-213.
  28. P. E. Martinez, B. N. Martinez, C. R. de Barbarin, *AZojomo*, 2006, **2**, 1-11.
  29. E. F. Pratt, M. J. Kamlet, *J. Org. Chem.*, 1961, **26**, 4029-4031.
  30. M. S. Newman, *J. Am. Chem. Soc.*, 1950, **72**, 4783-4786.

31. K. D. Karlin, J. Zuieta, *Copper coordination chemistry: biochemical & inorganic perspective*, New York, 1982, 332-366.
32. R. W. Layer, *Chem. Rev.*, 1962, **63**, 489-510.
33. D. J. Curran, S. Siggia, *The chemistry of carbon-nitrogen double bond*, S. Patai (Ed.), Wiley-Interscience, New York, 1970, 162-170.
34. J. Fabian, M. Legrand, *Bull. Soc. Chim. France*, 1956, 1461-1463.
35. M. D. Cohen, G. M. J. Schmidt, S. Flavian, *J. Chem. Soc.*, 1964, 2041-2051.
36. E. Hadjousdis, M. Vittorakis, I. Moustakali-Mavridis, *Tetrahedron*, 1987, **43**, 1345-1360.
37. M. D. Cohen, Y. Hirshberg, G. M. J. Schmidt, *J. Chem. Soc.*, 1964, 2051-2059.
38. M. D. Cohen, Y. Hirshberg, G. M. J. Schmidt, *J. Chem. Soc.*, 1964, 2060-2067.
39. M. Yildiz, Z. Kilic, T. Hokelec, *J. Mol. Struct.*, 1998, **441**, 1-10.
40. Z. Popovic, G. Pavlovic, V. Roje, N. Doslic, D. Matkovic-Calogovic, I. Leban, *J. Struct. Chem.*, 2004, **15**, 587-598.
41. M. Yildiz, H. Unver, D. Erdener, N. Ocak, A. Erdonmez, *Cryst. Res. Technol.*, 2006, **41**, 600-606.
42. H. Unver, D. M. Zengin, K. Guven, *J. Chem. Crystallogr.*, 2000, **30**, 359-364.
43. H. Nazir, M. Yildiz, H. Yilmaz, M. N. Tahir, D. Ylku, *J. Mol. Struct.*, 2000, **524**, 241-250.
44. A. M. Asiri, K. O. Badahdah, *Molecules*, 2007, **12**, 1796-1804.

45. G. O. Dudek, R. H. Holm, *J. Am. Chem. Soc.*, 1962, **84**, 2691-2696.
46. A. D. Marinkovic, N. V. Valentic, D. Z. Mijin, G. G. Uscumlic, B. V. Z. Johavonic, *J. Serb. Chem. Soc.*, 2008, **73**, 513-524.
47. B. Z. Jovanomic, M. Misic-Vukovic, A. D. Marinkovic, V. Vajs, *J. Mol. Struct.*, 1999, **482-483**, 375-378.
48. R. Akaba, K. Tokumaru, T. Kobayashi, C. Utsunomiya, *Bull. Chem. Soc. Jpn.*, 1980, **53**, 2002-2006.
49. P. M. Harrison, R. J. Hoare, *Metals in biochemistry*, New York, Champman & Hall, 1980, 9.
50. E. Ochiai, *Bioinorganic chemistry, an introduction*, Boston, Allyn & Bacon, 1977.
51. R. J. P. Williams, *New trends in bioinorganic chemistry*, J. R. R. F. da Silva (Ed.), Academic Press, New York, 1978, p.59.
52. S. A. K. Wilson, Progressive lenticular degeneration: a familial nervous disease associated with cirrhosis of the liver, *Brains*, 1912, **34**, 295-509.
53. M. Di Donato, B. Sarkar, *Biochimica et Biophysica Acta*, 1997, **1360**, 3-16.
54. R. Allen, *Copper ores*, London, Watson & Viney, 1923, 1.
55. A. Massey, chap 1, in, *Comprehensive inorganic chemistry*, J. C. Bailar, H. J. Emeleus, R. S. Nyholm, A. F. Trotman-Dickinson (Eds.), Pergamon, Oxford, 1973, vol 3, p. 1-3.
56. N. V. Sidwick, *Chemical elements and their compounds*, Clarendon, Oxford, 1942, vol. 1, p. 103.

57. C. K. Jorgenson, *Adsorption spectra and chemical bonding*, Academic Press, London, 1962.
58. C. K. Jorgenson, *Inorganic complexes*, Academic Press, London, 1963.
59. F. A. Cotton, G. Wilkinson, *Advanced inorganic chemistry*, Wiley Interscience, New York, 4<sup>th</sup> edn., 1980.
60. J. E. Huheey, *Inorganic chemistry: principles of structure and reactivity*, Harper International, Cambridge, 3<sup>rd</sup> edn., 1983.
61. B. J. Hathaway, M. Duggan, A. Murphy, J. Mullane, C. Power, A. Walsh, B. Walsh, *Coord. Chem. Rev.*, 1981, **36**, 267-324.
62. W. E. Hartfield, R. Whyman, *Trans. Met. Chem.*, 1969, **47**, 5-9.
63. K. Nakamoto, *Infrared and raman spectra of inorganic and coordination compounds*, Wiley Interscience, New York, 3<sup>rd</sup> edn., 1978.
64. J. Ferguson, *J. Chem. Phys.*, 1964, **40**, 3406-3410.
65. A. G. Karipides, T. S. Piper, *Inorg. Chem.*, 1962, **1**, 970-971.
66. B. Morosin, K. Lawson, *J. Mol. Spec.*, 1964, **12**, 98-178.
67. N. S. Hush, R. J. M. Hobbs, *Prog. Inorg. Chem.*, 1968, **10**, 259-486.
68. P. S. Braterman, *Inorg. Chem.*, 1963, **2**, 448-452.
69. R. L. Harlow, W. J. Wells, G. W. Watt, S. H. Simonsen, *Inorg. Chem.*, 1974, **13**, 2106-2111.
70. P. Cassidy, M. A. Hitchman, *Inorg. Chem.*, 1977, **16**, 1568-1570.

71. E. M. Gouge, J. F. Geldard, E. Sinn, *Inorg. Chem.*, 1980, **19**, 3356-3359.
72. O. R. Rodig, T. Brueckner, B. K. Hurlburt, R. K. Schlatzer, T. L. Venable, E. Sinn, *J. Chem. Soc. Dalton*, 1981, 196-199
73. A. M. Gouge, J. F. Geldard, *Inorg. Chem.*, 1978, **17**, 270-275.
74. A. B. P. Lever, *Inorganic electronic spectroscopy*, 2<sup>nd</sup> edn, Elsevier, New York, 1984.
75. E. L. Simmons, *Coord. Chem. Rev.*, 1974, **14**, 181-196.
76. M. A. Ali and S. E. Livingstone, *Coord. Chem. Rev.*, 1974, **13**, 101-132.
77. C. Battistoni, G. Mattogno, A. Monaci and F. Tarli, *J. Inorg. Nucl. Chem.*, 1971, **33**, 3815-3832.
78. M. A. Ali, D. A. Chowdhury-I and M. N. Uddin, *Polyhedron*, 1984, **3**, 595-598.
79. G. Davies, M. A. El-Sayed, E1-Toukhy and M. Henary, *Inorg. Chim. Acta.*, 1990, **168**, 65-76.
80. L. K. Johnson, C. M. Killian, M. Brookhart, *J. Am. Chem. Soc.*, 1995, **117**, 6414-6415
81. L. Canali, D. C. Sherrington, *Chem. Soc. Rev.*, 1998, **28**, 85-93.
82. A. A. Isse, A. Gennaro, E. Vianello, *J. Electroanal. Chem.*, 1998, **444**, 241-245.
83. D. Pletcher, H. Thompson, *J. Electroanal. Chem.*, 1999, **464**, 168-175.
84. P. H. Aubert, A. Neudeck, L. Dunsch, P. Audebert, P. Capdevielle, M. Maumy, *J. Electroanal. Chem.*, 1999, **470**, 77-88.
85. L. Mao, K. Yamamoto, W. Zhou, L. Jin, *Electroanalysis*, 2000, **12**, 72-75.

86. J. E. Weder, C. T. Dillon, T.W. Hambley, *Coord. Chem. Rev.*, 2002, **232**, 95-126.
87. J. R. J. Sorenson, *Progr. Med. Chem.*, 1989, **26**, 437-568.
88. A. Fini, G. Feroci, G. Fazio, *Euro. J. Pharmaceutical Sciences*, 2001, **13**, 213-217.
89. N. Armaroli, *Chem. Soc. Rev.*, 2001, **30**, 113-124.
90. D. R. McMillan, J. R. Krichhoff, K. V. Goodwin, *Coord. Chem. Rev.*, 1985, **64**, 83-92.
91. K. D. Karlin, Z. Tyeklar, in *„Bioinorganic chemistry of copper’*, Y. Lei, Z. Tyeklar(Eds), London: Champman & Hall, 1993.
92. S. Mahadevan, M. Palaniandavar, *Inorg. Chem.*, 1998, **37**, 693-700.
93. F. Liu, K. A. Meadows, D. R. McMillin, *J. Am. Chem. Soc.*, 1993, **115**, 6699-6704.
94. A. M. Samuni, M. Afeworki, W. Stein, A. T. Yordanov, W. Degraff, M. C. Krishna, J. B. Mitchell, M. W. Brechbiel, *Free Radical Biology & Medicine*, 2001, **30**, 170–177.
95. R. Muller, R. Gust, G. Bernhardt, C. Keller, H. Schonenberger, S. Seeber, R. Osieka, A. Eastman, M. Jennerwein, *J. Cancer Res. Clin. Oncol.*, 1990, **116**, 237-281.
96. M. Peyrone, *Liebigs Ann. Chem.*, 1844, **51**, 1-29.
97. P. J. Dyson, G. Sava, *J. Chem. Soc. Dalton Trans.*, 2006, 1929-33.
98. E.W. Gerner, D.H. Russell, *Cancer Res.*, 1977, **37**, 482-489.
99. A.B. Singh, T.J. Thomas, T. Thomas, T. Thomas, M. Singh, R. A. Mann,

- Cancer Res.*, 1992, **52**, 1840-1847.
100. J.G. Delcros, S. Tomasi, S. Duhieu, M. Foucault, B. Martin, M. Le Roch, J. Renault, P. Uriac, *J. Med. Chem.*, 2006, **49**, 232-245.
101. R.A. Gardner, J.G. Delcros, F. Konate, F. Breitbeil, B. Martin, M. Sigman, M. Huang, *J. Med. Chem.*, 2004, **47**, 6055-6069.
102. M.F. Brana, G. Dominguez, B. Saez, C. Romerdahl, S. Robinson, T. Barlozzari, *Eur. J. Med. Chem.*, 2002, **37**, 541-551.
103. C. Wang, J.G. Delcros, L. Cannon, J. Biggerstaff, *J. Med. Chem.*, 2003, **46**, 5129-5138.
104. Z.D. Xu, M. Wang, S.L. Xiao, M. Yang, *Bioorg. Med. Chem Letter*, 2005, **15**, 3996-4005.
105. T. Takeuchi, *J. Cancer Res. Clin. Oncol.*, 1995, **121**, 505-515.
106. C. Wang, J.G. Delcros, J. Biggerstaff, O. T. Phanstiel, *J. Med. Chem.*, 2003, **46**, 2672-2682.
107. M. A. Esteves, M. C. T. Vaza, M. L. S. Simiies, E. Farkasb, M. A. Santos, *J. Chem. Soc. Dalton Trans.*, 1995, 2565-2573.
108. G. E. Jackson, L. Mkhonto-Gama, A. Voye, M. Kelly, *J. Inorg. Biochem.* 2000, **97**, 147-152.
109. M. O. F. Khan, M. S. Levi, B. L. Tekwani, N. H. Wilson, R. Borne, *Bioorg. Med. Chem.*, 2007, **15**, 3919-3925.

110. P. B. Madrid, N. T. Wilson, J. L. DeRisi, R. K. Guy, *J. Comb. Chem.*, 2004, **6**, 437-442.
111. M. Amacker, N. Ruel, U. Hubscher, S. Spadari, *J. Mol. Bio.*, 1997, **274**, 738-747.
112. K. A. Cohen, J. Hopkins, R. H. Ingraham, C. Pargellis, J. C. Wu, D. E. H. Palladino, P. Kinkade, T. C. Warren, S. Rogers, J. Adams, P. R. Farina, P. M. Grob, *J. Bio. Chem.*, 1991, **266**, 14670-14674.
113. S. Akyuz, *J. Mol. Struct.*, 2003, **651-653**, 541-545.
114. K. Chibale, Barker lecture series, Rhodes University, 2006.
115. C. Biot, B. Pradines, M. Sergeant, J. Gut, P. J. Rosenthal, K. Chibale, *Bioorganic & Medicinal Chemistry Letters*, 2007, **17**, 6434-6438.
116. X.M. Zhou, Z.Q. Wang, J.W. Chang, K. H. Lee, Y. Cheng, H. X. Chen, *J. Med. Chem.*, 1991, **34**, 3346-3350.
117. K. Wakabayashi, H. Miyachi, Y. Hashimoto, *Bioorg. Med. Chem.*, 2005, **13**, 3996-4999.
118. A. E. Ozel, S. Akyuz, J. E. D. Davies, *J. Mol. Struct.*, 1995, **348**, 77-80.
119. S. Rai, K. D. Mandal, *Can. J. Chem.*, 1989, **67**, 239-244.
120. H. Ozeki, K. Okuyama, M. Takahashi, K. Kimura, *J. Phys. Chem.*, 1991, **95**, 4308-4313.
121. E. Rodriguez-Castellon, P. Olivera-Pastor, A. Jimenez-Lopez, P. Maireles-Torres,

- M. J. Hudson, P. Sylvester, *Can. J. Chem.*, 1989, **67**, 2095-2101.
122. E. Akalin, S. Akyzu, *Vib. Spectrosc.*, 2000, **22**, 3-10.
123. P. J. Kruger, D. W. Smith, *Can. J. Chem.*, 1967, **45**, 1611-1618.
124. A. M. Buswell, J. R. Downing, W. H. Rodebush, *J. Am. Chem. Soc.*, 1939, **61**,  
3252-3256.
125. S. F. Mason, *J. Chem. Soc.*, 1959, 1281-1288.
127. A. Bryson, *J. Am. Chem. Soc.*, 1960, **82**, 4862-4871.
128. T. Orville, *J. Chem. Soc.*, 1968, 1048-1052.
129. S. Patai, *The chemistry of carbon-nitrogen double bond*, ed. S. Patai,  
Wiley-Interscience, New York, 1970, 187-189.
130. E. A. Basso, G. F. Gauze, R. J. Abraham, *Magn. Reson. Chem.*, 2007, **45**, 749-757.
131. I. Alkorta, J. Elguero, *J. Magn. Reson. Chem.*, 2004, **42**, 955-961.
132. M. A. Warne, L. Griffiths, *J. Chem. Soc., Perkin Trans*, 1997, **2**, 203-207.
133. F. D. Rochon, C. Bonnier, *Inorganic Chimica Acta*, 2007, **360**, 461-472.
134. J. N. Bronsted, K. Pedersen, *J. Phys. Chem.*, 1924, **108**, 185-188.
135. L. P. Hammett, *J. Am. Chem. Soc.*, 1937, **59**, 96-103.
136. S. G. Williams, F. E. Norrington, *J. Am. Chem. Soc.*, 1976, **98**, 508-516.
137. K. Sung, *J. Org. Chem.*, 1999, **64**, 8984-8989.
138. J. Shorter, *J. Chem. Listy*, 2000, **94**, 210-214.

139. R. W. Taft, *J. Am. Chem. Soc.*, 1953, **75**, 4231-4238.
140. H. H. Jaffe, *J. Am. Chem. Soc.*, 1954, **76**, 5843-5846.
141. D. H. McDaniel, H. C. Brown, *J. Org. Chem.*, 1958, **23**, 420-427.
142. R. W. Taft, I. C. Lewis, *J. Am. Chem. Soc.*, 1958, **80**, 2436-2443.
143. R. W. Taft, I. C. Lewis, *J. Am. Chem. Soc.*, 1959, **81**, 5343-5352.
144. C. G. Swain, E. C. Lupton, *J. Am. Chem. Soc.*, 1968, **90**, 4328-4337.
145. Y. Yukawa, Y. Tsuno, M. Swada, *Bull. Chem. Soc. Jpn.*, 1966, **39**, 2274-2284.
146. J. D. Rorbert, W. T. Moreland, *J. Chem. Soc.*, 1953, **75**, 2167-2173.
147. G. K. Hamer, I. R. Peat, W. F. Reynolds, *Can. J. Chem.*, 1973, **51**, 897-915.
148. D.A. Dawson, G. K. Hamer, W. F. Reynolds, *Can. J. Chem.*, 1974, **52**, 39-45.
149. W. G. Paterson, N. R. Tipman, *Can. J. Chem.*, 1962, **40**, 2122-2125.
150. L. K. Dyall, *Austr. J. Chem.*, 1964, **17**, 419-27.
151. Y. Kondo, K. Kondo, T. Takemoto, T. Ikenoue, *Chem. Pharm. Bull., Jpn*, 1966, **14**,  
1322-1328.
152. J. M. Haigh, D. A. Thornton, *Tetrahedron Letters*, 1970, 2043.
153. R. W. Taft, Jr., I. W. Lewis, *J. Am. Chem. Soc.*, 1958, **80**, 2436-43.
154. P. J. Krueger, D. W. Smith, *Can. J. Chem.*, 1967, **45**, 1605-1610.

155. C. G. Swain, E. C Lupton, *J. Am. Chem. Soc.*, 1968, **90**, 4328-37.
156. P. J. Krueger, H. W. Thompson, *Proc. Roy. Soc.*, 1957, **234A**, 143-148.
157. H. W. Thomson, *Spectrochim. Acta*, 1958, **13**, 236-47.
158. P. J. Stone, H. W. Thomson, *Spectrochim. Acta*, 1957, **10**, 17-20
159. G. C. Percy, D. A. Thornton, *J. Inorg. Nucl. Chem.*, 1972, **34**, 3357-3367.
160. C. Hansch, A. Leo, R. W. Taft, *Chem. Rev.*, 1991, **91**, 165-195
161. K. Sung, *J. Org. Chem.*, 1999, **64**, 8984-8989.
162. J. McMurry, *Fundamental of organic chemistry*, 5<sup>th</sup> ed., Thomson-Brook/Cole, Australia, 2003.
163. D. F. Church, G. J. Gleicher, *J. Org. Chem.*, 1975, **40**, 536-537.
164. G. Medina, PhD Thesis, Rhodes University, Grahamstown, 2004.
165. D. L. Johnston, I. Bertini, W. D. Horrocks, *J. Inorg. Chem.*, 1971, **10**, 865-868.
166. C. G. Swain, S. H. Unger, N. R. Rosenquist, M. S. Swain, *J. Am. Chem. Soc.*, 1983, **105**, 492-502.
167. S. G. Williams, F. E. Norrington, *J. Am. Chem. Soc.*, 1976, **98**, 508-516.

## **2. EXPERIMENTAL**

### **2.1 Physical methods**

#### **2.1.1 Mid infrared spectroscopy (MIR)**

The mid infrared spectra were recorded on a Perkin-Elmer spectrum 2000 FT-IR spectrometer equipped with a KBr beam splitter and a DTG detector, in a region 4000 – 400  $\text{cm}^{-1}$ , with typically 16 scans at an average resolution of 4  $\text{cm}^{-1}$ . Samples were run in a KBr disc.

#### **2.1.2 Nuclear magnetic resonance (NMR)**

$^1\text{H}$  and  $^{13}\text{C}$ -NMR spectra were obtained on an Avance Bruker AMX 400 MHz spectrometer. All samples were prepared using deuterated solvents. Chemical shifts are reported in parts per million (ppm) relative to an internal standard tetramethylsilane (TMS).

#### **2.1.3 Mass spectrometry**

Mass spectrometry: Finnigan Mat LCQ, was performed by the Rhodes University Mass Spectrometry Unit. Both the Electrospray mass spectrometry and Atmospheric Pressure Chemical Ionization were used for mass analysis of the compounds.

##### **2.1.3.1 Electrospray ionization mass spectrometry (ESI-MS)**

The interface parameters for electrospray mass spectrometry were set as follows: sheath gas flow rate, 40 psi, auxiliary gas flow rate, 20 units; capillary temperature, 220  $^{\circ}\text{C}$ ; the solutions of the compounds were directly infused with a 250  $\mu\text{L}$  unimetrics at a flow rate of 8.00  $\mu\text{l}/\text{min}$ .

### **2.1.3.2 Atmospheric pressure chemical ionization mass spectrometry (APCI-MS)**

Solutions of the compounds were directly infused with a 250  $\mu$ L unimetrics at a flow rate of 8.00  $\mu$ l/min and the interface parameters were set as follows: sheath gas flow rate, 40 psi, auxiliary gas flow rate, 0; capillary temperature, 150  $^{\circ}$ C.

### **2.1.4 Electronic spectra (UV/vis solution)**

Electronic spectra were recorded on a Varian Cary 500 spectrophotometer. The spectra for the ligands and the complexes were recorded in solution.

### **2.1.5 Microanalyses**

Combustion microanalyses for carbon, hydrogen and nitrogen were performed on Virio Elementar EL111 CHNS Analyzer, (Rhodes University, South Africa) or were obtained from the University of Cape Town, South Africa, with a Fisons Elemental Analyzer 1108 CHNS-O.

### **2.1.6 Melting point**

All melting points were determined using a Gallenkamp melting point apparatus. The results were uncorrected.

### **2.1.7 Thin-layer chromatography (TLC)**

Thin-layer chromatography was performed on silica gel sheets 60F254 (Merck, Darmstadt). The purity of Schiff bases were confirmed by TLC in a mixture of suitable polar or non-polar solvents. The polar solvents used for separation were ethanol and methanol. Ethyl acetate, and hexane and chloroform were used.

## 2.2 Reagents and instrumentation

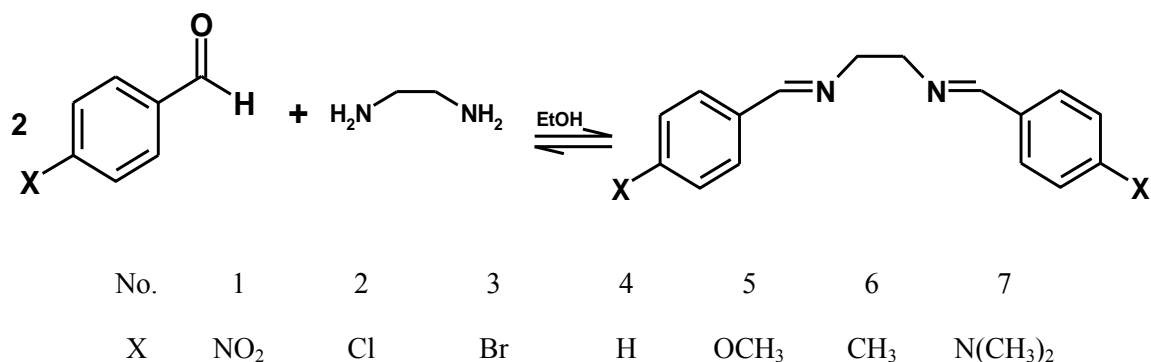
All chemicals and reagents used for the preparation of ligands and complexes were commercial products (Sigma–Aldrich) and used as received unless otherwise noted. Ethylenediamine was distilled over potassium hydroxide under nitrogen and trans-cinnamaldehyde was distilled from anhydrous sodium sulphate before use. The solvents were dried and distilled before use according to the standard procedures <sup>1</sup>.

## 2.3 Synthetic methods

### 2.3.1 Synthesis of N, N'-(aryl)benzylidene ligands

The Schiff bases were synthesized according to a well-established synthetic procedure <sup>2</sup> which involved the condensation of benzaldehyde or its derivatives with the ethylenediamine in 95 % ethanol, as shown in scheme 2.1. The synthetic scheme in the figure below presents the various Schiff base ligands that were synthesized for the study.

For the synthesis of all the Schiff bases, a 1:2 ratio of amine to aldehyde was used. The Schiff bases were obtained as solid precipitates. Upon recrystallization of the compounds from suitable solvents, clean compounds were obtained and their microanalyses are reported in table 3.1.



**Scheme 2.1** The *para*-substituted benzylideneethylenediamine ligands (**R-BEN**) employed in the study

### 2.3.1.1 Preparation of N, N'-bis(4-nitrobenzyl)ethylenediimine

Ethylenediamine (1.4646 g, 24.4 mmol) in 20 mL ethanol was added drop-wise to an ethanolic solution of 4-nitrobenzaldehyde (7.3643 g, 48.7 mmol). The mixture was refluxed for 2 hours. The resulting diimine precipitated as a yellow-pink solid. The crude solid was filtered off and washed with ethanol. The Schiff base was then recrystallized from hot ethanol to remove impurities and was left in the fume-hood to evaporate slowly. The product precipitated out as light peach fine crystals. The Schiff base was filtered and washed with cold ethanol (3 x 10 mL). The resulting product was dried at room temperature for 48 hours. The purity was confirmed by TLC in chloroform – ethanol (4: 1). The physical data are reported in table 3.1.

### 2.3.1.2 Preparation of N, N'-bis(4-chlorobenzyl)ethylenediimine

Ethylenediamine (1.5650 g, 26.0 mmol) in 20 mL ethanol was added drop-wise to an ethanolic solution of 4-chlorobenzaldehyde (7.320 g, 52.0 mmol). The mixture was refluxed for 2 hours. The resulting diimine precipitated as a white solid. The crude solid was filtered off and washed with methanol. The Schiff base was then recrystallized from hot ethanol to remove impurities and was left in the fume-hood to evaporate slowly. The product precipitated out as shiny white crystals which were collected and washed with cold ethanol

(3 x 10 mL). The shiny white crystals were dried at room temperature for 48 hours. The purity was confirmed by TLC in chloroform – methanol (3:1). The physical data are reported in table 3.1.

#### **2.3.1.3 Preparation of N, N'-bis(4-bromobenzyl)ethylenediimine**

Ethylenediamine (1.2138g, 20.2mmol) in 20 mL ethanol was added drop-wise to an ethanolic solution of 4-bromobenzaldehyde (7.4739 g, 40.4 mmol). The mixture was refluxed for 2 hours. The resulting diimine precipitated as white crystals. The product was filtered off and washed with cold methanol (3 x 10 mL) to remove excess 4-bromobenzaldehyde. The resulting Schiff base was dried at room temperature for 48 hours. The purity was confirmed by TLC in chloroform – methanol (3: 1). The physical data are reported in table 3.1.

#### **2.3.1.4 Preparation of N, N'-bis(benzyl)ethylenediimine**

Ethylenediamine (2.0170 g, 33.6 mmol) in 20 mL ethanol was added drop-wise to an ethanolic solution of benzaldehyde (7.1248 g, 67.1 mmol). The mixture was refluxed for 20 hours. The volume was reduced using a Rotavapour until yellow oil remained. The resulting diimine was precipitated out by adding hexane in a drop-wise manner with constant stirring. After the addition of about 15 mL hexane, a yellow precipitate formed. The resulting Schiff base was filtered and then recrystallised from hot hexane to remove the impurities and was left in the fume hood to evaporate slowly. The yellow crystals were filtered and dried at room temperature for 48 hours. The purity was confirmed by TLC in ethyl acetate – hexane (4: 1). The physical data are reported in table 3.1.

#### **2.3.1.5 Preparation of N, N'-bis(4-methylbenzyl)ethylenediimine**

Ethylenediamine (1.8048 g, 30.0 mmol) in 20 mL ethanol was added drop-wise to an ethanolic solution of p-methoxybenzaldehyde (7.2169 g, 60.1 mmol). The mixture was refluxed for 2 hours. The resulting diimine precipitated as white crystals. The crude solid was filtered off and washed with methanol. The Schiff base was then recrystallized from hot methanol to remove impurities. The filtrate was left in the fume-hood to evaporate slowly.

The product precipitated out as light yellow crystals which were collected and washed with cold methanol (3 x 10 mL). The light yellow crystals were dried at room temperature for 48 hours. The purity was confirmed by TLC in chloroform – ethanol (4: 1). The physical data are reported in table 3.1.

#### **2.3.1.6 Preparation of N, N'-bis(4-methoxybenzyl)ethylenediimine**

Ethylenediamine (1.6113 g, 26.8 mmol) in 20 mL ethanol was added drop-wise to an ethanolic solution of p-methoxybenzaldehyde (7.301 g, 53.6 mmol). The mixture was refluxed for 2 hours. The resulting diimine precipitated as a yellow solid. The crude solid was filtered off and washed with methanol. The Schiff base was then recrystallized from hot ethanol to remove impurities and was left in the fume-hood to evaporate slowly. The product precipitated out as light yellow crystals which were collected and washed with cold ethanol (3 x 10 mL). The Schiff base was dried at room temperature for 48 hours. The purity was confirmed by TLC in chloroform – methanol (3: 1). The physical data are reported in table 3.1.

#### **2.3.1.7 Preparation of N, N'-bis(4-dimethylaminobenzyl)ethylenediimine**

Ethylenediamine (1.4818 g, 24.7 mmol) in 20 mL ethanol was added drop-wise to an ethanolic solution of 4-dimethylaminobenzaldehyde (7.3574 g, 49.3 mmol). The mixture was refluxed for 2 hours. The reaction mixture was allowed to cool to room temperature. The resulting diimine precipitated as a yellow solid. The crude solid was filtered off and washed with methanol. The Schiff base was then recrystallized from hot chloroform to remove insoluble impurities and was left in the fume-hood to evaporate slowly. The product precipitated out as a light yellow solid which was collected and washed with anhydrous cold methanol (3 x 10 mL) until the wash was no longer coloured dark red due to the unreacted starting material. The fine light yellow crystals were filtered and dried at room temperature for 48 hours. The purity was confirmed by TLC in ethyl acetate – hexane (4: 1). The physical data are reported in table 3.1.

### 2.3.1.8 Attempted preparation of N, N'-bis(4-dihydroxybenzyl)ethylenediimine

For the preparation of N, N'-bis(4-dihydroxybenzyl)ethylenediimine three methods<sup>3-4</sup> were used in an attempt to obtain the Schiff base. All three methods were unsuccessful. One problem associated with the synthesis of this Schiff base is that it suffers a degree of hydrolysis. This is because the hydroxyl substituent at the para position of the 4-hydroxybenzaldehyde is more acidic, instead of the formation of iminic bond the hydroxyl substituent acts as acid, in which it breaks the azomethine bond and resulting in the undesired product.

#### 2.3.1.8.1 Method 1

To 7.2783 g (59.6 mmol) of 4-hydroxybenzaldehyde in 10 mL ethanol, was added drop-wise a 15 mL ethanolic solution of ethylenediamine (1.7909 g, 29.8 mmol). To this reaction mixture a quantity of silica (0.1120 g, 1.9 mmol) was added. The mixture was placed under ultrasound irradiation for an hour. The resulting product precipitated as a brown solid. The crude solid was filtered off and washed with ethanol. The product was then recrystallized from hot ethanol to remove impurities and was left in the fume-hood to evaporate slowly. The product precipitated out as light yellow crystals which are collected and washed with ethanol and left to dry out.

#### 2.3.1.8.2 Method 2

In this method, a solvent free synthesis was used for the preparation of N, N'-bis(4-hydroxybenzylideneamino)ethane. A 1:2 molar ratio of amine to aldehyde was used. Both the (0.9104 g, 7.5 mmol) 4-hydroxybenzaldehyde and (0.2240 g, 3.7 mmol) of ethylenediamine were mixed together through grinding until a melt product was formed. The resulting product was allowed to dry in the fume hood for 24 hours. The solidified melt was recrystallized from hot ethanol.

### 2.3.1.8.3 Method 3

The procedure for method 3 is similar to that used for the synthesis of N, N'-bis(benzyl)ethylenediimine, but a two fold excess of sodium hydroxide (0.1600 g, 4.0 mmol) was added to the ethanolic solution (10 mL) of 4-hydroxybenzaldehyde (0.4550 g, 4.0 mmol). The solution mixture was stirred at room temperature until the base dissolved completely. 0.1335 g of ethylenediamine in 20 ml ethanol was added drop-wise to the solution mixture. The mixture was refluxed for 2 hours. The resulting brown solution was acidified with methanolic hydrochloric acid (8.33 M) to remove the sodium and to precipitate the Schiff base.

### 2.3.2 Synthesis of N, N'-(aryl)benzyaldiamine dihydrochloride salt

The synthesis of *para*-substituted benzyethylenediamine dihydrochloride ligands, involved two separate reaction steps. The first step required the reduction<sup>5</sup> of Schiff bases with a five-fold molar excess of solid sodium borohydride in dry methanol. The second step involved the protonation of the amine ligands with concentrated methanolic hydrochloric acid (8.33 M) in methanol medium or 0.1 M of hydrochloric acid of pH=1 in an acetone medium. The concentrated methanolic hydrochloric acid solution was prepared in a similar manner to the preparation described by Sanches-Silva<sup>6</sup> and Taber.<sup>7</sup>

#### 2.3.2.1 Preparation of Methanolic HCl

A separating funnel with 50 mL of concentrated sulphuric acid was inserted, through a glass adaptor, into a 250 ml round bottom flask with 40.0 g of sodium chloride. By drop-wise addition of concentrated sulphuric acid into the sodium chloride, HCl gas was produced and it was transferred into a 250 mL round bottom flask containing methanol (100 mL). The concentration of the resulting solution was determine by potentiometric titration against silver nitrate solution using silver titrate and working electrode. The concentration was found to be 8.33 M methanolic HCl solution.

### 2.3.2.2 Preparation of N, N'-bis(4-nitrobenzyl)ethylenediamine dihydrochloride

To a solution of N, N'-bis(4-nitrobenzyl)ethylenediimine (0.1363 g, 0.4 mmol) in 10 ml methanol was slowly added a five-fold molar excess of solid sodium borohydride (0.07902 g, 2.1 mmol). After which the reaction mixture was refluxed for 3 hours. The solvent was distilled off. Then, 20 ml of cold water was added to the reaction mixture to liberate the secondary amine. The white product was then extracted with chloroform (4 x 20 ml). The combined extracts were washed with water and dried over anhydrous sodium sulphate. The solvent was removed by a Rotavapour and an oily product was obtained.

N, N'-bis(4-nitrobenzyl)ethylenediamine dihydrochloride salt was prepared by diluting 0.2272 g (0.7 mmol) in 200 mL of acetone. The solution was filtered and allowed to cool down to room temperature. The resulting colourless filtrate was acidified with hydrochloric acid (0.1 M = 15 mL) until pH = 1. During the course of the addition of acid, a fine white crystalline powder precipitated. After the addition of hydrochloric acid, the solution mixture was allowed to stir at room temperature for 1 hour. The resulting fine amine salt was filtered washed with cold acetone (3 x 10 mL) and dried at room temperature for 48 hours. The physical data are given in table 3.2.

### 2.3.2.3 Preparation of N, N'-bis(4-chlorobenzyl)ethylenediamine dihydrochloride

To a solution of N, N'-bis(4-chlorobenzyl)ethylenediimine (2.2909 g, 7.5 mmol) in 10ml methanol was slowly added a five-fold molar excess of solid sodium borohydride (1.4195 g 37.5 mmol). After which the reaction mixture was refluxed for 3 hours. The solvent was distilled off. Then, 20 ml of cold was added to the reaction mixture to liberate the secondary amine. The white product was then extracted with chloroform (4 x 20 ml). The combined extracts were washed with water and dried over anhydrous sodium sulphate. The solvent was removed by a Rotavapour and an oily product was obtained.

N, N'-bis(4-chlorobenzyl)ethylenediamine dihydrochloride was prepared by diluting 0.7125g (2.30 mmol) of N, N'-bis(4-chlorobenzyl)ethylenediamine in 150 mL of acetone. The solution was filtered and allowed to cool down to room temperature. The resulting colourless filtrate was acidified with hydrochloric acid (0.1 M = 15 mL) until pH = 1. During the course of the addition of acid, a fine white crystalline powder precipitated. After the addition of hydrochloric acid, the solution mixture was allowed to stir at room temperature for 1 hour. The resulting fine amine salt was filtered washed with cold acetone (3 x 10 mL) and dried at room temperature for 48 hours. The physical data are given in table 3.2.

#### **2.3.2.4 Preparation of N, N'-bis(4-bromobenzyl)ethylenediamine dihydrochloride**

To a solution of N, N'-bis(4-bromobenzyl)ethylenediamine (3.0 g, 7.6 mmol) in 10 ml methanol was slowly added a five-fold molar excess of solid sodium borohydride (1.4326 g, 37.9 mmol). After which the reaction mixture was refluxed for 3 hours. The solvent was distilled off. Then, 20 ml of cold water was added to the reaction mixture to liberate the secondary amine. The white product was then extracted with chloroform (4 x 20 ml). The combined extracts were washed with water and dried over anhydrous sodium sulphate. The solvent was removed by a Rotavapour and a yellow oily product obtained.

N, N'-bis(4-bromobenzyl)ethylenediamine dihydrochloride salt was prepared by diluting 1.0558g (2.7 mmol) of N, N'-bis(4-bromobenzyl)ethylenediamine in 250 mL of acetone. The solution was filtered and allowed to cool down to room temperature. The resulting filtrate was acidified with hydrochloric acid (0.1 M = 15 mL) until pH = 1. During the course of the addition of acid, a fine white crystalline powder precipitated. After the addition of hydrochloric acid, the solution mixture was allowed to stir at room temperature for 1 hour. The resulting fine amine salt was filtered, washed with cold acetone (3 x 10 mL) and dried at room temperature for 48 hours. The physical data are given in table 3.2.

### 2.3.2.5 Preparation of N, N'-bis(benzyl)ethylenediamine dihydrochloride

To a solution of the N, N'-bis(benzyl)ethylenediimine (1.6190 g, 6.8 mmol) in 15 ml methanol was slowly added a five-fold molar excess of solid sodium borohydride (1.2850 g, 34.0 mmol), after which the reaction mixture was refluxed for 3 hours. The solvent was distilled off. Then, 20 ml of cold water was added to the reaction mixture to liberate the secondary amine. The colourless product was then extracted with chloroform (3 x 20 mL). The combined extracts were washed with water and dried over anhydrous sodium sulphate. The solvent was removed by a Rotavapour and an oily product was obtained.

N, N'-bis(benzyl)ethylenediamine dihydrochloride salt was prepared by diluting N, N'-bis(benzyl)ethylenediamine (0.1716g, 1.75 mmol) in 150 mL of acetone. The solution was filtered and allowed to cool down to room temperature. The resulting colourless filtrate was acidified with hydrochloric acid (0.1 M = 15 mL) until pH = 1. During the course of the addition of acid, a fine white crystalline powder precipitated. After the addition of hydrochloric acid, the solution mixture was allowed to stir at room temperature for 1 hour. The resulting fine amine salt was filtered, washed with cold acetone (3 x 10 mL) and dried at room temperature for 48 hours. The physical data are given in table 3.2.

### 2.3.2.6 Preparation N, N'-bis(4-methylbenzyl)ethylenediamine dihydrochloride

To a solution of N, N'-bis(4-methylbenzyl)ethylenediimine (2.4256 g, 9.8 mmol) in 10 ml methanol was slowly added a five-fold molar excess of solid sodium borohydride (1.8624 g 49.3 mmol). The reaction mixture was then refluxed for 3 hours. The solvent was distilled off. Then, 20 ml of cold water was added to the reaction mixture to liberate the secondary amine. The white product was extracted with chloroform (4 x 20 ml). The combined extracts were washed with water and dried over anhydrous sodium sulphate. The solvent was removed by a Rotavapour and an oily product was obtained.

N, N'-bis(4-methylbenzyl)ethylenediamine dihydrochloride salt was prepared by dissolving 0.3468 g (1.3 mmol) of N, N'-bis(4-methylbenzyl)ethylenediamine in cold absolute methanol

(15 mL). The resulting solution was stirred for 30 min and then was filtered off. The filtrate was acidified with methanolic hydrochloric acid (8.33 M) until pH = 1. The solution was allowed to stir at room temperature for 1 hour, resulting in a fine white precipitate. The precipitate was filtered, washed with methanol (2 x 10 ml) and dried at room temperature. The salt was ground to a fine powder and then taken up in minimum amount of cold water, filtered and reprecipitated by evaporation of the solvent in the fume-hood. The precipitate was recrystallized again in warm acetone/ethanol and placed in the cold (5 °C) to form a crystalline solid. The physical data are given in table 3.2.

### 2.3.2.7 Preparation of N, N'-bis(4-methoxybenzyl)ethylenediamine dihydrochloride

To a solution of N, N'-bis(4-methoxybenzyl)ethylenediimine (2.3164 g, 7.8 mmol) in 10 ml methanol was slowly added a five-fold molar excess of solid sodium borohydride (1.4785g, 39.1 mmol). After which the reaction mixture was refluxed for 3 hours. The solvent was distilled off. Then, 20 ml of cold water was added to the reaction mixture to liberate the secondary amine. The white product was extracted with chloroform (4 x 20 ml). The combined extracts were washed with water and dried over anhydrous sodium sulphate. The solvent was removed by a Rotavapour and an oily product was obtained.

N, N'-bis(4-methoxybenzyl)ethylenediamine dihydrochloride salt was prepared by dissolving 0.5106g (1.7 mmol) of N, N'-bis(4-methoxybenzyl)ethylenediamine in 150 mL of acetone. The light yellow solution was filtered and allowed to cool down to room temperature. The resulting colourless filtrate was acidified with hydrochloric acid (0.1 M = 15 mL) until pH = 1. During the course of the addition of acid, a fine white crystalline powder precipitated. After the addition of hydrochloric acid, the solution mixture was allowed to stir at room temperature for 1 hour. The resulting fine amine salt was filtered, washed with cold acetone (3 x 10 mL) and dried at room temperature for 48 hours. The physical data are given in table 3.2.

### 2.3.2.8 Attempted preparation of N, N'-bis(4-dimethylaminobenzyl)ethylenediamine dihydrochloride

To a solution of N, N'-bis(4-dimethylaminobenzyl)ethylenediamine (1.0 g, 3.1 mmol) in 10 ml methanol was slowly added a five-fold molar excess of solid sodium borohydride (0.5830 g, 15.4 mmol). After which the reaction mixture was refluxed for 3 hours. The solvent was distilled off. Then, 20 ml of cold water was added to the reaction mixture to liberate the secondary amine. The white product was then extracted with chloroform (4 x 20 ml). The combined extracts were washed with water and dried over anhydrous sodium sulphate. The solvent was removed by a Rotavapour and an oily product was obtained.

The hydrochloride salt was prepared by adding the oily product 0.5137g (1.6 mmol) in cold absolute methanol (15 mL). The resulting solution was stirred for 30 min and then was filtered. The filtrate was acidified with methanolic hydrochloric acid (8.33 M) until pH = 1. The solution was allowed to stir at room temperature for 1 hour, resulting in a fine white precipitate. The precipitate was filtered, washed with methanol (2 x 10 ml) and dried at room temperature. The product was ground to a fine powder and then taken up in minimum amount of cold water, filtered and reprecipitated by evaporation of the solvent in the fume-hood. The precipitate was recrystallized again in warm acetone/ethanol and placed in the cold (5 °C) to form dark brown precipitate. Unfortunately the compound was not the desired product. This was confirmed by microanalysis.

### 2.3.3 Synthesis of N, N'-(aryl)benzaldiamine ligands

For the synthesis of the free *para*-substituted benzaldiamine ligands, a two-fold molar excess sodium acetate was used to ensure a complete stripping of the two molar ratio of hydrochloride acid from the N, N'(aryl)benzaldiamine dihydrochloride ligand and the procedure is illustrated using N, N'-bis(4-chlorobenzyl)ethylenediamine dihydrochloride and ethanol as solvent. For some of the diamines methanol was employed (see table 3.3). The physical data of the ligands are given in table 3.3. Since the preparation of N, N'-bis(4-dimethylaminobenzyl)ethylenediamine dihydrochloride salt was unsuccessful, the amine of

this was obtained directly from the reduced N, N'-bis(4-dimethylaminobenzyl)ethylenediamine, by the recrystallization method (2.3.3.2).

### 2.3.3.1 Preparation of N, N'-bis(benzyl)ethylenediamine ligand

A two-fold molar methanolic (5 ml) solution of (0.1551 g, 2.3 mmol) sodium acetate was added to a stirred methanolic (15 ml) solution of (0.4355 g, 1.1 mmol) N, N'-bis(benzyl)ethylenediamine dihydrochloride salt at -10 °C. The resulting light yellow mixture was stirred for 2 hours in ice-bath; then brought to stir for 30 min at room temperature. The resulting white precipitate was filtered off. The volume of the methanol from the filtrate was reduced by rotator evaporation until an oily precipitate remained. The oily product was then dissolved in chloroform (12 ml), followed by drying over anhydrous sodium sulphate. The solvent was then reduced by rotator evaporation and an oily product was obtained. The resulting amine was dried at room temperature for 3 days. The compounds were obtained as an oily form and are quite air stable.

### 2.3.3.2 Preparation of N, N'-bis(4-dimethylaminobenzyl)ethylenediamine

Since the attempted formation of the salt was unsuccessful, the amine ligand was prepared by recrystallizing 0.8 g of N,N'-bis(4-dimethylaminobenzyl)ethylenediamine from hot dichloromethane. The physical data of the ligand is given in table 3.3.

## 2.3.4 Synthesis of copper(II) halide complexes derived from

### N, N'-(aryl)benzyldiamine ligands

For the synthesis of Cu(R-BENH)Br<sub>2</sub> and Cu(R-BENH)Cl<sub>2</sub>, cupric chloride dihydrate {(Cu(II)Cl<sub>2</sub>.2H<sub>2</sub>O)} and anhydrous copper(II) bromide {(Cu(II)Br<sub>2</sub>)} were used. The synthesis procedure is generally common for all the complexes. The metal and amine ligand were reacted on a 1:1 basis in dry ethanol. The reactions were carried out at room temperature.

### 2.3.4.1 Synthesis of the copper bromide complexes

#### 2.3.4.1.1 Preparation of Cu(NO<sub>2</sub>-BENH)Br<sub>2</sub>, (1B)

A solution of N, N'-bis(4-nitrobenzyl)ethylenediamine (0.0252 g, 0.08 mmol) in ethanol (8 mL) was added drop-wise to a warm stirred solution of (0.0188 g, 0.08 mmol) copper(II) bromide in ethanol (10 mL). The drop-wise addition of N, N'-bis(4-nitrobenzyl)ethylenediamine resulted in a formation of fine green crystals of the product. The reaction mixture was stirred at room temperature for 30 min. The product was filtered, and washed with cold ethanol. The product was dried at room temperature for 2 days. The purity of the isolated complex was checked by elemental analysis, and the physical data are given in table 3.4.

#### 2.3.4.1.2 Preparation of Cu(Cl-BENH)Br<sub>2</sub>, (2B)

A solution of N, N'-bis(4-chlorobenzyl)ethylenediamine (0.0064 g, 0.02 mmol) in ethanol (8 mL) was added drop-wise to a warm stirred solution of (0.0461 g, 0.02 mmol) copper(II) bromide in ethanol (10 mL). The drop-wise addition of N, N'-bis(4-chlorobenzyl)ethylenediamine resulted in a formation of fine green crystals of the product. The reaction mixture was stirred at room temperature for 30 min. The product was filtered and washed with cold ethanol. The product was dried at room temperature for 2 days. The purity of the isolated complex was checked by elemental analysis, and the physical data are given in table 3.4.

#### 2.3.4.1.3 Preparation of Cu(Br-BENH)Br<sub>2</sub>, (3B)

A solution of N, N'-bis(4-bromobenzyl)ethylenediamine (0.0347 g, 0.09 mmol) in ethanol (8 mL) was added drop-wise to a warm stirred solution of (0.0194 g, 0.09 mmol) copper(II) bromide in ethanol (10 mL). The drop-wise addition of N, N'-bis(4-bromobenzyl)ethylenediamine resulted in a formation of fine green crystals of the product.

The reaction mixture was stirred at room temperature for 30 min. The product was filtered and washed with cold ethanol. The product was dried at room temperature for 2 days. The purity of the isolated complex was checked by elemental analysis, and the physical data are given in table 3.4.

#### **2.3.4.1.4 Preparation of Cu(H-BENH)Br<sub>2</sub>, (4B)**

A solution of N, N'-di(benzyl)ethylenediamine (0.0406 g, 0.2 mmol) in ethanol (8 mL) was added drop-wise to a warm stirred solution of (0.0378 g, 0.2 mmol) copper(II) bromide in ethanol (10 mL). The drop-wise addition of the ligand resulted in a formation of fine green crystals of the product. The reaction mixture was stirred at room temperature for 30 min. The product was filtered and washed with cold ethanol. The product was dried at room temperature for 2 days. The purity of the isolated complex was checked by elemental analysis, and the physical data are given in table 3.4.

#### **2.3.4.1.5 Preparation of Cu(CH<sub>3</sub>-BENH)Br<sub>2</sub>, (5B)**

A solution of N, N'-bis(4-methylbenzyl)ethylenediamine (0.0328 g, 0.1 mmol) in ethanol (8 mL) was added drop-wise to a warm stirred solution of (0.0273 g, 0.1 mmol) copper(II) bromide in ethanol (10 mL). The drop-wise addition of N, N'-bis(4-methylbenzyl)ethylenediamine resulted in a formation of fine green crystals of the product. The reaction mixture was stirred at room temperature for 30 min. The product was filtered and washed with cold ethanol. The product was dried at room temperature for 2 days. The purity of the isolated complex was checked by elemental analysis, and the physical data are given in table 3.4.

#### **2.3.4.1.6 Preparation of Cu(OCH<sub>3</sub>-BENH)Br<sub>2</sub>, (6B)**

A solution of N, N'-bis(4-methoxybenzyl)ethylenediamine (0.1103 g, 0.4 mmol) in ethanol (8 mL) was added drop-wise to a warm stirred solution of (0.0810 g, 0.4 mmol) copper(II)

bromide in ethanol (10 mL). The drop-wise addition of N, N'-bis(4-methoxybenzyl)ethylenediamine resulted in a formation of fine green crystals of the product. The reaction mixture was stirred at room temperature for 30 min. The product was filtered and washed with cold ethanol. The product was dried at room temperature for 2 days. The purity of the isolated complex was checked by elemental analysis, and the physical data are given in table 3.4.

### 2.3.4.2 Synthesis of the copper chloride complexes

#### 2.3.4.2.1 Preparation of Cu(NO<sub>2</sub>-BENH)Cl<sub>2</sub>, (1C)

The ligand, N, N'-bis(4-nitrobenzyl)ethylenediamine (0.0310 g, 0.1 mmol) was dissolved in absolute ethanol (8 mL) and was slowly added drop-wise to a warm stirred suspension of (0.0177 g, 0.1 mmol) cupric chloride dihydrate in the same solvent (10 mL). Upon addition of the ligand, fine blue crystals of the product immediately formed. The product was further stirred for 30 min. The fine blue crystals were filtered and washed with cold absolute ethanol (3 x 10 mL). The product was dried at room temperature for 3 days. The purity of the isolated complex was checked by elemental analysis, and the physical data are given in table 3.5.

#### 2.3.4.2.2 Preparation of Cu(Cl-BENH)Cl<sub>2</sub>, (2C)

The ligand, N, N'-bis(4-chlorobenzyl)ethylenediamine (0.0377 g, 0.1 mmol) was dissolved in absolute ethanol (8 mL) and was slowly added drop-wise to a warm stirred suspension of (0.0208 g, 0.1 mmol) cupric chloride dihydrate in the same solvent (10 mL). Upon addition of the ligand, fine blue crystals of the product immediately formed. The product was further stirred for 30 min. The fine blue crystals were filtered and washed with cold absolute ethanol (3 x 10 mL). The product was dried at room temperature for 3 days. The purity of the isolated complex was checked by elemental analysis, and the physical data are given in table 3.5.

#### 2.3.4.2.3 Preparation of Cu(Br-BENH)Cl<sub>2</sub>, (3C)

The ligand, N, N'-*bis*(4-bromobenzyl)ethylenediamine (0.0351 g, 0.09 mmol) was dissolved in absolute ethanol (8 mL) and was slowly added drop-wise to a warm stirred suspension of (0.0151 g, 0.09 mmol) cupric chloride dihydrate in the same solvent (10 mL). Upon addition of the ligand, blue fine crystals of the product immediately formed. The product was further stirred for 30 min. The fine blue crystals were filtered and washed with cold absolute ethanol (3 x 10 mL). The product was dried at room temperature for 3 days. The purity of the isolated complex was checked by elemental analysis, and the physical data are given in table 3.5.

#### 2.3.4.2.4 Preparation of Cu(H-BENH)Cl<sub>2</sub>, (4C)

The ligand, N, N'-*bis*(benzyl)ethylenediamine (0.0180 g, 0.08 mmol) was dissolved in absolute ethanol (10 mL) and was slowly added drop-wise to a warm stirred suspension of (0.0127 g, 0.08 mmol) cupric chloride dihydrate in the same solvent (10 mL). Upon addition of the ligand, fine blue crystals of the product immediately formed. The product was further stirred for 30 min. The fine blue crystals were filtered and washed with cold absolute ethanol (3 x 10 mL). The product was dried at room temperature for 3 days. The purity of the isolated complex was checked by elemental analysis, and the physical data are given in table 3.5.

#### 2.3.4.2.5 Preparation of Cu(CH<sub>3</sub>-BENH)Cl<sub>2</sub>, (5C)

The ligand, N, N'-*bis*(4-methylbenzyl)ethylenediamine (0.0333 g, 0.1 mmol) was dissolved in absolute ethanol (10 mL) and was slowly added drop-wise to a warm stirred suspension of (0.0212 g, 0.1 mmol) cupric chloride dihydrate in the same solvent (10 mL). Upon addition of the ligand, fine blue crystals of the product immediately formed. The product was further stirred for 30 min. The fine blue crystals were filtered and washed with cold absolute ethanol (3 x 10 mL). The product was dried at room temperature for 3 days. The purity of the isolated complex was checked by elemental analysis, and the physical data are given in table 3.5.

#### 2.3.4.2.6 Preparation of $\text{Cu}(\text{OCH}_3\text{-BENH})\text{Cl}_2$ , (6C)

The ligand, N, N'-*bis*(4-methoxybenzyl)ethylenediamine (0.0879 g, 0.4 mmol) was dissolved in absolute ethanol (8 mL) and was slowly added drop-wise to a warm stirred suspension of (0.0494 g, 0.4 mmol) cupric chloride dihydrate in the same solvent (10 mL). Upon addition of the ligand, fine blue crystals of the product immediately formed. The product was further stirred for 30 min. The fine blue crystals were filtered and washed with cold absolute ethanol (3 x 10 mL). The product was dried at room temperature for 3 days. The purity of the isolated complex was checked by elemental analysis, and the physical data are given in table 3.5.

#### 2.3.4.2.7 Preparation of $\text{Cu}(\text{N}(\text{CH}_3)_2\text{-BENH})\text{Cl}_2$ , (7C)

The ligand, N, N'-*bis*(4-dimethylaminobenzyl)ethylenediamine (0.0359 g, 0.1 mmol) was dissolved in absolute ethanol (10 mL) and was slowly added drop-wise to a warm stirred suspension of (0.0246 g, 0.1 mmol) cupric chloride dihydrate in the same solvent (10 mL). Upon addition of the ligand, fine blue crystals of the product immediately formed. The product was further stirred for 30 min. The fine blue crystals were filtered and washed with cold absolute ethanol (3 x 10 mL). The product was dried at room temperature for 3 days. The purity of the isolated complex was checked by elemental analysis, and the physical data are given in table 3.5.

### 2.3.5 Synthesis of N, N'-*bis*(cinnamaldiimine) ligands

The N, N'-*bis*(*trans*-cinnamaldehyde)-1, 2-diiminoethane ligand was prepared in the similar manner as described in the literature.<sup>8</sup>

#### 2.3.5.1 Preparation of N, N'-*bis*(*trans*-cinnamaldehyde)-1, 2-diiminoethane ligand, (21)

To a stirring solution of *trans*-cinnamaldehyde (12.61 mL, 100 mmol) in methanol (100 mL) cooled with an ice bath, was added dropwise 3.35 mL (50 mmol) ethylenediamine. The

mixture was then stirred for an additional 45 min. The reaction mixture was poured into a beaker containing 400 mL of water, and it was allowed to stir for a further 30 min. The resulting product was collected on a coarse fritted glass funnel, washed with water and dried at room temperature for 48 hours. The Schiff base was recrystallized from acetone and the resulting white crystals were collected and washed with cold acetone (10 x 2 mL). The physical data are given in table 3.6.

### **2.3.5.2 Preparation of N, N'-bis(4-dimethylaminocinnamaldehyde)-1,**

#### **2-diiminoethane ligand, (22)**

The cinnamaldiimine ligand, N, N'-bis(4-dimethylaminocinnamaldehyde)-1, 2-diiminoethane was synthesized via Schiff base condensation using 1.8615 g (10.6 mmol) of 4-dimethylaminocinnamaldehyde in 15mL ethanol and 0.3192 g (5.3 mmol) of ethylenediamine in 10 mL of the same solvent. The solution mixture was reflux for 2 hours. The resulting orange crude product was filtered, washed with cold ethanol (3 x 10 mL) and dried at room temperature for 48 hours. The physical data are given in table 3.6.

### **2.3.6 Synthesis of N, N'-bis(cinnamaldiamine) ligand**

#### **2.3.6.1 Preparation of N, N'-bis(trans-cinnamylbenzyl)ethylenediamine ligand, (23)**

To a solution of N, N'-bis(trans-cinnamaldehyde)-1, 2-diiminoethane (1.0208 g, 3.5 mmol) in 15 mL of methanol was slowly added a five-fold molar excess of solid sodium borohydride (0.5384 g, 14.2 mmol), after which the reaction mixture was refluxed for 3 hour. The solvent was distilled off. Then, 20 ml of cold water was added to reaction mixture to liberate the secondary amine. The colourless product was then extracted with chloroform (3 x 20 ml). The combined extracts were washed with water and dried over anhydrous sodium sulphate. The solvent was removed by rotator evaporation and a colourless oily solid was obtained. The physical data are given in table 3.6.

### 2.3.7 Synthesis of copper(I) complexes derived from N, N'-bis(*trans*-cinnamaldehyde)-

#### 1, 2-diiminoethane ligand

The syntheses were carried out using distilled, dry, degassed solvents. All the chemicals were degassed before use. Reactions were performed under high purity nitrogen atmosphere by purging the system with nitrogen. The synthesis of the bromo and chloro complexes were carried out using anhydrous CuCl<sub>2</sub> and CuBr<sub>2</sub> in the presence of copper wire, while the iodo complex was prepared directly from anhydrous CuI. The anhydrous CuCl<sub>2</sub> was prepared by heating cupric chloride dihydrate in a heating piston. For the entire synthesis 1:1 metal to ligand mole ratio was used. The preparation of Cu(I) compounds were done in an identical manner. The synthesis is described using Cu(I)(CA<sub>2</sub>EN)Cl. The physical data are given in table 3:7.

#### 2.3.7.1 Preparation of Cu(I)(CA<sub>2</sub>EN)Cl, (2I)

0.1008g (0.6 mmol) of anhydrous CuCl<sub>2</sub> was added to 8 mL of distilled acetonitrile, under a stream of purified N<sub>2</sub>. A Cu(0) coil was added to the suspension to repropionate any Cu(II) species that could form upon addition of the ligand, an excess of 2, 2-dimethoxypropane (1.23 mL, 5.9 mmol) was added to the CuCl suspension under nitrogen. After the addition of 2, 2-dimethoxypropane, the solution immediately became in a pale colourless solution after stirring under nitrogen. 0.1705g of N, N'-bis(*trans*-cinnamaldehyde)-1, 2-diiminoethane (5.9 mmol) was added to the colourless solution under nitrogen and an orange solid precipitated immediately. The orange product was filtered under nitrogen using a special glass frit. The compounds are air stable when they are completely dry, but a rapid oxidation to Cu(II) was observed in the presence of moisture. The compounds were stored in a degassed desicator. The physical data are given in table 3:7.

### 2.3.8 Synthesis of copper(II) complexes derived from N, N'-bis(*trans*-cinnamaldehyde)-1, 2-diaminoethane ligand, Cu(II)(CA<sub>2</sub>EN)Cl<sub>2</sub> and (Cu(II)(CA<sub>2</sub>EN)Br<sub>2</sub>)

The synthesis of dibromoN, N'-bis(*trans*-cinnamaldehyde)-1, 2-diaminoethanecopper(II) and dichloroN, N'-bis(*trans*-cinnamaldehyde)-1, 2-diaminoethanecopper(II) were carried out using cupric chloride anhydrous and anhydrous copper(II) bromide under high a purity nitrogen atmosphere. The anhydrous CuCl<sub>2</sub> was prepared by heating cupric chloride dihydrate in a heating pistol. The synthesis is described using Cu(II)(CA<sub>2</sub>EN)Cl<sub>2</sub>, because the preparation of Cu(II)(CA<sub>2</sub>EN)Br<sub>2</sub> was unsuccessful, yielding inconsistent results. This is possibly due to the bromide stabilising the reduction of Cu(II) to Cu(I). Thus synthesis of the Cu(II) iodide complex was not attempted.

#### 2.3.8.1 Preparation of Cu(II) (CA<sub>2</sub>EN)Cl<sub>2</sub>, (4I)

To a 0.1007 g (0.6 mmol) of anhydrous CuCl<sub>2</sub> was added 10 mL of distilled acetonitrile, under a stream of purified N<sub>2</sub>. An excess of 2, 2-dimethoxypropane (1.23 mL, 5.9 mmol) was added to the stirred CuCl<sub>2</sub> suspension under nitrogen. Upon the addition of 2, 2-dimethoxypropane, the solution turned colourless. 0.1705 g of N, N'-bis(*trans*-cinnamaldehyde)-1, 2-diiminoethane (0.6 mmol) was added to the colourless solution under nitrogen and blue crystals precipitated immediately. The compound is air and moisture stable and its physical data is given in table 3.8.

### 2.3.9 Attempt to synthesize copper(II) complexes derived from N, N'-bis(*trans*-cinnamylbenzyl)ethylenediamine ligand

Attempts were made to prepare the amine complexes, Cu(II)(CA<sub>2</sub>ENH)Br<sub>2</sub> and Cu(II)(CA<sub>2</sub>ENH)Cl<sub>2</sub> in a similar manner to the synthesis described in section 2.2.5 and 2.2.6. Unfortunately the syntheses for both compounds were unsuccessful. The attempted synthesis is described using Cu(II)(CA<sub>2</sub>ENH)Br<sub>2</sub>.

#### 2.3.9.1 Preparation of Cu(II)(CA<sub>2</sub>ENH)Br<sub>2</sub>

The complex was prepared by drop-wise addition of ethanolic solution (8 mL) of N, N'-bis(*trans*-cinnamaldehyde)-1, 2-diaminoethane (0.1456 g, 0.5 mmol) into a solution of Cu(II)Br<sub>2</sub> in ethanol. Upon the addition of the ligand solution, a green solid product precipitated out. The solution mixture was then stirred for 30 min at room temperature. The resulting green product was filtered, washed with absolute ethanol (10 x 3 mL) and dried at room temperature for 48 hours. The complex was then recrystallized from hot acetone – hexane and in hot ethanol. The microanalysis gave inconsistent results. This is possibly because the complexes undergo dissociation of the ligand in these solvents, leading to contamination of the metal salts on recrystallisation.

## 2.4 References

1. D. D. Perrin, W.L.F. Armarego, *Purification of laboratory chemicals*, 3<sup>rd</sup> ed. Pergamon Press. New York, 1988.
2. A. Toth, C. Floriani, M. Pasquali, A. Chiesi-Villa, A. Gaetani-Manfredotti, C. Guastini, *Inorg. Chem.*, 1985, **24**, 648-653.
3. K. P. Guzen, A. S. Guarezemini, A. T. G. Orfao, R. Cella, C. M. P. Pereira, H. A. Stefani, *Tetrahedron Letters*, 2007, **48**, 1845-1848.
4. C. Imrie, V. O. Nyamori, T. I.A. Gerber, *J. Organometallic. Chem.*, 2004, **689**, 1617–1622.
5. J. H. Billman, A. C. Diesing, *J. Org. Chem.*, 1957, **22**, 1068-1070.
6. A. Sanches-Silva, A. Rodriguez-Bernaldo de Quiros, J. Lopez-Hernandez, P. Paseiro-losada, *J. Chromatogr.* 2004, **1032**, 7-15.
7. D. F. Taber, Y. Wang, *J. Am. Chem. Soc.*, 1997, **119**, 22-26.
8. M. Amirasr, K. J. Schenk, M. Salavati, S. Dehghanpour, A. Taeb, A. Tadjarodi, *J.Coord.Chem.*, 2003, **56**, 231-243.

### 3. RESULTS (PHYSICAL AND CHEMICAL STUDY)

All the results obtained from the techniques used in characterizing the ligands and their complexes are listed in this chapter.

The interpretation of the experimental spectra data (including the IR,  $^1\text{H}$ - and  $^{13}\text{C}$ -NMR, UV/vis and MS in table 3.1-3.22) and the elucidation of the chemical structure of the respective compounds and their complexes are based on known reported structures in literature <sup>1-2</sup>. Since the N, N'-*bis*(cinnamaldehyde)-1, 2-diiminoethane ligand is not a new compound, the interpretation and the assignment of the proton and carbon chemical shifts for the N, N'-*bis*(cinnamaldehyde)-1, 2-diiminoethane ligand and its dimethylamine analogue were made by comparing the NMR spectra of the ligand with those reported in literature <sup>3,4</sup>.

### 3.1 Physicochemical data for ligands and complexes

Table 3.1 Microanalysis and analytical data for the of N, N'-(aryl)benzaldimine ligands

No.	Ligand	Molecular formula	Found ( Calculated)			Color	Yield (%)	Mp	Molar	M <sup>+</sup>
			%C	%H	%N			(°C)	mass	
1	NO <sub>2</sub> -BEN	C <sub>16</sub> H <sub>14</sub> N <sub>4</sub> O <sub>4</sub>	58.94 (58.89)	4.31 (4.33)	17.17 (17.17)	yellow-pink	97.6	200-202	326.3	328.1
2	Cl-BEN	C <sub>16</sub> H <sub>14</sub> Cl <sub>2</sub> N <sub>2</sub>	62.95 (62.97)	4.71 (4.62)	9.23 (9.18)	shinny white	92.6	145-147	305.2	306.4
3	Br-BEN	C <sub>16</sub> H <sub>14</sub> Br <sub>2</sub> N <sub>2</sub>	48.67 (48.76)	3.65 (3.58)	7.24 (7.11)	shinny white	88.2	160-161	394.1	396.9
4	H-BEN	C <sub>16</sub> H <sub>16</sub> N <sub>2</sub>	81.18 (81.32)	7.04 (6.83)	11.84 (11.85)	light yellow	80.5	40-42	236.3	237.9

Table 3.1 (continued)

No.	Ligand	Molecular formula	Found ( Calculated)			Color	Yield (%)	Mp	Molar	M <sup>+</sup>
			%C	%H	%N			(°C)	mass	
5	CH <sub>3</sub> -BEN	C <sub>18</sub> H <sub>20</sub> N <sub>2</sub>	81.33 (81.77)	7.86 (7.63)	10.55 (10.59)	white	78.3	150-152	264.4	266.3
6	OCH <sub>3</sub> -BEN	C <sub>18</sub> H <sub>20</sub> N <sub>2</sub> O <sub>2</sub>	72.57 (72.95)	6.99 (6.80)	9.44 (9.45)	yellow	73.6	110-111	296.4	298.3
7	N(CH <sub>3</sub> ) <sub>2</sub> -BEN	C <sub>20</sub> H <sub>26</sub> N <sub>4</sub>	74.24 (74.49)	8.39 (8.13)	17.13 (17.38)	light cream	65.2	185-186	322.5	324.1

OH-BEN see section 2.3.1.8.

Table 3.2 Microanalysis and analytical data for the N, N'-(aryl)benzaldiamine dihydrochloride salts

No.	Ligand	Molecular formula	Found ( Calculated)			Color	Yield (%)	Mp (°C)	Molar mass <sup>a</sup>	M <sup>+</sup>
			%C	%H	%N					
8	NO <sub>2</sub> -BENH•2HCl	C <sub>16</sub> H <sub>18</sub> Cl <sub>2</sub> N <sub>4</sub> O <sub>4</sub> •2HCl	47.65 (47.66)	5.22 (5.00)	13.32 (13.89)	light yellow	73	205-207	332.4	333.2
9	Cl-BENH•2HCl	C <sub>16</sub> H <sub>18</sub> N <sub>2</sub> Cl <sub>2</sub> •2HCl	50.41 (50.29)	5.44 (5.28)	7.24 (7.33)	shinny white	56	245-246	311.3	311.8
10	Br-BENH•2HCl	C <sub>16</sub> H <sub>18</sub> N <sub>2</sub> Br <sub>2</sub> •2HCl	40.97 40.80	4.44 (4.28)	5.87 (5.95)	shinny white	62	240-241	400.	400.1
11	H-BENH•2HCl	C <sub>16</sub> H <sub>20</sub> N <sub>2</sub> •2HCl	61.28 (61.35)	7.17 (7.08)	8.78 (8.94)	shinny white	57	249-250	242.4	243.4
12	CH <sub>3</sub> -BENH•2HCl	C <sub>18</sub> H <sub>24</sub> N <sub>2</sub> •2HCl	63.54 (63.34)	7.59 (7.68)	8.33 (8.21)	shinny white	82	219-220	270.4	271.0
13	OCH <sub>3</sub> -BENH•2HCl	C <sub>18</sub> H <sub>24</sub> N <sub>2</sub> O <sub>2</sub> •2HCl	57.32 (57.91)	6.51 (7.02)	7.46 (7.02)	shinny white	65	255-257	302.4	303.0

a (LH<sub>2</sub><sup>2+</sup>) ion

Table 3.3 Microanalysis and analytical data for the N, N'-(aryl)benzaldiamine ligands

No.	Ligand	Molecular formula	Found ( Calculated)			Color	Yield (%)	Mp (°C)	Molar mass	M <sup>+</sup>
			%C	%H	%N					
14	NO <sub>2</sub> -BENH•MeOH	C <sub>16</sub> H <sub>18</sub> N <sub>4</sub> O <sub>4</sub>	52.93 (53.00)	5.80 (5.01)	15.74 (15.46)	light orange	62	o	330.3	331.9
15	Cl-BENH•MeOH	C <sub>16</sub> H <sub>18</sub> Cl <sub>2</sub> N <sub>2</sub>	56.86 (56.31)	6.27 (5.32)	8.71 (8.21)	yellow	63	o	309.2	310.6
16	Br-BENH	C <sub>16</sub> H <sub>18</sub> Br <sub>2</sub> N <sub>2</sub>	47.88 (48.27)	4.70 (4.56)	6.96 (7.04)	yellow	54	o	398.1	400.2
17	H-BENH•MeOH•H <sub>2</sub> O	C <sub>16</sub> H <sub>20</sub> N <sub>2</sub>	68.88 (68.78)	7.47 (7.22)	9.07 (10.23)	white	68	56-58	240.3	242.0
18	CH <sub>3</sub> -BENH•½EtOH	C <sub>18</sub> H <sub>24</sub> N <sub>2</sub> •½C <sub>2</sub> H <sub>5</sub> OH	74.63 (74.18)	8.51 (9.01)	9.24 (9.61)	white	72	74-75	268.4	270.5
19	OCH <sub>3</sub> -BENH•½EtOH	C <sub>18</sub> H <sub>24</sub> N <sub>2</sub> O <sub>2</sub> •½C <sub>2</sub> H <sub>5</sub> OH	66.36 (66.84)	7.44 (7.48)	8.24 (8.66)	cream	55	94-95	300.4	302.2
20	N(CH <sub>3</sub> ) <sub>2</sub> -BENH•MeOH	C <sub>20</sub> H <sub>30</sub> N <sub>4</sub> •CH <sub>3</sub> OH	67.35 (67.00)	8.91 (8.46)	15.15 (15.63)	yellow	44	87-89	326.5	327.8

o oils

Table 3.4 Microanalysis and analytical data for the N, N'-(aryl)benzaldiaminedibromidecopper(II) complexes

No.	Complex	Molecular formula	Molar mass	Found ( Calculated)			Color	Yield (%)	Mp (°C)
				%C	%H	%N			
1B	Cu(NO <sub>2</sub> -BENH)Br <sub>2</sub>	C <sub>16</sub> H <sub>18</sub> Br <sub>2</sub> CuN <sub>4</sub> O <sub>4</sub>	553.7	34.98 (34.71)	3.38 (3.28)	10.06 (10.12)	green	74	160-161
2B	Cu(Cl-BENH)Br <sub>2</sub>	C <sub>16</sub> H <sub>18</sub> Br <sub>2</sub> Cl <sub>2</sub> CuN <sub>2</sub>	532.6	41.88 (41.08)	4.25 (4.41)	6.31 (6.26)	green	69	192-193
3B	Cu(Br-BENH)Br <sub>2</sub>	C <sub>16</sub> H <sub>18</sub> Br <sub>4</sub> CuN <sub>2</sub>	621.5	30.51 (30.92)	2.91 (2.92)	4.70 (4.51)	green	57	147-149
4B	Cu(H-BENH)Br <sub>2</sub>	C <sub>16</sub> H <sub>20</sub> Br <sub>2</sub> CuN <sub>2</sub>	463.7	41.03 (41.44)	4.27 (4.35)	6.30 (6.04)	green	64	163-164
5B	Cu(CH <sub>3</sub> -BEHN)Br <sub>2</sub>	C <sub>18</sub> H <sub>24</sub> Br <sub>2</sub> CuN <sub>2</sub>	491.7	44.99 (44.03)	5.08 (4.93)	5.69 (5.69)	green	81	153-154
6B	Cu(OCH <sub>3</sub> -BENH)Br <sub>2</sub>	C <sub>18</sub> H <sub>24</sub> Br <sub>2</sub> CuN <sub>2</sub> O <sub>2</sub>	523.7	40.08 (40.58)	4.75 (4.62)	5.23 (5.35)	green	56	111-112

Table 3.5 Microanalysis and analytical data for the N, N'-(aryl)benzaldiaminedichloridecopper(II) complexes

No.	Complex	Molecular formula	Molar mass	Found ( Calculated)			Color	Yield (%)	Mp (°C)
				%C	%H	%N			
1C	Cu(NO <sub>2</sub> -BENH)Cl <sub>2</sub>	C <sub>16</sub> H <sub>18</sub> Cl <sub>2</sub> CuN <sub>4</sub> O <sub>4</sub>	464.79	41.07 (41.35)	3.97 (3.90)	11.99 (12.05)	blue	52	196-197
2C	Cu(Cl-BENH)Cl <sub>2</sub>	C <sub>16</sub> H <sub>14</sub> Cl <sub>2</sub> CuN <sub>2</sub>	443.7	43.09 (43.31)	4.08 (4.10)	6.25 (6.32)	blue	63	192-193
3C	Cu(Br-BENH)Cl <sub>2</sub>	C <sub>16</sub> H <sub>18</sub> Br <sub>2</sub> Cl <sub>2</sub> CuN <sub>2</sub>	532.6	35.95 (36.08)	3.33 (3.41)	5.33 (5.26)	blue	59	189-190
4C	Cu(H-BENH)Cl <sub>2</sub>	C <sub>16</sub> H <sub>16</sub> Cl <sub>2</sub> CuN <sub>2</sub>	374.8	50.51 (51.27)	5.38 (5.38)	7.29 (7.47)	blue	68	192-194
5C	Cu(CH <sub>3</sub> -BENH)Cl <sub>2</sub> • $\frac{1}{3}$ EtOH	C <sub>18</sub> H <sub>20</sub> Cl <sub>2</sub> CuN <sub>2</sub> • $\frac{1}{3}$ C <sub>2</sub> H <sub>5</sub> OH	418.2	53.59 (53.67)	6.22 (6.01)	6.36 (6.95)	blue	73	190-191

Table 3.5 (continued)

No.	Complex	Molecular formula	Molar mass	Found ( Calculated)			Color	Yield (%)	Mp (°C)
				%C	%H	%N			
6C	Cu(OCH <sub>3</sub> -BENH)Cl <sub>2</sub>	C <sub>18</sub> H <sub>20</sub> Cl <sub>2</sub> CuN <sub>2</sub> O <sub>2</sub>	343.8	50.18 (49.71)	5.53 (5.57)	6.41 (6.44)	blue	74	178-179
7C	Cu((NCH <sub>3</sub> ) <sub>2</sub> -BEN)Cl <sub>2</sub> •½H <sub>2</sub> O	C <sub>20</sub> H <sub>30</sub> Cl <sub>2</sub> CuN <sub>4</sub> •½H <sub>2</sub> O	469.9	51.58 (51.12)	6.57 (6.44)	11.96 (11.92)	blue	67	204-206

Table 3.6 Microanalysis and analytical data for the N, N'-bis(cinnamaldiimine) ligands

No.	Ligand	Molecular formula	Found ( Calculated)			Color	Yield (%)	Mp (°C)	Molar mass	M <sup>+</sup>
			%C	%H	%N					
21	CA <sub>2</sub> EN	C <sub>20</sub> H <sub>20</sub> N <sub>2</sub>	83.11 (83.29)	6.87 (6.87)	9.70 (9.72)	white	85	108-109	288.4	290.5
22	N(CH <sub>3</sub> ) <sub>2</sub> CA <sub>2</sub> EN•½H <sub>2</sub> O	C <sub>24</sub> H <sub>30</sub> N <sub>4</sub> •½H <sub>2</sub> O	76.01 (76.96)	7.83 (8.07)	14.41 (14.96)	orange	77	193-194	374.5	379.4
23	CA <sub>2</sub> ENH•MeOH	C <sub>20</sub> H <sub>22</sub> N <sub>2</sub> •CH <sub>3</sub> OH	74.55 (74.50)	7.57 (6.88)	8.16 (8.69)	white	62	76-79	290.3	292

Table 3.7 Microanalysis and analytical data for the N, N'-bis(cinnamaldehyde)-1, 2-diiminoethanecopper(I)halide

No	Complex	Molecular formula	Molar mass	Found ( Calculated)			Color	Yield (%)	Mp (°C)
				%C	%H	%N			
1I	Cu(I) (CA <sub>2</sub> EN)Br•(4CH <sub>3</sub> CN)	C <sub>24</sub> H <sub>32</sub> N <sub>2</sub> BrCu(CN) <sub>4</sub>	596.0	40.38 (40.58)	3.49 (3.88)	5.15 (5.39)	dark orange	71	209-211
2I	Cu(I)(CA <sub>2</sub> EN)Cl•(1½ CH <sub>3</sub> CN)	C <sub>21</sub> H <sub>24</sub> N <sub>2</sub> ClCuCN	449.0	53.85 (53.51)	4.47 (4.49)	6.43 (6.24)	orange	67	166-168
3I	Cu(I)(CA <sub>2</sub> EN)•(½ CH <sub>3</sub> CN)I	C <sub>20</sub> H <sub>21</sub> N <sub>2</sub> ICu	499.4	48.01 (48.11)	3.88 (4.08)	5.74 (5.61)	red-orange	88	215-216

Table 3.8 Microanalysis and analytical data for the N, N'-bis(cinnamaldehyde)-1, 2-diiminoethanecopper(II)dihalide

No	Complex	Molecular formula	Molar mass	Found ( Calculated)			Color	Yield (%)	Mp (°C)
				%C	%H	%N			
4I	Cu(CA <sub>2</sub> EN)Cl <sub>2</sub>	C <sub>20</sub> H <sub>20</sub> CuCl <sub>2</sub> N <sub>2</sub>	422.9	56.08 (56.80)	4.62 (4.78)	6.78 (6.63)	green	89	156-157

### 3.2 NMR spectroscopy spectra data for the ligands

Table 3.9 Proton nuclear magnetic resonance data for the N, N'-(aryl)benzaldimine ligands

No.	Ligand	H-5	H-4	H-2	H-1	X
1	NO <sub>2</sub> -BEN	8.28 (m, 2H)	7.90 (m, 2H)	8.41 (s, 1H)	4.09 (s, 2H)	-
2	Cl-BEN	7.62 (m, 2H)	7.35 (m, 2H)	8.22 (s, 1H)	3.95 (s, 2H)	-
3	Br-BEN	7.55 (m, 2H)	7.51 (m, 2H)	8.21 (s, 1H)	3.95 (s, 2H)	-
4	H-BEN	7.70 (m, 2H)	7.39 (m, 2H)	8.29 (s, 1H)	3.98 (s, 2H)	7.71 (m, 2H)

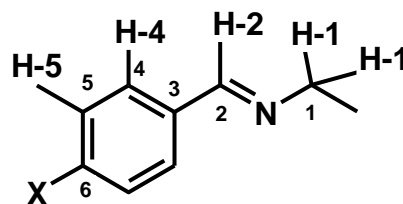


Figure 3.1 Numbering system used for the Schiff bases

Table 3:9 continues

No	Ligand	H-5	H-4	H-2	H-1	X
5	CH <sub>3</sub> -BEN	7.19 (m, 2H)	7.58 (m, 2H)	8.25 (s, 1H)	3.95 (s, 2H)	2.36 (s, 3H)
6	OCH <sub>3</sub> -BEN	6.87 (m, 2H)	7.61 (m, 2H)	8.18 (s, 1H)	3.79 (s, 2H)	3.86 (s, 3H)
7	N(CH <sub>3</sub> ) <sub>2</sub> -BEN	6.67 (m, 2H)	7.57 (m, 2H)	8.16 (s, 1H)	3.87 (s, 2H)	2.99 (s, 6H)

Table 3:10 Carbon nuclear magnetic resonance data for the N, N'-(aryl)benzaldimine ligands

No.	Ligand	C-6	C-5	C-4	C-3	C-2	C-1	X
1	NO <sub>2</sub> -BEN	149.51	124.36	129.21	141.78	160.86	61.91	-
2	Cl-BEN	136.66	128.91	129.31	134.56	161.41	61.51	-
3	Br-BEN	125.00	131.75	129.42	134.91	161.33	61.37	-
4	H-BEN	130.78	128.71	128.24	136.25	162.89	61.79	-
5	CH <sub>3</sub> -BEN	140.79	129.22	128.00	133.50	162.52	61.66	21.45
6	OCH <sub>3</sub> -BEN	162.38	114.35	130.07	129.58	161.98	62.18	55.78
7	N(CH <sub>3</sub> ) <sub>2</sub> -BEN	151.61	111.35	129.29	124.20	162.23	61.85	40.03

Table 3:11 Proton nuclear magnetic resonance data for the N, N'-(aryl)benzaldiamine dihydrochloride salts

No.	Ligand	H-5	H-4	H-2	H-1	NH <sub>2</sub>	X
8	NO <sub>2</sub> -BEN•2HCl	8.27 (m, 2H)	7.80 (m, 2H)	4.22 (s, 2H)	3.50 (s, 2H)	3.39 (s, 2H)	-
9	Cl-BEN•2HCl	7.55 (m, 2H)	7.36 (m, 2H)	3.52 (s, 2H)	2.72 (s, 2H)	2.89 (s, 2H)	-
10	Br-BEN•2HCl	7.58 (m, 2H)	7.39 (m, 2H)	3.89 (s, 2H)	3.51 (s, 2H)	3.36 (s, 2H)	-
11	H-BEN•2HCl	7.57 (m, 2H)	7.56 (m, 2H)	4.18 (s, 2H)	3.71 (s, 2H)	3.35 (s, 2H)	7.44 (s, 1H)
12	CH <sub>3</sub> -BEN•2HCl	7.20 (m, 2H)	7.33 (m, 2H)	3.95 (s, 2H)	2.98 (s, 2H)	3.39 (s, 2H)	2.30 (s, 3H)
13	OCH <sub>3</sub> -BEN•2HCl	6.98 (m, 2H)	7.49 (m, 2H)	4.10 (s, 2H)	3.30 (s, 2H)	3.32 (s, 2H)	3.77 (s, 3H)

Table 3:12 Proton nuclear magnetic resonance data for the N, N'-(aryl)benzaldiamine ligands

No.	Ligand	H-5	H-4	H-2	H-1	N-H	X
14	NO <sub>2</sub> -BENH	8.18 (m, 2H)	7.50 (m, 2H)	3.90 (s, 2H)	2.77 (s, 2H)	1.95 (s, 1H)	-
15	Cl-BENH	7.28 (m, 2H)	7.23 (m, 2H)	3.74 (s, 2H)	2.73 (s, 2H)	1.73 (s, 1H)	-
16	Br-BENH	7.43 (m, 2H)	7.18 (m, 2H)	3.72 (s, 2H)	2.72 (s, 2H)	1.16 (s, 1H)	-
17	H-BENH	7.31 (m, 2H)	7.26 (m, 2H)	3.78 (s, 2H)	2.78 (s, 2H)	2.28 (s, 1H)	7.21 (s, 1H)
18	CH <sub>3</sub> -BENH	7.13 (m, 2H)	7.20 (m, 2H)	3.74 (s, 2H)	2.76 (s, 2H)	2.08 (s, 1H)	2.34 (s, 3H)
19	OCH <sub>3</sub> -BENH	6.85 (m, 2H)	7.23 (m, 2H)	3.79 (s, 2H)	2.75 (s, 2H)	2.07 (s, 1H)	3.71 (s, 3H)
20	N(CH <sub>3</sub> ) <sub>2</sub> -BENH	6.78 (m, 2H)	7.25 (m, 2H)	3.75 (s, 2H)	2.82 (s, 2H)	1.61 (s, 1H)	2.99 (s, 3H)

Table 3:13 Carbon nuclear magnetic resonance data for the N, N'-(aryl)benzaldiamine ligands

No.	Ligand	C-6	C-5	C-4	C-3	C-2	C-1	X
14	NO <sub>2</sub> -BENH	147.53	124.09	129.03	148.42	53.54	49.21	-
15	Cl-BENH	132.42	128.29	129.22	138.65	52.94	48.43	-
16	Br-BENH	120.79	131.56	129.91	139.58	53.34	48.82	-
17	H-BENH	127.17	128.57	128.35	140.12	53.86	48.51	127.17
18	CH <sub>3</sub> -BENH	136.30	128.85	127.91	136.91	53.29	48.27	20.87
19	OCH <sub>3</sub> -BENH	158.74	113.88	129.46	132.36	53.28	48.51	55.38
20	N(CH <sub>3</sub> ) <sub>2</sub> -BENH	150.25	113.19	129.04	129.52	53.87	49.17	41.27

Table 3:14 Proton and Carbon nuclear magnetic resonance data for the N, N'-bis(cinnamaldiimine) ligands

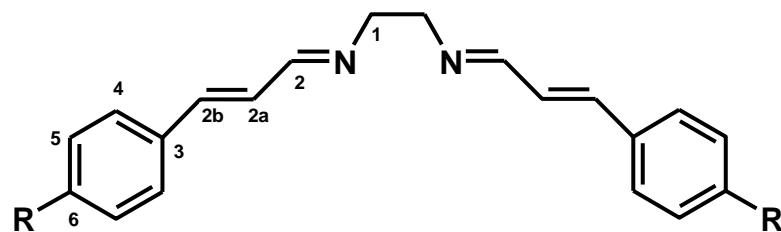


Figure 3.2 Numbering system used for the N, N'-bis(cinnamaldiimine) ligands

No		R	1	2	2a	2b	3	4	5	6	X
21	$^1\text{H}$	H	3.85 (s, 2H)	8.05 (d, 1H)	6.94 (d, 1H)	6.89 (d, 1H)	-	7.34 (d, 2H)	7.46 (d, 2H)	7.46 (d, 2H)	-
	$^{13}\text{C}$		61.55	164.01	127.05	141.64	135.52	127.87	128.60	128.93	-
22	$^1\text{H}$	4N(CH <sub>3</sub> ) <sub>2</sub>	3.79 (s, 2H)	7.99 (d, 1H)	6.72 (d, 1H)	6.66 (d, 1H)	-	7.35 (d, 2H)	6.85 (d, 2H)	-	2.98 (s, 3H)
	$^{13}\text{C}$		61.38	164.21	123.35	141.76	123.11	128.08	111.49	150.41	39.73

### 3.3 Electronic spectra data for the ligands

Table 3:15 UV/visible spectral data for the N, N'-(aryl)benzaldimine ligands, (Extinction coefficient in parentheses (log  $\epsilon$ , l/mol cm))

No.	R	Solvent	$\pi \rightarrow \pi^*$ (benzene)	$\pi \rightarrow \pi^*$ (imine)	CT	$n \rightarrow \pi^*$ (imine)	others
1	4-NO <sub>2</sub>	EtOH	216 (3.03) 218 sh	237 (2.67) 238	282 (3.65)	321 (2.50)	324 (2.42)
2	4-Cl	EtOH	210 (3.68)	masked	254 (2.82)	284 (2.96) 294 (2.65)	293 (2.69)
3	4-Br	EtOH	212 (3.45)	masked	258 (2.85)	285 (2.75)	292 (2.55)
4	H	EtOH	204 (3.85)	211 (3.65)	247 (4.00)	274 (2.78)	-
5	4-CH <sub>3</sub>	EtOH	208 (3.44)	masked	256 (3.73)	288 (2.60)	294 (2.45)
6	4-OCH <sub>3</sub>	EtOH	216 (3.43)	masked	271 (4.00)	287 (3.36)	297 (3.19), 302 (2.96)
7	4-N(CH <sub>3</sub> ) <sub>2</sub>	EtOH	203 (3.50)	215 (3.07)	235 (3.15)	336 (4.08)	408 (2.44)

The UV spectra of the N, N'-(aryl)benzaldimine dihydrochloride ligands due to the poor solubility of the salts. (No. 8-13)

Table 3:16 UV/visible spectral data for the N, N'-(aryl)benzaldiamine ligands

(Extinction coefficient in parentheses (log  $\epsilon$ , l/mol cm))

No.	Assignment:		n $\rightarrow$ $\zeta^*$ transition		$\pi \rightarrow \pi^*$ transition	
	Compound	Solvent	200-240 nm	250-300 nm	305-350 nm	360-700 nm
14	4-NO <sub>2</sub>	Ethanol	214 (3.92)	271 (4.00)	-	-
		CHCl <sub>3</sub>	-	-	313 (3.50)	448 (2.00)
15	4-Cl	EtOH	222 (4.26)	271 (2.75)	-	-
		CHCl <sub>3</sub>	-	264 (2.82)	-	438 (1.43)
16	4-Br	EtOH	221 (4.40)	272 (2.85)	-	-
		CHCl <sub>3</sub>	-	262 (3.45)	-	433 (1.82)
17	H	EtOH	212 (4.15)	260 (2.93)	-	-
		CHCl <sub>3</sub>	-	268 (3.51)	333 (2.58)	-

Table 3.16 continues

No.	Assignment:		n → ζ* transition		π → π* transition	
	R	Solvent	200-240 nm	250-300 nm	305-350 nm	360-700 nm
18	4-CH <sub>3</sub>	EtOH	214 (4.17)	270 (2.71)	-	-
		CHCl <sub>3</sub>	-	261 (3.87)	332 (2.66)	-
19	4-OCH <sub>3</sub>	EtOH	214 (4.17)	268 (2.71)	-	-
		CHCl <sub>3</sub>	-	258 (3.87)	332 (2.66)	-
20	4-N(CH <sub>3</sub> ) <sub>2</sub>	EtOH	210 (2.54)	264 (3.0)	311 (3.62)	
		CHCl <sub>3</sub>		266 (4.38)	315 (4.00), 351(3.89)	-

### 3.4 Electronic spectral data for the N, N'-(aryl)benzaldiaminedihalidecopper(II) complexes

Table 3:17 UV/visible spectral data for the N, N'-(aryl)benzaldiaminedibromidecopper(II) complexes

(Extinction coefficient in parentheses (log  $\epsilon$ , l/mol cm))

No	Assignment:		$n \rightarrow \zeta^*$ transition	$\pi \rightarrow \pi^*$ transition	CT (M $\rightarrow$ L)	CT (M $\rightarrow$ L)	$d \rightarrow d$ transition
	R	Solvent	200-240 nm	250-300 nm	305-350 nm	360-500 nm	505-900 nm
1B	4-NO <sub>2</sub>	Ethanol	214, (3.99)	271, (4.01)	308, (3.91)	479, (3.70)	872, (2.33)
		CHCl <sub>3</sub>		271, (4.02)	-	485, (3.63)	850, (2.20)
2B	4-Cl	Ethanol	224 (4.16)	274 (3.62)	311, (3.77)	465 (2.81)	699,(2.81)
		CHCl <sub>3</sub>		272, (4.08)	308, (3.93)	464, (2.90)	708 (2.66)
3B	4-Br	Ethanol	228 (4.21)	277, (3.64)	308, (3.80)	466, (2.84)	735, (2.86)
		CHCl <sub>3</sub>		279, (4.10)	301, (3.99)	468, (3.07)	755, (2.95)
4B	H	Ethanol	212 (4.05)	271 (3.58)	308 (3.79)	456 (2.76)	728 (2.77)
		CHCl <sub>3</sub>	-	273, (4.01)	307, (3.94)	465, (2.90)	686, (2.63)
5B	4-OCH <sub>3</sub>	Ethanol	231 (4.17)	277 (3.80)	314 (3.70)	469 (2.77)	686 (2.78)
		CHCl <sub>3</sub>		277, (4.03)	307, (3.87)	464, (3.04)	686, (2.77)
6B	4-CH <sub>3</sub>	Ethanol	221 (4.04)	276 (3.63)	308, (3.72)	477 (2.70)	740, (2.77)
		CHCl <sub>3</sub>		279, (3.77)	308, (3.82)	469, (2.81)	694, (2.60)

Table 3:18 UV/visible spectral data for the N, N'-(aryl)benzaldiaminedichloridecopper(II) complexes

(Extinction coefficient in parentheses (log  $\epsilon$ , l/mol cm))

No	Assignment:		$n \rightarrow \zeta^*$ transition	$\pi \rightarrow \pi^*$ transition	CT (M $\rightarrow$ L)	CT (M $\rightarrow$ L)	$d \rightarrow d$ transition
	R	Solvent	200-240 nm	250-300 nm	305-350 nm	360-500 nm	505-900 nm
1C	4-NO <sub>2</sub>	Ethanol	211 (3.99)	267 (3.05)		-	859 (2.63)
		CHCl <sub>3</sub>	-	272 (3.76)	308 (3.54)	-	698 (2.22)
2C	4-Cl	Ethanol	226 (4.07)	271 (3.91)	308 (3.86)	-	860 (3.06)
		CHCl <sub>3</sub>	-	265 (3.82)	306 (3.90)	-	757 (2.78)
3C	4-Br	Ethanol	225 (4.05)	277 (3.73)	448 (3.43)		880 (2.43)
		CHCl <sub>3</sub>		268 (3.74)	473 (3.56)	-	866(2.11)
4C	H	Ethanol	272 (3.95)	281 (3.73)	308 (3.68)	-	857 (3.14)
		CHCl <sub>3</sub>	-	270 (3.76)	308 (3.64)	-	656 (2.58)
5C	4-CH <sub>3</sub>	Ethanol	221 (4.00)	275 (3.81)	308 (3.72)	-	619 (3.04)
		CHCl <sub>3</sub>	-	271 (3.84)	308 (3.67)	-	684 (2.31)
6C	4-OCH <sub>3</sub>	Ethanol	232 (4.07)	277 (3.88)	308 (3.63)	-	621 (3.01)
		CHCl <sub>3</sub>	-	275 (3.92)	308 (3.58)	-	719 (2.18)
7C	4-N(CH <sub>3</sub> ) <sub>2</sub>	Ethanol	-	262 (4.19)	316 (3.67)	405 (3.29)	562 (2.7)
		CHCl <sub>3</sub>	-	270 (5.01)	317 (4.78)	456 (4.72)	-

### 3.5 Electronic spectral data for the copper(I) and copper(II) complexes with N, N'-bis(cinnamaldehyde)-1, 2-diiminoethane

Table 3:19 UV/visible spectral data for the N, N'-bis(cinnamaldehyde)-1, 2-diiminoethanecopper(I)halide and copper(II) dihalide

(Extinction coefficient in parentheses (log  $\epsilon$ , l/mol cm))

No	Assignment:		$\pi \rightarrow \pi^*$ (benzene)	$\pi \rightarrow \pi^*$ (imine)	CT	$n \rightarrow \pi^*$ (imine)	CT (M $\rightarrow$ L)	d $\rightarrow$ d transition
	Complex	Solvent	250 - 300 nm	305 - 350 nm		360 - 400 nm	410 - 500 nm	500 -900 nm
21	CA <sub>2</sub> EN	DCM	249 (3.50)	masked	311 (4.82)	339 (3.76)	-	
22	N(CH <sub>3</sub> ) <sub>2</sub> -CA <sub>2</sub> EN	DCM	251 (3.67)	masked	317 (4.75)	mask		
1I	Cu(I)(CA <sub>2</sub> EN)Br	DCM	252 (3.85)	masked	321 (4.04)	-	442 (2.98)	-
2I	Cu(I)(CA <sub>2</sub> EN)Cl	DCM	250 (3.86)	masked	320 (4.00)	-	448 (2.90)	-
3I	Cu(I)(CA <sub>2</sub> EN)I	DCM	250 (3.87)	masked	320 (4.02)	-	449 (2.91)	-
4I	Cu(II)(CA <sub>2</sub> EN)Cl <sub>2</sub>	DCM	249 (3.75)	masked	313 (3.81)	389 (3.57)	-	741 (2.22)

### 3.6 Mid-infrared spectral data for the N, N'-(aryl)benzaldimine ligands

Table 3:20 The mid-infrared spectral data for the N, N'-(aryl)benzaldimine ligands

R	$\nu_{\text{C=N}}$
4-NO <sub>2</sub>	1649
4-Cl	1644
4-Br	1643
H	1614
4-CH <sub>3</sub>	1608
4-OCH <sub>3</sub>	1614
4-N(CH <sub>3</sub> ) <sub>2</sub>	1636

### 3.7 Mid-infrared spectral data for the N, N'-(aryl)benzaldiamine dihydrochloride salts

Table 3:21 The mid-infrared spectral data for the N, N'-(aryl)benzaldiamine dihydrochloride salts

R	$\nu\text{NH}_2^+$	$\delta\text{NH}_2^+$
4- NO <sub>2</sub>	2519	1598
4- Cl	2548	1589
4- Br-	2503	1598
H	2501	1587
4- CH <sub>3</sub>	2500	1605
4- OCH <sub>3</sub>	2597	1600

### 3.8 Mid-infrared spectral data for the N, N'-(aryl)benzaldiamine ligands and their copper(II) halide complexes

Table 3:22 The mid-infrared spectral data for the copper(II) N, N'-(aryl)benzaldiaminebromide and chloride complexes

R	$\nu$ N-H	$\nu$ H-N <sub>(CuBr)</sub>	$\nu$ H-N <sub>(CuCl)</sub>
4-NO <sub>2</sub>	3387	3209	3219
4-Cl	3380	3196	3215
4-Br	3357	3203	3213
H	3372	3212	3212
4-CH <sub>3</sub>	3269	3207	3208
4-OCH <sub>3</sub>	3359	3212	3212
4-N(CH <sub>3</sub> ) <sub>2</sub>	3365	3210	3214

### 3.9 Mid-infrared spectral data for the N, N'-bis(cinnamaldiimine) ligands and their copper(I) and copper(II) halide complexes

Table 3:23 The mid-infrared spectral data for the N, N'-bis(cinnamaldiimine) ligands and their copper(I) and copper(II) halide complexes

No	Compound	$\nu_{\text{C=N}}$
21	CA <sub>2</sub> EN	1615
22	N(CH <sub>3</sub> ) <sub>2</sub> -CA <sub>2</sub> EN	1620
1I	Cu(I)(CA <sub>2</sub> EN)Br	1625
2I	Cu(I)(CA <sub>2</sub> EN)Cl	1627
3I	Cu(I)(CA <sub>2</sub> EN)I	1627
4I	Cu(II)(CA <sub>2</sub> EN)Cl <sub>2</sub>	1618

### 3.1 References

1. E. Pretsch, P. Bühlman, C. Affolter, “*Structure determination of organic compounds: Table of spectral data*”, 3<sup>rd</sup> ed, Springer, Berlin, 2000.
2. E. Pretsch, J. Selbl, *Table of spectra data for structure determination of organic compounds*, 2<sup>nd</sup>, New York, Berlin:Springer, 1989.
3. M. Amirnasr, K. J. Schenk, M. Salavati, S. Dehghanpour, A. Taeb, A. Tadjarodi, *J. Coord. Chem*, 2003, **56**, 231-243.
4. S. Derinkuyu, K. Ertekin, O. Oter, S. Denizalti, E. Cetinkaya, *Dyes and Pigment*, 2008, **76**, 133-141.

## **4. DISCUSSION (PHYSICAL AND CHEMICAL STUDY)**

### **4.1 Elemental analyses**

#### **4.1.1 Micro-analyses of Schiff base ligands and their copper(II) halide complexes**

The proposed structure for the N, N'-(aryl)benzylaldimine based ligands (the imines, amines and amine salts) and their copper complexes are based upon the elemental analysis as shown in table 3.1, 3.2 and 3.3 and upon spectrometry data discussed below. In some cases a trace of water or other solvents was found in the crystal lattice. From the elemental analysis results, the ratio between the ligand and the metal ion was found to be 1:1, and the results show good agreement with proposed structures.

#### **4.1.2 Micro-analyses of N, N'-bis(cinnamaldiimine) ligands and their copper(I) halide and copper(II) dihalide complexes**

The data from the microanalysis for N, N'-bis(cinnamaldehyde)-1, 2-diiminoethane showed good agreement with the proposed structure, while the microanalysis for N, N'-bis(4-dimethylaminocinnamaldehyde)-1, 2-diiminoethane showed the presence of water. Both the microanalysis of copper(I) and copper(II) complexes of N, N'-bis(cinnamaldehyde)-1, 2-diiminoethane confirmed the 1:1 metal : ligand ratio. The data for the microanalyses is summarized in tables 6 and 7.

## 4.2 Mass spectrometry studies of Schiff base ligands

For this study electrospray mass spectrometry (ESI-MS) and atmospheric pressure chemical ionization (APCI-MS) were used for the characterization of the stoichiometry of the ligands in solution. ESI-MS uses a soft ionization technique to generate ions or to transform molecules in solution into ions, and the ions produced are negative. It generates less fragmentation and is suitable for polar and ionic compounds.

APCI is a method used in mass spectrometers to form ions from molecules. This method is very useful for non-polar substances and is a less soft ionization technique than ESI-MS. It was developed and optimized for Positive and Negative Ion Chemical Ionization. This ionization technique can produce multiple charged molecules  $[M + nH]^{n+}$ , depending on the type of solvent used.

Both ESI and APCI were found to be useful for the study of *para*-substituted Schiff base ligands, and they both confirmed the expected molecular weights of the obtained compounds.

#### 4.2.1 APCI-MS studies of the N, N'-(aryl)benzaldimine ligands

The solutions of N, N'-(aryl)benzaldimine ligands in chloroform were characterized with atmospheric pressure chemical ionization, which confirmed the structure of the expected compounds. The observed parent ion  $m/z$  values for N, N'-(aryl)benzaldimine ligands are listed in table 3.1. The  $m/z$  values for the parent ions of all the N, N'-(aryl)benzaldimine ligands showed a high mass ions due to  $[M + 2H]^+$  and this is due to the presence of the two imine groups within the N, N'-(aryl)benzaldimine ligand. To illustrate the behaviour of the Schiff bases the mass spectra obtained for N, N'-*bis*(4-dimethylaminobenzyl)-1, 2-diiminoethane, N, N'-*bis*(4-chlorobenzyl)-1, 2-diiminoethane and N, N'-*bis*(4-bromobenzyl)-1, 2-diiminoethane are shown in figure 4.2.1, 4.2.2 and 4.2.3.

For the mass spectrum studies of the N, N'-*bis*(4-dimethylaminobenzyl)-1, 2-diiminoethane is note that the expected parent ion  $m/z$  value for the ligand,  $\{(N(CH_3)_2-BEN)\}$  is  $[M + 4H]$  due to the additional two available  $(CH_3)_2N$  groups of the ligand, but only  $[M + 2H]^+$  is observed. This indicates that the protonation of the  $(CH_3)_2N$  group of the Schiff base,  $\{(N(CH_3)_2-BEN)\}$  is not stable in the mass spectrometer.

The mass spectrum of N, N'-*bis*(4-dimethylaminobenzyl)-1, 2-diiminoethane  $\{(N(CH_3)_2-BEN)\}$  (Fig 4.2.1), shows a molecular ion ( $M^{2+}$ ) peak at  $m/z$  324 and the presence of another species at  $m/z$  186. The fragment at  $m/z$  186 came from cleavage of the amine ligand.<sup>1, 2</sup> It has been shown that in APCI nitrogen-aromatic compounds such as imines are reduced to the corresponding amines.<sup>1, 2</sup> The degree of the reduction was found to be dependent on the compound, the nature of the solvent and the temperature of the nebulizer probe. The reduction of the imines it is known to be more prominent in protic solvents such as methanol, water and in acid solutions. These complicate the APCI-MS spectra. This process can be limited by using dried acetonitrile or methylene chloride solvent.

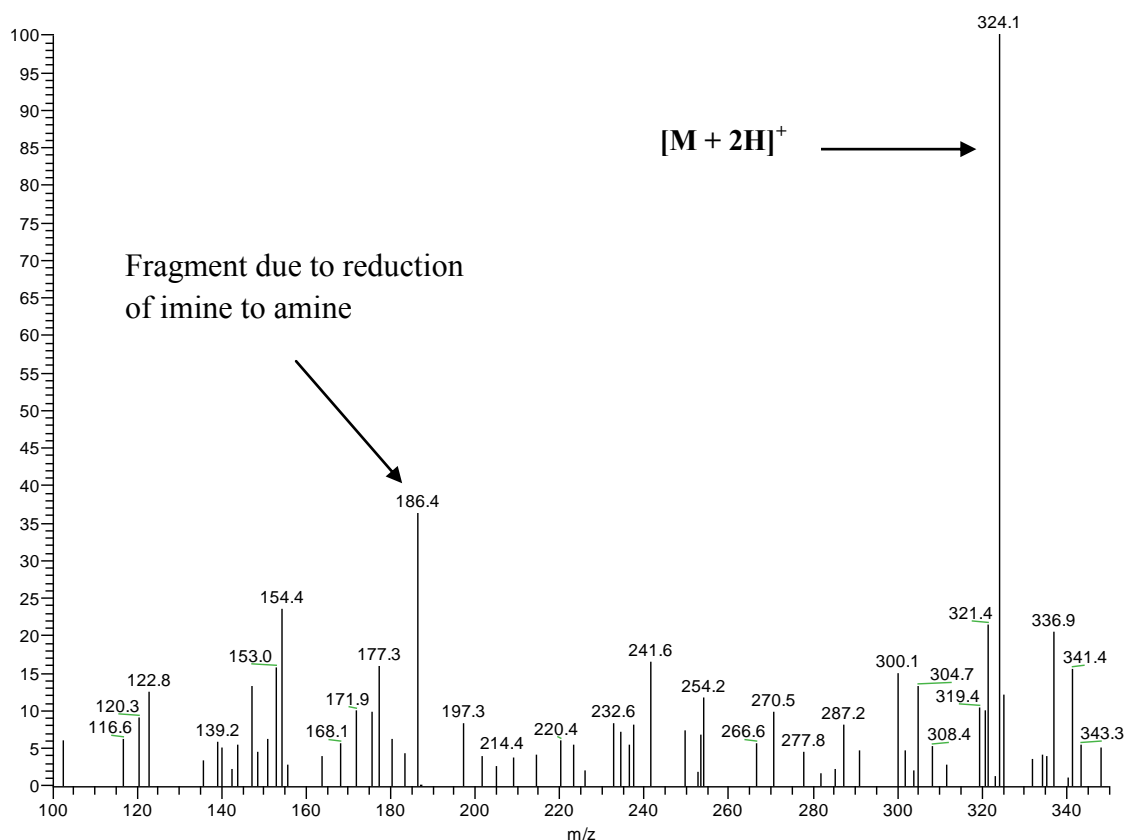


**Figure 4.2.1 APCI-MS spectrum obtained for  $N(CH_3)_2$ -BEN in chloroform solution**

The mass spectra of the Cl and Br analogues are shown in figure 4.2.2 and 4.2.3. From the mass spectrum of the Schiff base, Cl-BEN, the signal at  $m/z$  306 corresponds to  $[M + 2H]^+$  for two  $^{35}Cl$ . The signal at  $m/z$  308 is due to  $^{35}Cl$  and  $^{37}Cl$  for  $[M + 2H]^+$ . At  $m/z$  310 the weak signal corresponds to  $[M + H]^+$  for the two  $^{37}Cl$ . From the mass spectrum of the Cl-BEN can be concluded that the ratio is 9:6:1 due to the relative heights of the 306.4, 308.4 and 310.4 lines. The pattern of the three peaks in the spectrum of Cl-BEN confirms clearly that the ligand contains two chlorides with the natural chlorine isotope distribution of  $^{35}Cl$  and  $^{37}Cl$  (75.77 % and 24.23 %, respectively) <sup>3</sup>.

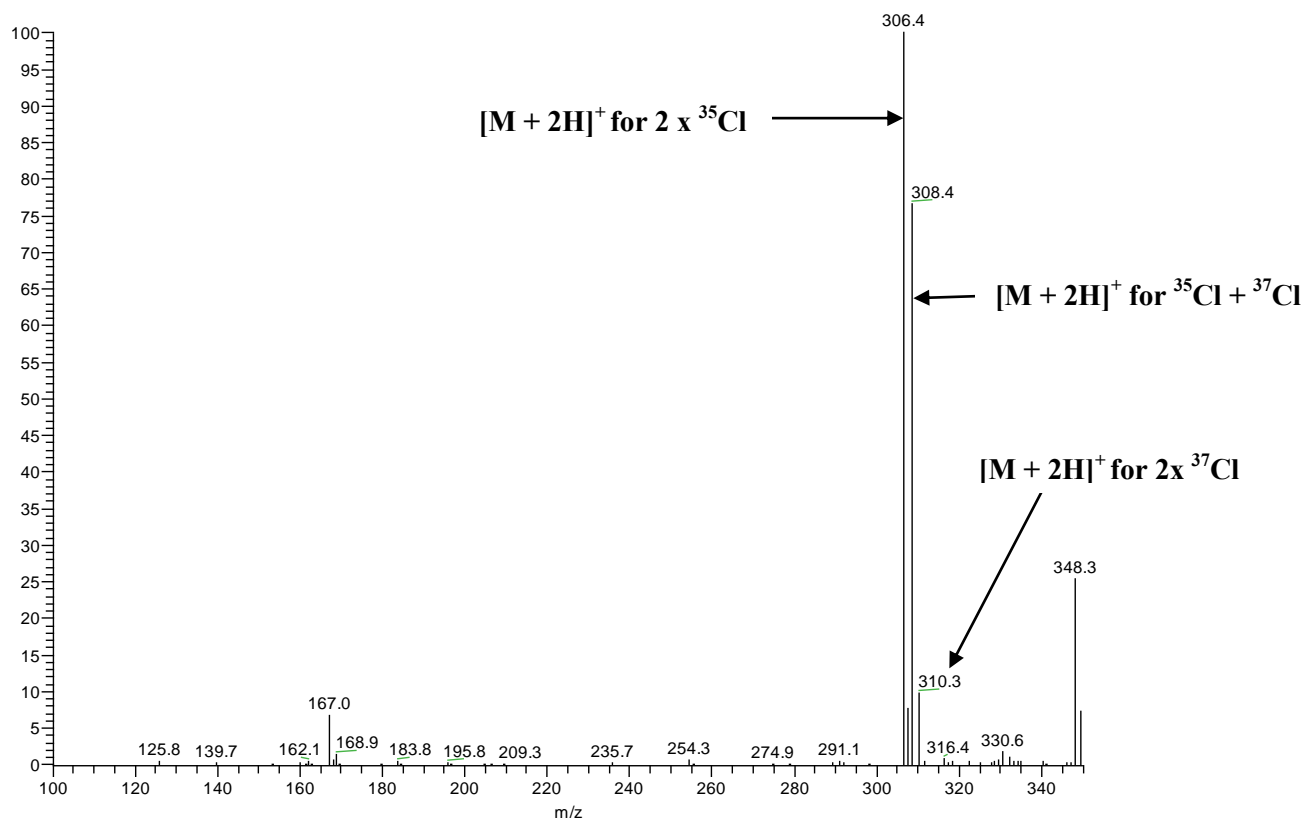


**Figure 4.2.2 APCI-MS spectrum obtained for Cl-BEN in chloroform solution**

The mass spectrum of Br-BEN, show a mass ion at m/z 393.9 due to  $[M + 2H]^+$  for two <sup>79</sup>Br, the alternative explanation for this is signal may be due to  $[M]^+$  for <sup>79</sup>Br and <sup>81</sup>Br. At m/z 394.8 the parent ion corresponds to  $[M + H]^+$  for <sup>79</sup>Br and <sup>81</sup>Br. The ion peak at m/z 395.9 corresponds to  $[M + 2H]^+$  for <sup>79</sup>Br and <sup>81</sup>Br, with the alternative explanation  $[M]^+$  for two <sup>81</sup>Br. The latter interpretation is unlikely give the absence of a  $[M]^+$  for two <sup>79</sup>Br. The strong signal at m/z 396.9 is due to  $[M + H]^+$  for two <sup>81</sup>Br. The signal at m/z 398.1 corresponds to  $[M + 2H]^+$  for two <sup>81</sup>Br. The relative heights of the peaks observed in the mass spectrum of Br-BEN demonstrate clearly that the Schiff base consists of the mixture of <sup>79</sup>Br and <sup>81</sup>Br, the apparent abundance of <sup>81</sup>Br is a reflection of two bromines in the molecule <sup>3</sup>. The natural abundance for <sup>79</sup>Br and <sup>81</sup>Br are 50.52 % and 49.48 % respectively <sup>3</sup>.

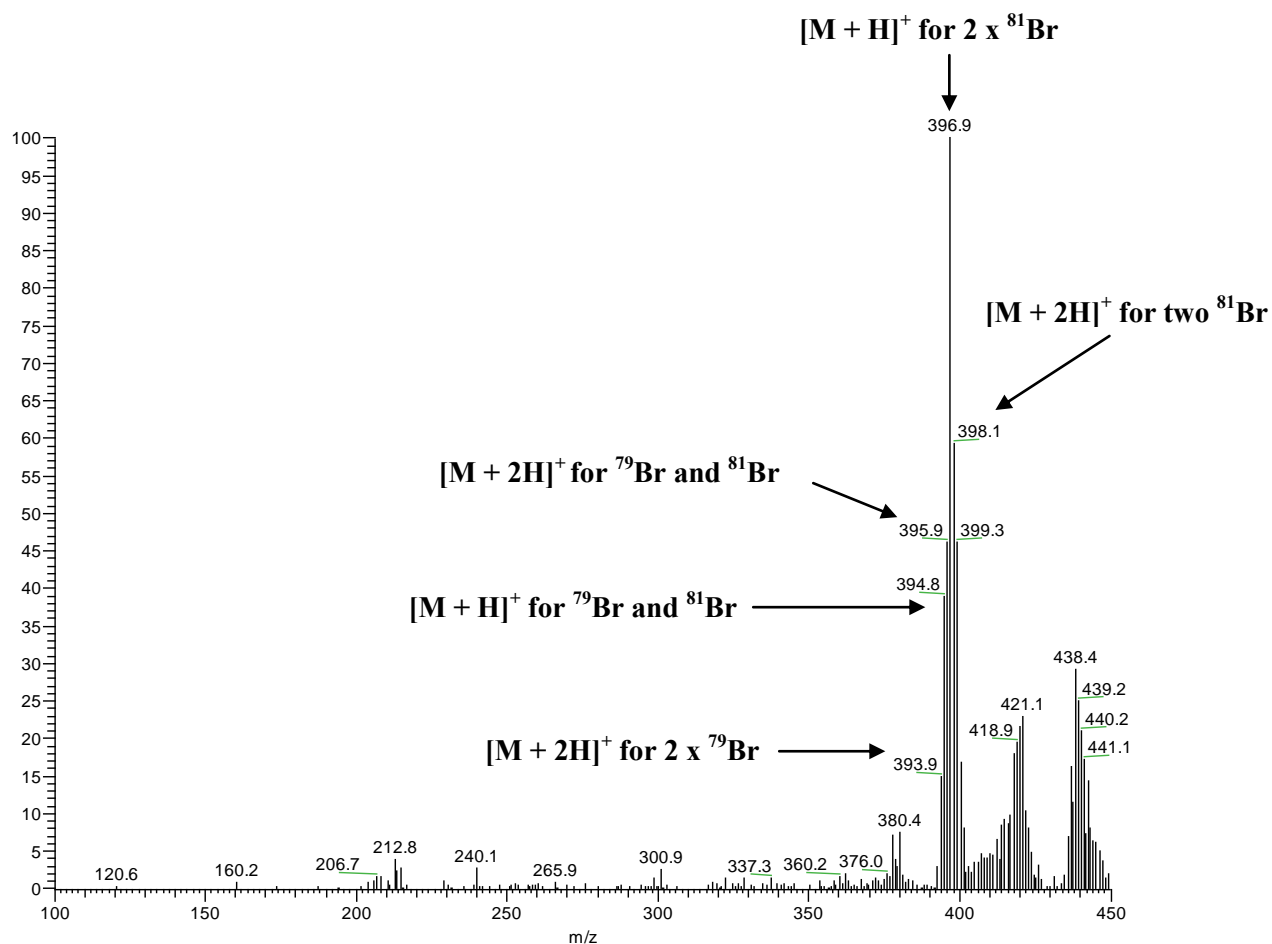
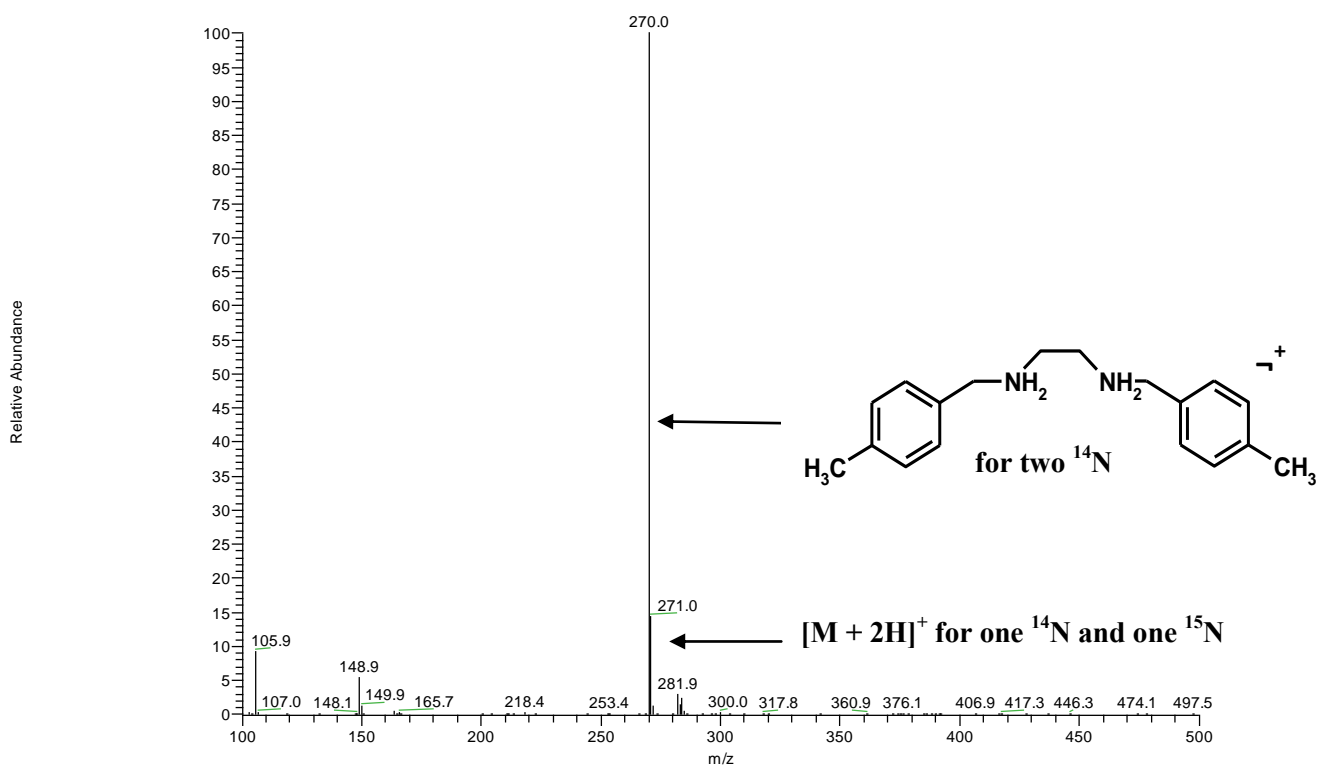


Figure 4.2.3 APCI-MS spectrum obtained for Br-BEN in chloroform solution

#### 4.2.2 APCI-MS and ESI studies of the N, N'-(aryl)benzaldiamine dihydrochloride salts

The mass spectra of the N, N'-(aryl)benzaldiamine dihydrochloride ligands were analysed with atmospheric pressure chemical ionization and with electrospray ionization in deionised water solutions. The mass spectra of the N, N'-(aryl)benzaldiamine dihydrochloride salts are shown in figures 4.2.4, 4.2.5 and 4.2.6. The m/z values for the parental ion of all the amine ligand salts showed higher mass ions due to  $[M + H]^+$ . The results obtained from the mass spectra of the ligands confirmed the structure of the expected ligands. The observed parent ion m/z values for all the N, N'-(aryl)benzaldiamine dihydrochloride ligands are listed in table 3.2.



**Figure 4.2.4 APCI spectrum obtained for (CH<sub>3</sub>)-BENH•2HCl in water**

The mass spectrum of the N, N'-*bis*(4-methylbenzyl)-1, 2-diaminoethane dihydrochloride ligand is shown in figure 4.2.4. The mass spectrum shows a base peak at m/z 270 which corresponds to [M + 2H]<sup>+</sup> for two <sup>14</sup>N, and at m/z 271 a higher mass ion is observed and the signal corresponds to [M + 2H]<sup>+</sup> for <sup>14</sup>N and possibly <sup>15</sup>N. The natural abundance of <sup>14</sup>N and <sup>15</sup>N are 100 and 0.4 %.

The bromide and chloride analogues of the N, N'-(aryl)benzaldiamine dihydrochloride ligands were characterized with electrospray ionization for two reasons:

- (i) For better mass spectral resolution for both bromide and chloride analogues.
- (ii) For an easy comparison between the N, N'-(aryl)benzaldiamine dihydrochloride and N, N'-(aryl)benzaldiamine ligands.

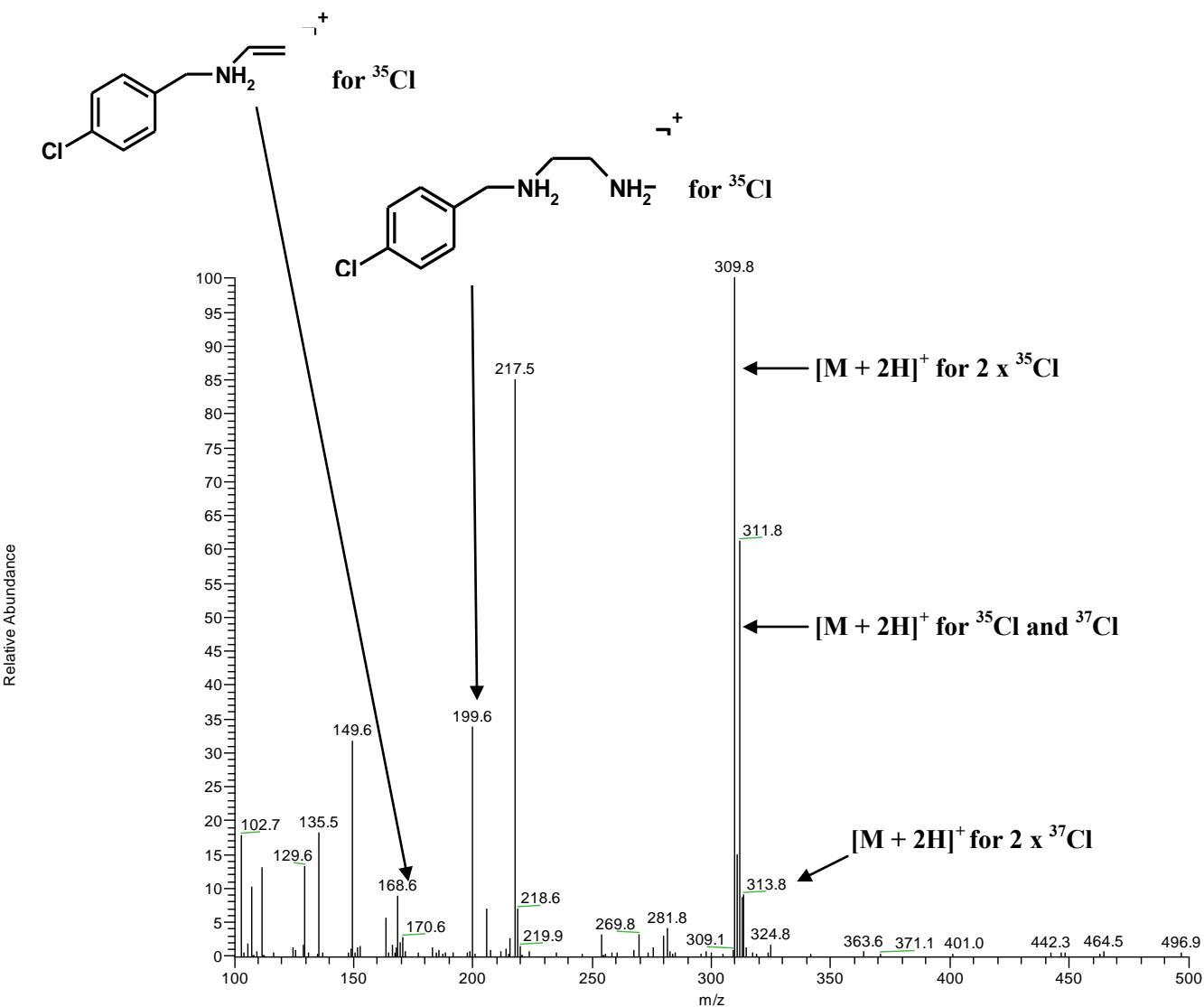


**Figure 4.2.5 ESI spectrum obtained for Cl-BENH•2HCl in water**

The mass spectrum of N, N'-bis(4-chlorobenzyl)-1, 2-diaminoethane dihydrochloride (fig 4.2.5) shows a strong signal or parent ion at m/z 309.8 that corresponds to  $[\text{M} + 2\text{H}]^+$  for 2 x  $^{35}\text{Cl}$ . The signal at m/z 311.8 represents  $[\text{M} + 2\text{H}]^+$  for  $^{35}\text{Cl}$  and  $^{37}\text{Cl}$ , while the weak signal at m/z 313.8 corresponds to  $[\text{M} + 2\text{H}]^+$  for two  $^{37}\text{Cl}$ . The signals at m/z 199.8 and at m/z 168.6 are the result of the fragmentation of the molecule. The relative heights of the peaks due to the isotopes pattern shows a 9:6:1 ratio, typical for a molecule with two chlorines<sup>3</sup>.

From the electrospray ionization mass spectrum of the *N, N'*-bis(4-bromobenzyl)-1, 2-diaminoethane dihydrochloride (fig 4.2.6), the amine salt shows a typical bromide isotope pattern. At  $m/z$  398.4 a parent ion which corresponds to  $[M + 2H]^+$  for two  $^{79}\text{Br}$  is observed. The signal at  $m/z$  400.1 represents  $[M + 2H]^+$  for  $^{79}\text{Br}$  and  $^{81}\text{Br}$  as has been discussed above the alternative explanation for the signal is  $[M + 2H]^+$  for two  $^{79}\text{Br}$ . The signal at  $m/z$  402.1 is due to  $[M + 2H]^+$  for two  $^{81}\text{Br}$ . The isotope pattern of the *N, N'*-bis(4-bromobenzyl)-1, 2-diaminoethane dihydrochloride ligand indicates the natural isotopes distribution of any compound containing a single Br group in an approximately 1:1 ratio as observed for the *N, N'*-bis(4-bromobenzyl)-1, 2-diaminoethane analysis discussed above.

The signals at  $m/z$  122.1 and 312.5 correspond to the fragmentation of the ligand as presented in the figure below (fig 4.2.6)

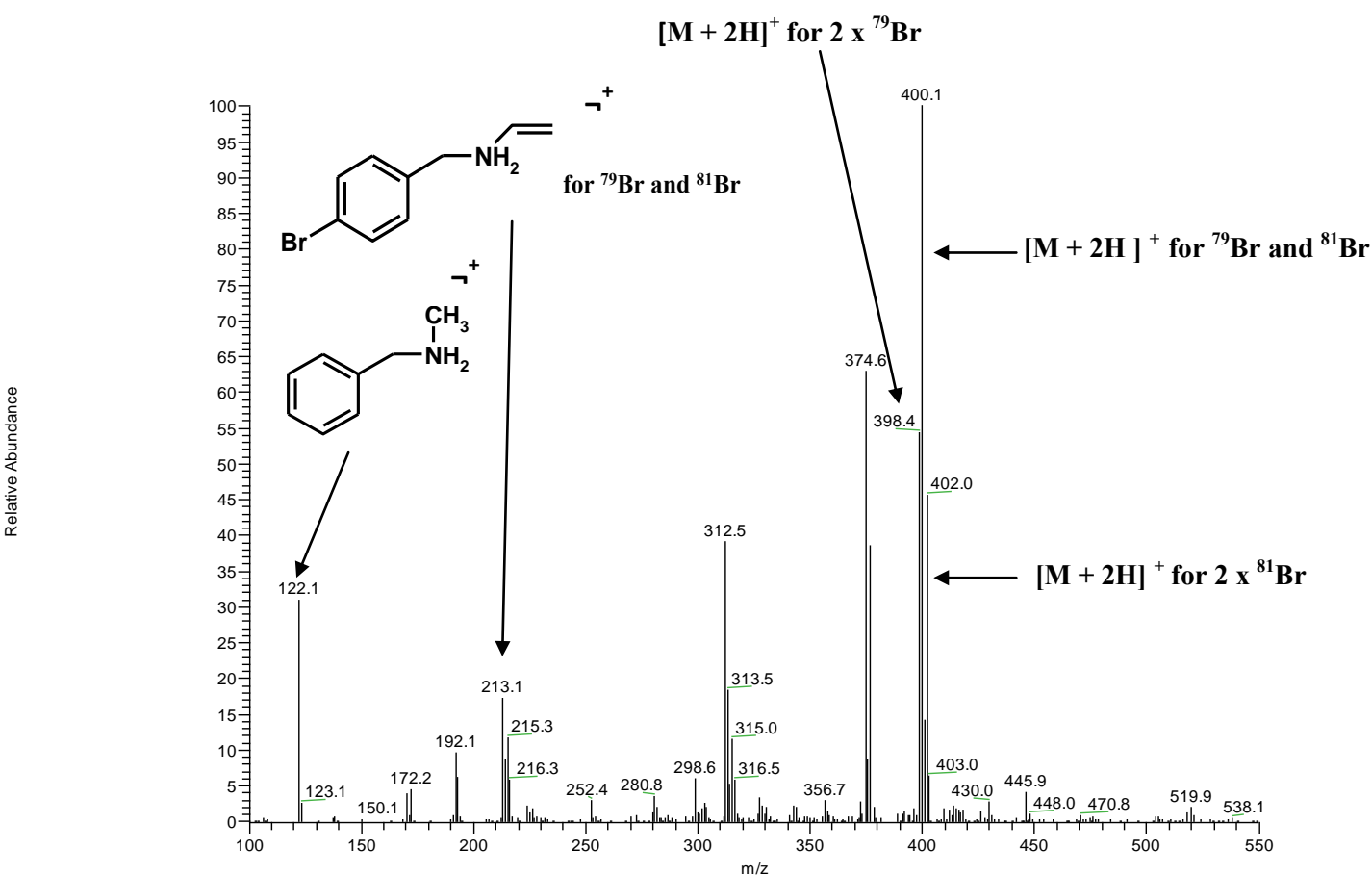


Figure 4.2.6 ESI spectrum obtained for Br-BENH•2HCl in water

### 4.2.3 ESI-MS studies of N, N'-(aryl)benzaldiamine ligands

The N, N'-(aryl)benzaldiamine ligands were all characterized with electrospray ionization mass spectrometry in methanol. The ESI mass spectra of the N, N'-(aryl)benzaldiamine ligands showed a very strong signal due to the molecular ion peak for all the N, N'-(aryl)benzaldiamine ligands. The parent ion  $m/z$  values for the ligands were the  $[M + 2H]^+$  ion, and are listed in table 3.3. The mass spectra of N, N'-bis(4-chlorobenzyl)-1, 2-diaminoethane and N, N'-bis(4-bromobenzyl)-1, 2-diaminoethane are shown in figures 4.2.7 and 4.2.8.

The mass spectrum of N, N'-bis(4-chlorobenzyl)-1, 2-diaminoethane shows a mass ion at  $m/z$  310.6 which corresponds to  $[M + 2H]^+$  for two  $^{35}\text{Cl}$ . At  $m/z$  312 a signal due to  $[M + 2H]^+$  for  $^{35}\text{Cl}$  and  $^{37}\text{Cl}$  is observed and the alternative explanation for this signal is  $[M]^+$  for two  $^{37}\text{Cl}$ . The alternative explanation is unlikely given the absence of  $[M]^+$  for two  $^{35}\text{Cl}$  and  $[M]^+$  for  $^{35}\text{Cl}$  and  $^{37}\text{Cl}$ . The signal at  $m/z$  313.5 corresponds to  $[M + H]^+$  for two  $^{37}\text{Cl}$ . At  $m/z$  314 the signal is due to  $[M + H]$  for two  $^{37}\text{Cl}$ . This pattern indicates the presence of two halogens ( $^{35}\text{Cl} : ^{37}\text{Cl}$  of 75.77 : 24, 23).

It can be concluded, due to the isotope patterns, that the parent ion for the Cl-BEN•2HCl in water (fig 4.2.5) is similar to that of the Cl-BENH in methanol (fig 4.2.7). But it is observed that the manner in which the fragmentation in the mass spectrum of Cl-BEN•2HCl in water occurs is more complicated and complex below  $m/z$  250 when compared to the Cl-BENH in methanol. This is because of the nature of the solvent used for each analysis, and the intense signals observed in the Cl-BEN•2HCl spectrum are the indication of stabilisation of the fragmentations due to the use of water as solvent.

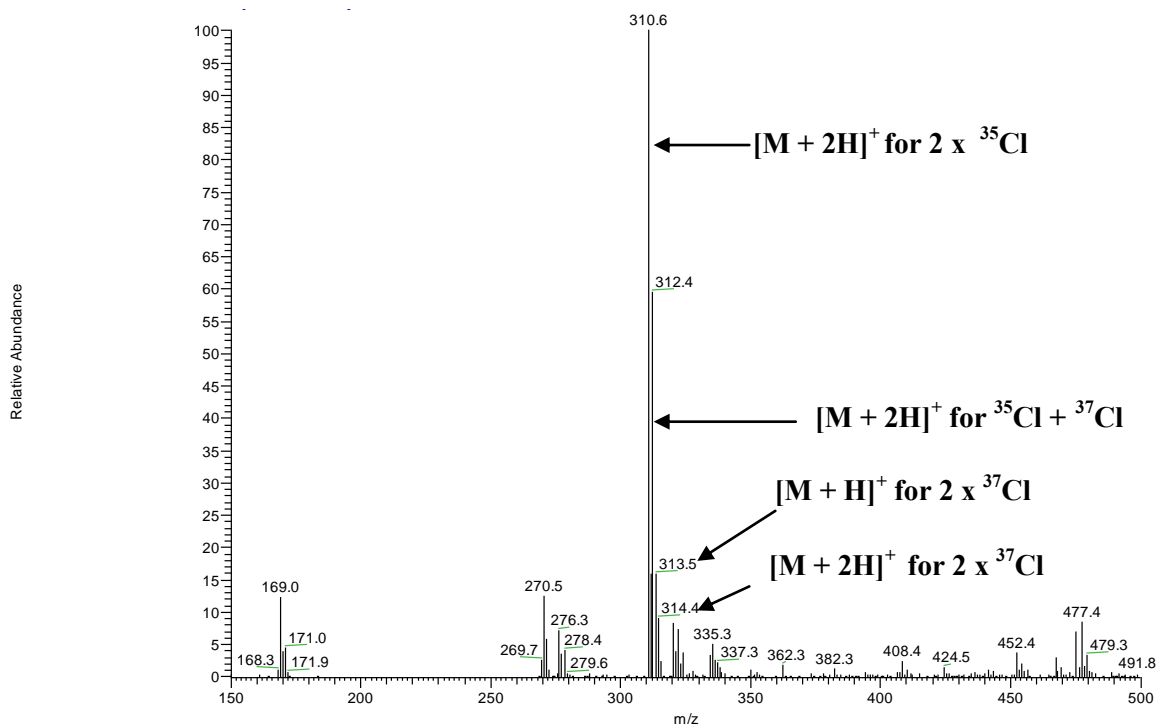


**Figure 4.2.7** ESI spectrum obtained for Cl-BENH in methanol

The mass spectrum of the N, N'-bis(4-bromobenzyl)-1, 2-diaminoethane shows three signals which correspond to the isotope pattern at  $m/z$  398.3,  $m/z$  400.2 and  $m/z$  402.1. The signal at  $m/z$  398.3 represents  $[M + 2H]^+$  for two  $^{79}\text{Br}$  and the alternative explanation is  $[M]^+$  for  $^{79}\text{Br}$  and  $^{81}\text{Br}$ . The molecular peak at  $m/z$  400.2 corresponds to  $[M + 2H]^+$  for  $^{79}\text{Br}$  and  $^{81}\text{Br}$  and the alternative explanation for this signal is  $[M]^+$  for two  $^{81}\text{Br}$ . However the alternative explanations are unlikely, given that there is no signal at  $m/z$  396 due to  $[M]^+$  for two  $^{79}\text{Br}$ . The parent ion at  $m/z$  402.1 is due to  $[M + 2H]^+$  for two  $^{81}\text{Br}$ . From the mass spectrum of the amine ligand it can be concluded from the relative heights of the peaks that the ratio of the isotope pattern is 9:6:1, typical of dibrominated molecule<sup>3</sup>.

The fragments at  $m/z$  169.8 and  $m/z$  212.7 correspond to the cleavage of the N, N'-bis(4-bromobenzyl)-1, 2-diaminoethane as shown in figure 4.2.8.

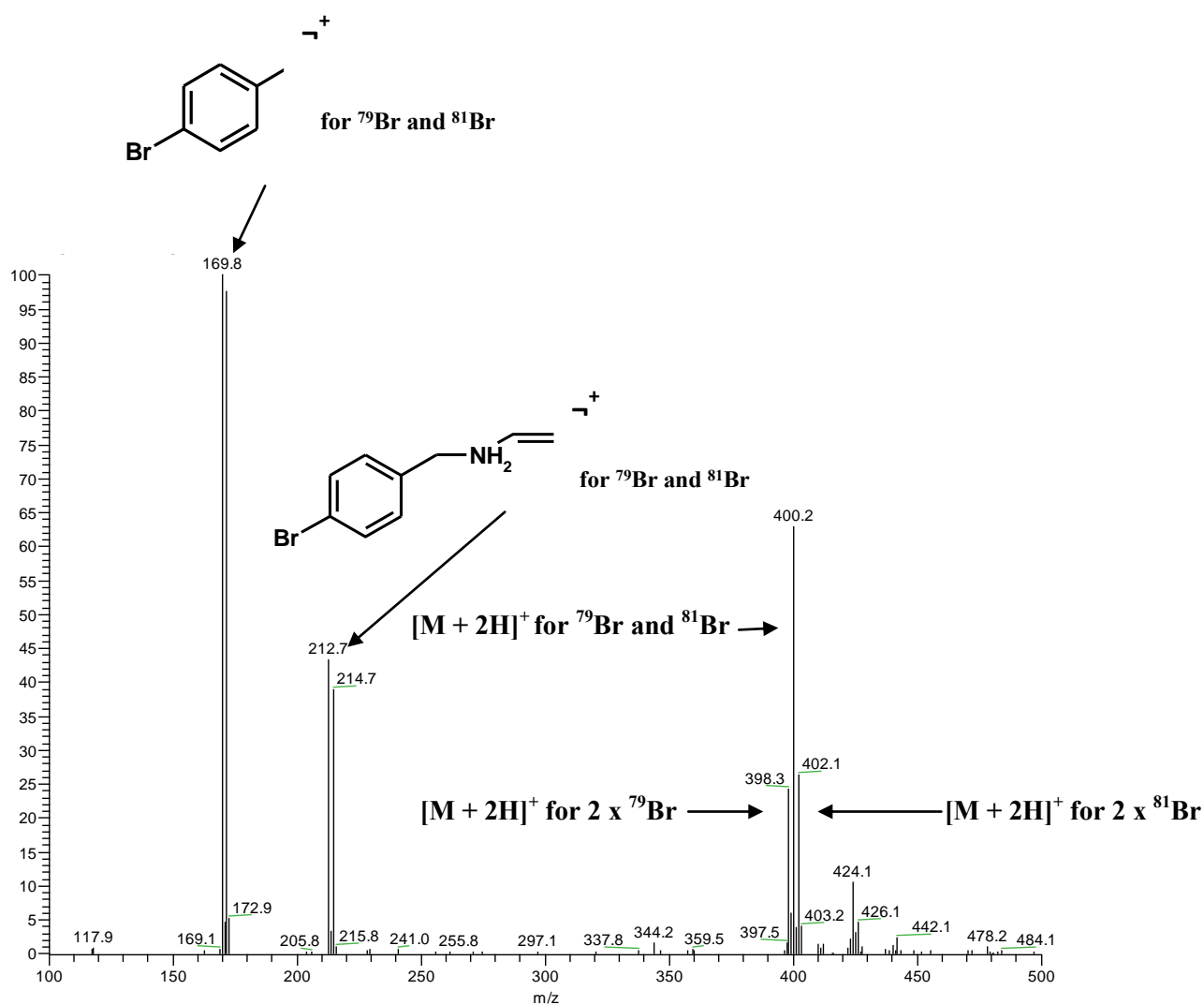


Figure 4.2.8 ESI spectrum obtained for Br-BENH in methanol

#### 4.2.4 Comparison between the mass spectral patterns of the ligands

##### N, N'-(aryl)benzaldiamine ligands and N, N'-(aryl)benzaldiamine dihydrochloride salts

From the mass spectrometry studies of N, N'-(aryl)benzaldiamine ligands and N, N'-(aryl)benzaldiamine salts (tables 3.2 and 3.3) it may be concluded that base peak for the imines and the amine ligands were  $[\text{M} + \text{H}]$  and  $[\text{M} + 2\text{H}]^+$ . This shows that these ligands easily pick up protons. This is due to the lone pair electrons on the nitrogen atom of the molecule. The studies indicate that the base peak of the amine salts is the already existing  $[\text{M}$

+ 2H]<sup>+</sup> of the amine salts. This implies that the N, N'-(aryl)benzaldiamine salts are very stable in the mass spectrometer compared to the N, N'-(aryl)benzyaldiamine ligands.

#### **4.2.5 Comparison between the mass spectral patterns of the N, N'-(aryl)benzaldiamine dihydrochloride salts analogues**

The distinct difference observed between the fragmentation pattern in the mass spectra of the N, N'-*bis*(4-bromobenzyl)-1, 2-diaminoethane dihydrochloride (fig 4.2.6) and N, N'-*bis*(4-chlorobenzyl)-1, 2-diaminoethane dihydrochloride ligands (fig 4.2.5) may be associated with the differences in the electron clouds of the two halogen atoms, chlorine and bromine. Bromine is more polarisable compared to the chlorine as its electron shell is larger than that of chlorine. This will alter the stability of the ions produced in the mass spectrometer, so explaining the difference in their respective patterns.

The ESI mass spectra of the amine ligands in methanol solutions, Cl-BENH and Br-BENH (fig 4.2.7 and 4.2.8) exhibit some differences in the fragmentation pattern. In the mass spectrum of Br-BENH in methanol, two sharp peaks at *m/z* 169.8 and *m/z* 212.7 are observed, while in the mass spectrum of Cl-BENH no intense signals are observed in that region. This is the result of the bromo analogue being more polarisable than the chloro analogue.

### **4.3 <sup>1</sup>H- and <sup>13</sup>C-NMR studies**

#### **4.3.1 Linear Free Energy Relationship and NMR chemical shifts**

NMR chemical shifts have been used to exploit and evaluate the electronic effect (inductive, resonance, steric and polar effects) produced by the substituents, because of the important information they provide to study perturbations in electronic density, especially with <sup>1</sup>H- and <sup>13</sup>C-NMR. Electron density is the measure of the probability of an electron released by a

substituent (donating or withdrawing groups) being present at a specific location within the molecule.

The effects of the substituents may be monitored using  $^1\text{H}$ - and  $^{13}\text{C}$ -NMR substituent chemical shifts based on the principles of linear free energy relationships (LFER) comprising the single substituent parameters (SSP) or dual substituent parameters (DSP). This is achieved by correlating the substituent parameters (SSP or DSP) with the  $^{13}\text{C}$ - or  $^1\text{H}$ -NMR shifts to obtain a correlation coefficient and the resultant trend. The slope of the trend-line indicates the extent to which the spectroscopic properties are influenced by the substituent.

Single substituent parameters can be ascribed by the classical Hammett equation while the dual substituent parameters are used in determining both the inductive and resonance effect transmitted by the substituent within the molecule. The Hammett equation <sup>4, 5</sup> is given in equation 1. The equation represent a combination of inductive and resonance effects.

$$\log(k / k_0) = \rho\zeta \dots\dots\dots (1)$$

Dual substituent parameters, such as Swain <sup>6</sup> and Williams & Norrington <sup>7</sup> allow the separation and identification of the relative contributions of inductive and resonance electronic influence by the substituent on chemical reactivities and physical properties. These dual substituent parameters are an example of the extension of the Hammett equation and are described using equation 2.

$$\text{Log}(k / k_0) = \rho_I\zeta_I + \rho_R\zeta_R \dots\dots\dots (2)$$

A negative  $\rho$  value is an indication of a positive charge within the ring and positive values indicate resonance stabilization. When the signs of  $\rho_I$  and  $\rho_R$  are opposing each other, Taft <sup>8</sup>

explains this as an indication of a charge migration going from reactant to the transition state, for example a positive charge moving towards the substituent.

#### 4.3.2 $^1\text{H}$ - and $^{13}\text{C}$ -NMR studies of N, N'-(aryl)benzaldimine ligands

In this section, the attention will be on the effect produced by substituents, this will be done by using the slope of the resultant trend line.

The spectra were all run in deuterated chloroform. The  $^1\text{H}$ - and  $^{13}\text{C}$ -NMR spectral data for the assignment of the carbon and proton signals was followed using figure 4.1. Chemical shifts for the Schiff bases together with the relevant assignment are provided in tables 3:9 and 3:10. The data obtained supports the structures presented in scheme 2:1.

From the spectroscopic data obtained from the  $^{13}\text{C}$ -NMR studies of the N, N'-(aryl)benzaldimine ligands, given in table 3.10, it can be concluded that the electron-donor substituents {4- $\text{CH}_3$ , 4- $\text{OCH}_3$  and 4- $\text{N}(\text{CH}_3)_2$ } on the benzene ring of the Schiff base cause an increase of electron density at C-5 and C-3 (upfield shifts; see chapter 3, table 3.10). The same electron donor substituents decrease the electron density at C-6 (downfield shifts) as shown in table 4.1. The spectroscopic data from the  $^1\text{H}$ -NMR studies (table 3.11) indicate that the electron donor substituents at *para*-positions of the benzene ring of the Schiff base cause an increase of electron density at H-5, H-2, and H-1 (except for the 4- $\text{CH}_3$ ). The same substituents cause a decrease of electron density at H-4. This means that the sequence of the electron density for the hydrogen atom is as follows: H-5 >> H-4, H-2 >> H-4, H-2 >> H-1 and H-1 > H-4.

The manner in which the electron donor substituents influence the chemical shifts of the ring carbon and ring protons of the N, N'-(aryl)benzaldimine ligands was found to be similar to the behaviour of the ring protons and ring carbons of the Titanocene benzoates <sup>9</sup>.

Table 4.1 Trends of the electron donor substituents on the N, N'-(aryl)benzaldimine ligands

	6	5	4	3	2	1
$^1\text{H}$	—	↑	↓	—	↑	↑
$^{13}\text{C}$	↓	↑	↓	↑	↑	↓

↑ = Upfield shift, ↓ = Downfield shift

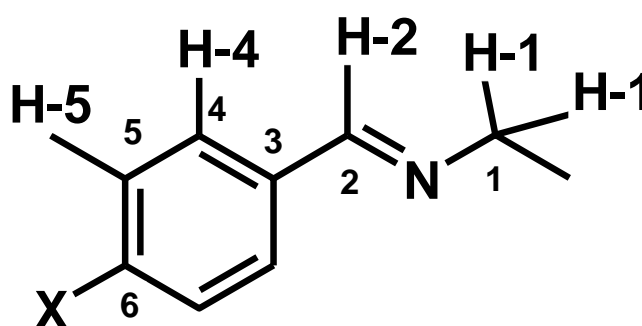


Figure 4.3.1 Numbering system used for the Schiff bases

Early work has shown that there is no simple relationship that exists between the proton or carbon chemical shifts and the substituents, this cannot easily be explained by the relationship that exists between the chemical shifts and the local electron densities <sup>10</sup>.

From the above observation it can be deduced that the electronic effect subjected onto the carbon and hydrogen atoms of the N, N'-(aryl)benzaldimine ligands by the donor substituent may not be clearly understood by using Hammett parameters only, this shows the need for the use of dual parameters, because there is no simply general relationship that exists between the  $^1\text{H}$ - and  $^{13}\text{C}$ -NMR chemical shifts and the local electron density .

The opposite trends were observed for electron-acceptor substituents as compared to those of electron-donor substituents. Since the Hammett parameters<sup>3, 4</sup> use the combined inductive and resonance effect, dual substituent parameters such as those of Swain<sup>5</sup> and of Williams & Norrington<sup>6</sup> may be suitable to measure the separately the contributions of inductive and resonance effect on the N, N'-(aryl)benzaldimine ligands.

The Hammett constants are derived from the protonation of a substituted benzoic acid and Swain constants are also based on the aromatic system. Both these parameters are applicable in monitoring the effect of the substituents on the carbon atoms of aromatic ring of the Schiff base ligands. The Williams & Norrington parameters are based on the aliphatic system and should be more applicable to understand the electronic effect on the side chain of the Schiff base ligands.

According to the size of the correlation coefficient obtained between the correlation of the <sup>1</sup>H-NMR chemical shifts and the three substituent parameters {(Hammett ( $\zeta_p$ ), Swain ( $\zeta_R$ ) and Williams & Norrington ( $\zeta_R$ ))}, the results indicate that there is a positive resonance correlation at positions H-5, H-2 and H-1 (see table 4.2), this implies that the conjugation of the electrons from the substituent move up to the nitrogen atom (see table 4.2 and figure 4.3.2).

In addition, looking at the sign of the constants  $\rho$  from table 4.2, similar observations are observed. All the parameters, Hammett ( $\zeta_p$ ), Swain and Williams & Norrington suggest a conjugation of the electrons up to the nitrogen atom for the correlation of protons.

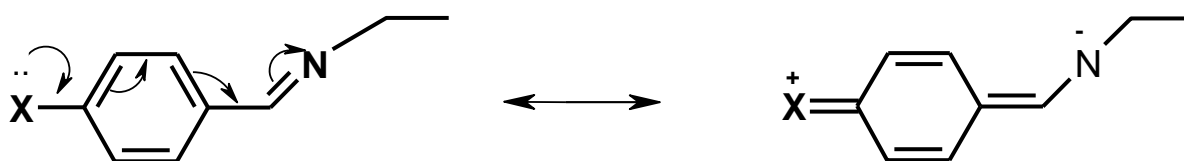


**Figure 4.3.2 The delocalisation of electrons to the imine nitrogen**

Table 4.2 Correlation coefficients for protons derived from the H-NMR data of N, N'-(aryl)benzaldimine ligands and various substituents parameters

Parameters	Correlation coefficient			
	H-5	H-4	H-2	H-1
Hammett ( $\zeta_p$ )	0.9478	0.3334	0.7988	0.7826
Swain ( $\zeta_I$ )	0.6414	0.4611	0.1303	0.1629
Swain ( $\zeta_R$ )	0.9048	0.1577	0.7822	0.7617
Williams & Norrington ( $\zeta_I$ )	0.6652	0.4573	0.4812	0.4661
Williams & Norrington ( $\zeta_R$ )	0.9162	0.1543	0.8295	0.8142

Table 4.3 Correlation coefficients for carbons derived from the  $^{13}\text{C}$ -NMR data of N, N'-(aryl)benzaldimine ligands and various substituents parameters

Parameters	Correlation coefficient					
	C-6	C-5	C-4	C-3	C-2	C-1
Hammett ( $\zeta_p$ )	-0.0214	0.6389	-0.0119	0.9575	-0.6715	-0.2499
Swain ( $\zeta_I$ )	0.2552	-0.2616	0.7491	0.1085	-0.8969	0.0009
Swain ( $\zeta_R$ )	-0.4584	0.8027	-0.3057	0.9747	-0.3705	-0.2967
Williams & Norrington ( $\zeta_I$ )	-0.0019	0.2091	0.5376	0.6063	-0.9644	-0.1215
Williams & Norrington ( $\zeta_R$ )	0.4795	0.7999	-0.4154	0.9771	-0.2817	-0.2812

While for the carbon atoms of the N, N'-(aryl)benzaldimine ligands no positive resonance correlation is observed up through the side chain using the three substituent parameters {(Hammett ( $\zeta_p$ ), Swain ( $\zeta_R$ ) and Williams & Norrington ( $\zeta_R$ ))}, see table 4.3. The only positive resonance correlation observed for the carbon atoms is at C-5 and C-3, this is expected due the distance between the substituents and positions five and three. The

correlation analysis shows a negative inductive effect at C-2, and this was better described by Williams & Norrington parameters. This is not surprising, because the parameters are derived from aliphatic system. The results for the carbon chemical shifts indicate that the phenyl ring is not parallel to the imine bond, and that there is no conjugation into the side chain. Clearly the apparent conjugation indicated by the proton spectral must be due to the through space interaction.

Using both the size and sign of the correlation coefficient obtained from the correlation between the proton chemical shifts and the substituent parameters, evidence of the conjugation observed in the proton spectrum, may be associated with the flexibility of the molecule. A model of the system shows that the rotation of the N, N'-(aryl)benzaldimine ligand about the methylene bridge brings H-1 and H-2 under the benzene ring, see figure 4.3.3. This would allow the H-2 and H-1 to be affected by the electron cloud of the benzene ring and increasing the inductive effect through space, as shown in figure 4.3.3. From the statements mentioned above it can be concluded that there is no electron delocalization from the substituent up to the imine group. This shows that the phenyl group is not parallel with the azomethine functional group<sup>11</sup>. The absence of the through space inductive effect within the carbon atoms is due to the distance between the carbon atoms (C-2 or C-1) and the electron cloud generated by the benzene ring. This system should possibly be examined more through molecular modelling studies as it might give greater insight into what is happening here.

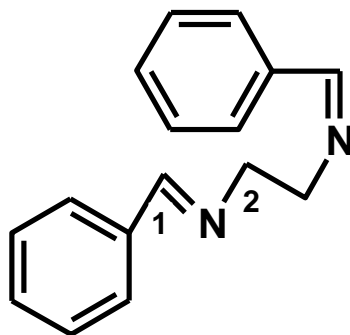


**Figure 4.3.3** The rotation of the imine ligand about the methylene

### 4.3.3 $^1\text{H}$ - and $^{13}\text{C}$ -NMR studies of N, N'-(aryl)benzaldiamine ligands

The spectra were all run in deuterated chloroform. The  $^1\text{H}$ - and  $^{13}\text{C}$ -NMR spectral data for the assignment of the carbon and proton signals was followed using figure 4.1. Chemical shifts for the N, N'-(aryl)benzaldiamine ligands together with the relevant assignment are provided in table 3:12.

The correlation analysis between the hydrogen atoms and substituent parameters, shows that the use of Hammett parameter decreases the resonance correlation as from position 5 (H-5) up to N-H. Similar observations were found with Swain and Williams & Norrington parameters (see table 4.4). This implies that the reduction of the imine bond decreases the possibility of the suggested through space inductive effect observed in the N, N'-(aryl)benzaldiamine ligands.

Table 4.4 Correlation coefficients for protons derived from the  $^1\text{H}$ -NMR data of N, N'-(aryl)benzaldiamine ligands and various substituents parameters

Parameters	Correlation coefficient				
	H-5	H-4	H-2	H-1	N-H
Hammett ( $\zeta_\rho$ )	0.9278	0.5838	0.5468	-0.5519	-0.0070
Swain ( $\zeta_I$ ) <sup>b</sup>	0.4031	0.4932	0.3861	-0.1248	-0.5718
Swain ( $\zeta_R$ ) <sup>c</sup>	0.8216	0.4016	0.4026	-0.5698	0.1977
Williams & Norrington ( $\zeta_I$ )	0.7429	0.5746	0.5179	-0.5050	-0.3722
Williams & Norrington ( $\zeta_R$ )	0.8276	0.4363	0.4265	-0.4559	0.2676

Looking at the signs of the constants  $\rho$  and the size of the correlation coefficient, using the three substituent parameters, the correlation of the protons for the N, N'-(aryl)benzaldiamine ligands suggest that there are two different effects stabilising the aromatic ring and the side chain. The analyses from the three parameters (the signs of the constants  $\rho$ ) indicate that there is conjugation of electrons within the ring, but not up to the nitrogen atom (same signs for  $\rho_I$  and  $\rho_R$ ). These observations are in agreement with the results obtained when using the size of the correlation coefficient. The size of correlation coefficient, indicates that at H-5 there is a pronounced resonance effect ( $r = 0.8216$  and  $r = 0.8276$ ), this was better described using Swain ( $\zeta_R$ ) and Williams & Norrington ( $\zeta_R$ ) parameters. While a moderate inductive effect is observed at H-2 and H-1 ( $r = 0.5179$  and  $r = -0.5050$ ), this was described better with Williams & Norrington ( $\zeta_I$ ) parameters. This is not surprising given that Williams & Norrington ( $\zeta_I$ ) parameters are a better model to understand the effect of the substituents on the side chain of the molecule. Again Swain ( $\zeta_I$ ) parameters show that at nitrogen atom (N-H) there is a negative inductive effect ( $r = -0.5718$ ). From the above statement it can be concluded that the benzene ring is not co-planar with the amine bond.

The correlation analysis for the carbon atoms show a good correlation between C-3 and Hammett parameters, a similar effect is observed between C-3 and Swain ( $\zeta_R$ ) and Williams & Norrington ( $\zeta_R$ ) parameters (see table 4.5). Again the analysis indicates that there is a moderate positive resonance correlation between C-5 and the three parameters {Hammett, Swain ( $\zeta_R$ ) and Williams & Norrington ( $\zeta_R$ )}. The signs of the constants  $\rho$  and the magnitude of correlation coefficient for all the three substituent parameters suggest two different effects are exerted in benzene ring and side chain. Swain ( $\zeta_R$ ) and Hammett ( $\zeta_\rho$ ) parameters suggest that the conjugation moves up to C-3 ( $r = 0.9536$ ,  $r = 0.9153$ ). These observations are in agreement with the results found when using Williams & Norrington ( $\zeta_R$ ) parameters ( $r = 0.9253$  for C-3). At position C-1 an inductive effect is observed ( $r = 0.7202$ , Swain ( $\zeta_I$ )). The Hammett parameters suggest that the delocalization of the electrons from the substituents only occurs within the benzene ring. This implies that there is no conjugation of the electrons from the substituent up to the nitrogen atom, and thus indicates no parallelism between the benzene ring and the amine bond, but there is resonance within the ring.

Table 4.5 Correlation coefficients for carbons derived from the  $^{13}\text{C}$ -NMR data of N, N'-(aryl)benzaldiamine ligands and various substituents parameters

Parameters	Correlation coefficient					
	C-6	C-5	C-4	C-3	C-2	C-1
Hammett ( $\zeta_\rho$ )	-0.3242	0.6054	0.1542	0.9536	-0.3443	0.08766
Swain ( $\zeta_I$ )	0.2869	-0.2632	0.7558	0.2402	-0.1814	0.7202
Swain ( $\zeta_R$ )	-0.4752	0.7671	-0.1249	0.9153	-0.3294	-0.2122
Williams & Norrington ( $\zeta_I$ )	0.0069	0.1790	0.6288	-0.6653	-0.4091	0.4206
Williams & Norrington ( $\zeta_R$ )	-0.4900	0.7717	-0.2353	0.9253	-0.2144	-0.1906

#### 4.3.4 $^1\text{H}$ -NMR studies of N, N'-(aryl)benzaldiamine dihydrochloride salts

The spectra were all run in deuterated dimethylsulfoxide. The  $^1\text{H}$ -NMR spectra data for the proton signals was followed using figure 4.3.1. Chemical shifts for the N, N'-(aryl)benzaldiamine dihydrochloride ligands together with the relevant assignment are provided in table 3.11.

Table 4.6 Correlation coefficients for protons derived from the  $^1\text{H}$ -NMR data of N, N'-(aryl)benzaldiamine dihydrochloride salts and various substituents parameters

Parameters	Correlation coefficient				
	H-5	H-4	H-2	H-1	N-H <sub>2</sub>
Hammett ( $\zeta_\rho$ )	0.9701	0.6590	0.0743	0.1944	-0.0482
Swain ( $\zeta_I$ )	0.5626	0.4159	-0.1516	-0.0307	-0.2546
Swain ( $\zeta_R$ )	0.9406	0.5686	0.1601	0.2499	0.0925
Williams & Norrington ( $\zeta_I$ )	0.6817	0.4920	-0.0961	0.0351	-0.1997
Williams & Norrington ( $\zeta_R$ )	0.8775	0.5640	0.2438	0.3001	0.1555

The correlation analysis studies of the proton chemical shifts of the N, N'-(aryl) benzyaldiamine dihydrochloride salts show a good correlation (see table 4.6) between H-5 and the three parameters {Hammett ( $\zeta_\rho$ ), Swain ( $\zeta_R$ ) and Williams & Norrington ( $\zeta_R$ )}. This is expected because of the short distance between the substituent and the benzene ring. A moderate positive resonance correlation is also observed at the H-4 for the three parameters.

Looking at the signs of the values of  $\rho$  and the magnitude of the correlation coefficient, all three parameters are in agreement that the resonance effect is more pronounced within the benzene ring ( $r = 0.9701$ ,  $r = 0.9406$  and  $r = 0.8775$  for H-5 and  $r = 0.6590$ ,  $r = 0.5686$  and  $r = 0.5640$  for H-4). Hammett parameters suggest that the conjugation of electrons from the substituent move up to H-2 (positive signs of the values of  $\rho$ ). Both Swain and Williams & Norrington parameters contradict Hammett parameters (signs of  $\rho_I$  and  $\rho_R$ ). These two parameters suggest that the conjugation of the electrons do not reach side chain, H-2. This is expected, because Hammett parameters give a combination of the two electronic effects, resonance and inductive effect, while the Swain and Williams & Norrington parameters separate the two effects.

From the both the size of the correlation coefficient and the signs of the values of  $\rho$ , it can be concluded that the benzene ring is not parallel to the amine salt bond and there is no through space inductive effect which is observed among the imines. The reduction or disappearance of the through space inductive effect might, when compared to the free amines, be restricted by the solvent effect (deuterated dimethyl sulfoxide). The presence of solvent might have hindered the effect of the electron cloud of the benzene ring onto the H-1 and H-2.

#### 4.3.5 $^1\text{H}$ - and $^{13}\text{C}$ -NMR studies of N, N'-bis(cinnamaldiimine) ligands

The spectra was run in deuterated chloroform. The  $^1\text{H}$ - and  $^{13}\text{C}$ -NMR spectral data for the assignment of the carbon and proton signals was followed using figure 4.3.4. Chemical shifts for the N, N'-bis(cinnamaldiimine) ligands together with the relevant assignment are provided in table 3:14.

Due to the absence of a series of substituted N, N'-bis(cinnamaldiimine) ligands, no correlation analyses were made. However, from the experimental data in table 3.14 it can be concluded that the presence of the electron donor substituent {4-N(CH<sub>3</sub>)<sub>2</sub>} at the para-position of the Schiff base decreases the electron density of carbon and hydrogen atoms at positions, H-4, C-2, C-2b and C-4. This is expected, because of the possible overlapping of the orbitals containing lone pair of electrons on the azomethine group with the π-orbitals of the π system of the alkene group. The trend effect of the substituent {4-N(CH<sub>3</sub>)<sub>2</sub>} is presented in table 4.7

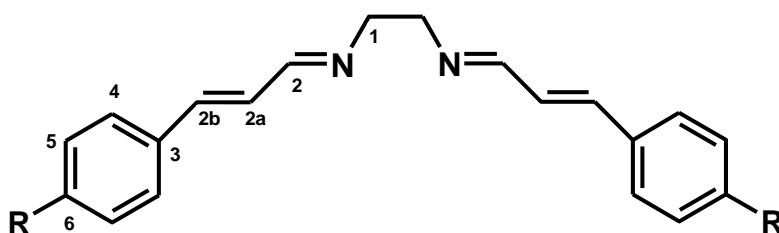


Figure 4.3.4 Numbering system used for the N, N'-bis(cinnamaldiimine) ligand

Table 4.7 Trends of the electron donor substituent on the N, N'-bis(4-dimethyl aminocinnamaldehyde)-1, 2-diiminoethane

		6	5	4	3	2b	2a	2	1
N(CH <sub>3</sub> ) <sub>2</sub> -CA <sub>2</sub> EN	<sup>1</sup> H	—	↓	↓	—	↑	↑	↑	↑
	<sup>13</sup> C	↓	↑	↓	↑	↓	↑	↓	↑

↑ = Upfield shift, ↓ = Downfield shift

#### 4.3.6 Comparison between <sup>13</sup>C-NMR studies of CA<sub>2</sub>EN and BEN ligands.

From the nuclear magnetic resonance studies of the Schiff bases, both the N(CH<sub>3</sub>)<sub>2</sub>-CA<sub>2</sub>EN ligands and N(CH<sub>3</sub>)<sub>2</sub>-BEN ligands, it can be concluded, that the presence of the conjugated double bond within the system results in an increase of an electron density at C-6, C-4 and C-2 for the N(CH<sub>3</sub>)<sub>2</sub>-CA<sub>2</sub>EN ligand and hence the signals of these are shifted downfield.

While at C-5, C-3 and C-1 positions the electron density decreases and these carbon atoms are observed in the upfield region.

The change in chemical shift for the ligands are give in table 4.8. The alkene group (position 2b) highly affect the side chain of the Schiff base ligand and C-4. As observed in table 4.8, C-2 of the Schiff base, CA<sub>2</sub>EN appears downfield; while the same carbon for Schiff base, N(CH<sub>3</sub>)<sub>2</sub>-CA<sub>2</sub>EN is observed upfield. Similar findings were observed at C-1. The large shift of 0.86 and 0.84 for C-4 and C-2 reflect the conjugation experienced by the imine carbon and C-4, especially when compared to the smallest shifts (0.23) expected for C-1.

Table 4.8 Change in substituent chemical shift values for CA<sub>2</sub>EN and BEN ligands

No	Ligand	C-6	C-5	C-4	C-3	C-2	C-1
7	N(CH <sub>3</sub> ) <sub>2</sub> -BEN	20.83	-17.36	1.05	-12.05	-0.66	0.06
22	N(CH <sub>3</sub> ) <sub>2</sub> -CA <sub>2</sub> EN	21.81	-17.11	0.21	-12.41	0.20	-0.17
	( $\Delta$ SCS)	0.02	0.25	0.84	0.44	0.86	0.23

$$\text{Change SCS } (\Delta\text{SCS}) = \text{SCS}_{(\text{subst.})} - \text{SCS}_{(\text{unsubst.})}$$

#### 4.4 Electronic spectral studies

The Ultraviolet and visible spectrometer is an important analytical instrument in the modern day laboratory. It is used to understand the behaviour of molecular electrons when they are exposed to light having an energy that matches possible electronic transition within the organic and inorganic molecules.

The spectra of the Ultraviolet-visible-NIR consist of three different regions, the ultraviolet region (200 – 380 nm), the visible region (ranging from blue through to red, 430 nm to 750 nm) and the near infrared region (800 nm – 2000 nm), as shown in figure 4.4.1.

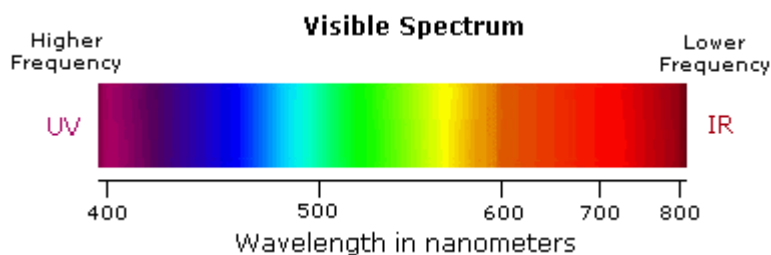


**Figure 4.4.1 The Ultraviolet-visible-NIR spectrum**

The UV-vis spectroscopic studies can be conducted in solid or solution state. In solution state different solvents may be used and these solvents may have little or major effect on the electronic spectra of samples. The effect of solvent on the electronic spectra of the organic and inorganic molecules is well established<sup>12</sup>. The nature of the solvent plays a major role in the position of the wavelength of a molecular electronic absorption band. Polar solvents such as ethanol (protic) can stabilise cations using the unshared electron pairs, and can stabilise anions by hydrogen bonding. In the case of aprotic solvents (for example chloroform), a large frequency shift can be observed on the electronic spectra of samples, due to the  $n \rightarrow \sigma^*$  transition of the chloroform.

For the electronic spectral studies of the ligands and their metal complexes two solvents were used, depending on the solubility of the ligands and their metal complexes. This was done to enable easy comparison of absorption bands. The section is divided into two parts; the first part will involve the assignment of the absorption bands. The last part will focus on the elucidation of the effect of the substituent in the UV/vis spectrum of the ligands and their metal complexes.

#### **4.4.1 The electronic spectra of the ligands and copper complexes**

The solution electronic spectra of (concentration  $1 \times 10^{-4}$  to  $1 \times 10^{-5}$  mol/L) of Schiff base ligands, the amines derived from the reduction of the Schiff base ligands and the copper complexes were studied in various organic solvents of different polarities: chloroform ( $\text{CHCl}_3$ ), ethanol (EtOH), acetonitrile ( $\text{CH}_3\text{CN}$ ) and dichloromethane (DCM). The purpose of this section is to study the spectral behaviour of the Schiff bases and their complexes using

different solvents. It has been observed that the molecular structure of the compounds and the nature (polarity) of the solvent contribute to the spectral behaviour.

#### 4.4.1.1 The electronic spectra of the N, N'-(aryl)benzaldimine ligands

This section will focus on the interpretation of electronic spectra and the effect produced by the substituents on the HOMO and LUMO orbitals of the N, N'-(aryl)benzaldimine ligands. This will be done by monitoring the shifts of the electronic transitions in the electronic spectra of the ligands.

N, N'-(aryl)benzaldimine ligands were examined spectroscopically from 200 nm up to 900 nm in ethanol solution. Representative ultraviolet absorption spectra of the Schiff bases in ethanol are shown in figures 4.4.2 and 4.4.3. The visible region was omitted from figures 4.4.2 and 4.4.3 because there were no maximum absorption bands observed at the longer wavelength region. The corresponding data are also summarized for the N, N'-(aryl)benzaldimine ligands in table 3.12.

The electronic spectra of the N, N'-(aryl)benzaldimine ligands in ethanol showed dissimilarities in absorption bands of all the imines, this is due to the influence of the various substituents at the *para*-position of the benzene ring and the effect of the solvent. For the N, N'-(aryl)benzaldimine ligands, four to five absorption bands are expected, since the ligand has two different types of  $\pi$  electrons, lone pairs and  $\zeta$  electrons. The numbers of absorption bands for each electronic spectrum of the Schiff bases depend on the nature of the substituent at the *para*-position.

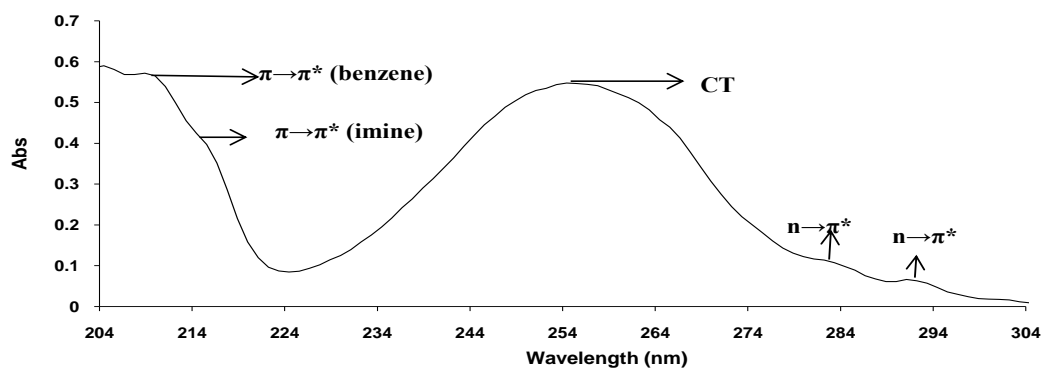
The absorption bands expected for the N, N'-(aryl)benzaldimine ligands, include two  $\pi \rightarrow \pi^*$  transitions,  $n \rightarrow \pi^*$  transitions and intramolecular charge transition<sup>13,14</sup>. The whole spectrum is expected in the ultraviolet region.

In the electronic spectra of the Schiff bases in ethanol, the first  $\pi \rightarrow \pi^*$  transition is due to excitation of the  $\pi$  electrons of the aromatic ring, and the other  $\pi \rightarrow \pi^*$  transition is due to the presence of unpaired electrons in the azomethine group<sup>13, 14</sup>. Schiff bases also exhibit a charge transfer transition. Since it has been observed that the polar solvents enhanced bathochromic shifts<sup>15</sup>, the focus will be on the electronic effect of the substituent in ethanol.

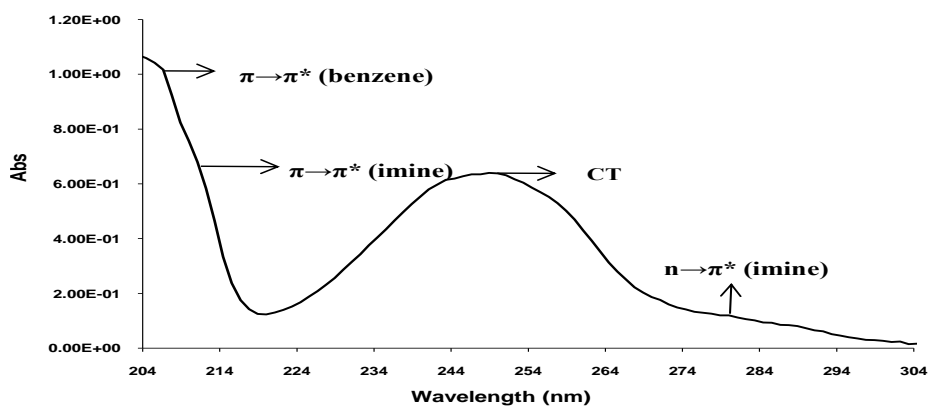
The electronic spectra of N, N'-bis(4-chlorobenzyl)-1, 2-diiminoethane, N, N'-bis(benzyl)-1, 2-diiminoethane and N, N'-bis(4-methylbenzyl)-1, 2-diiminoethane ligands in ethanol are shown in figure 4.4.2 respectively. As observed from the spectra of Cl-BEN, H-BEN and CH<sub>3</sub>-BEN ligands in ethanol, the absorption bands ( $\pi \rightarrow \pi^*$  transition, CT and  $n \rightarrow \pi^*$  transition) of the Cl and CH<sub>3</sub> analogues suffered bathochromic shifts when compared to the absorption bands of H-BEN in ethanol solution. This is not surprising, because polar solvents enhances bathochromic shifts. This indicates that the HOMO state of these absorption bands are destabilized relative to LUMO state. This indicates that the effects exerted by these groups (4-Cl and 4-CH<sub>3</sub>) on the absorption bands of the N, N'-(aryl)benzylideneimine system in ethanol solution are similar.

The spectrum of the nitro-substituted Schiff base in ethanol is given in figure 4.4.3 and several absorption bands are observed. These absorption bands consist of the three  $\pi \rightarrow \pi^*$  transitions, two  $n \rightarrow \pi^*$  transitions, two  $n \rightarrow \sigma^*$  transitions and two charge transfer bands (within the Schiff base, the nitro functional group). The three  $\pi \rightarrow \pi^*$  transitions are due to the azomethine group, benzene ring and the extra conjugated double bond from 4-NO<sub>2</sub> substituent. The  $n \rightarrow \pi^*$  transitions are the result of the lone pair of electrons from 4-NO<sub>2</sub> substituent and the azomethine group<sup>13, 14, 16, 17</sup>.

(a)



(b)



(c)

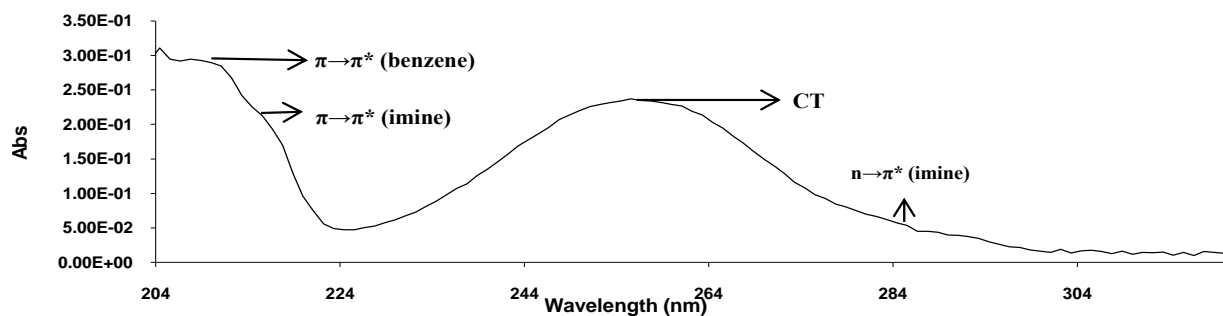
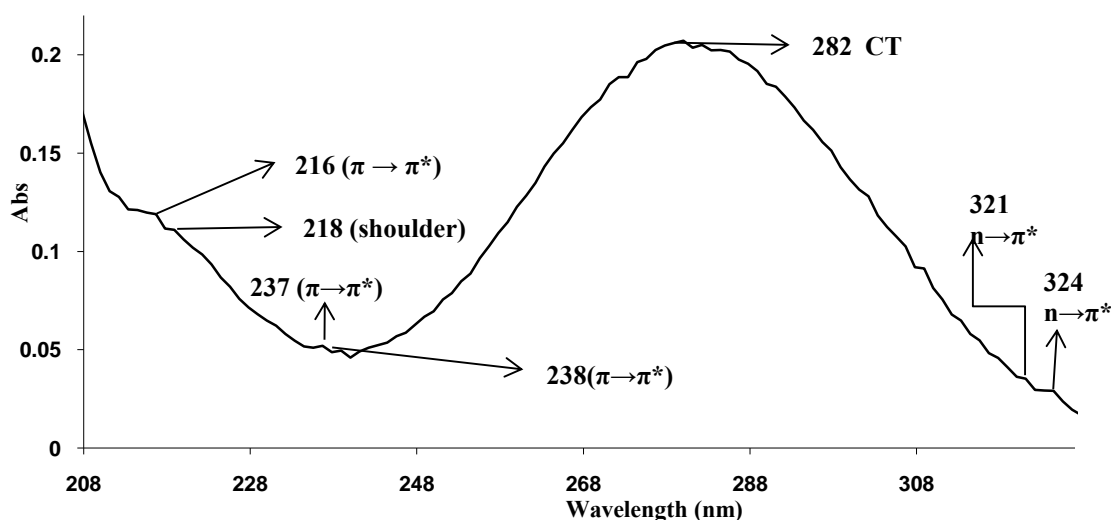


Figure 4.4.2 Ultraviolet absorption spectra of ligands, (a) Cl-BEN, (b) H-BEN and (c) CH<sub>3</sub>-BEN in EtOH

In the electronic spectra of N, N'-bis(4-nitrobenzyl)-1, 2-diiminoethane ligand, the three  $\pi \rightarrow \pi^*$  transitions due to the benzene ring, nitro-substituent and azomethine group are observed between 216 nm to 238 nm region. While one charge transfer band is observed around 282 nm and the other one is masked. The two  $n \rightarrow \pi^*$  transitions due to the nitro substituent and imine group are observed in the 321 nm to 324 nm region. The two  $n \rightarrow \sigma^*$  transitions absorb in the far-ultraviolet region (10-200 nm), as the result of this they can not be observed.



**Figure 4.4.3 Ultraviolet absorption spectrum of NO<sub>2</sub>-BEN in EtOH**

Some general conclusions from the spectra of all the ligands can be made. From the analysis of the spectroscopic data collected in table 3.12 of the Schiff bases in ethanol, it can be concluded that the absorption bands in the wavelength range 202 – 216 nm are due to the excitation of the  $\pi$  electrons of the benzene ring<sup>15</sup>. The results indicate that these bands are sensitive to both the nature of the substituent attached to the benzene ring and the polarity of the solvent. The data show that the presence of the electron acceptor groups at the *para* position of the Schiff base and the use of polar solvent shifts the  $\pi \rightarrow \pi^*$  transitions (benzene) to longer wavelength. This implies that both the solvent and the electron-acceptor groups stabilize the excited state  $\pi^*$  (LUMO) relative to the ground state (HOMO)<sup>15, 16</sup>. Electron-donor substituents {4-CH<sub>3</sub> and 4-OCH<sub>3</sub>, but not for 4-N(CH<sub>3</sub>)<sub>2</sub>} shift the absorption bands towards longer wavelength (fig 4.4.4), relatively destabilizing the excited state  $\pi^*$  (LUMO), this results in a smaller energy gap between the  $\pi$  orbital to  $\pi^*$  orbitals of the benzene ring.

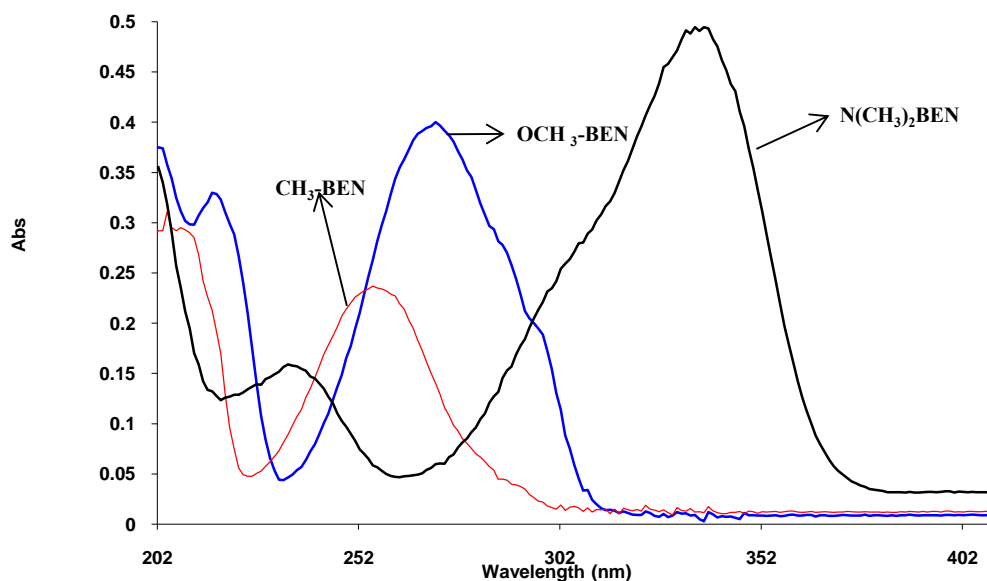


**Figure 4.4.4 Ultraviolet absorption spectra of ligands of CH<sub>3</sub>-BEN, OCH<sub>3</sub>-BEN and N(CH<sub>3</sub>)<sub>2</sub>-BEN in EtOH**

The weak absorption bands between 211 to 237 nm in ethanol solution (fig 4.4.4) may be assigned to the  $\pi \rightarrow \pi^*$  transition of the azomethine group<sup>18</sup>. The electronic spectroscopic data show that the electron-donor substituents decreases the energy gap between the  $\pi$  and  $\pi^*$  orbital of the imine group destabilizing the HOMO relative the LUMO.

The strong absorption bands within the range 247 to 336 nm are due to the charge transfer bands<sup>15</sup>. These bands are more sensitive to solvents and also to the nature of substituent. Since the spectroscopic data of these absorption bands are non-linear (fig 4.4.4 and table 3.15), no correlation was conducted.

The bands located in the range 283 to 289 nm correspond to  $n \rightarrow \pi^*$  transition due to the azomethine group. The effect exerted by donor and withdrawing substituents on  $n \rightarrow \pi^*$  transition are non-linear (fig 4.4.4 and table 3.15) and no correlation analysis was conducted on these transitions.

Since the spectroscopic data obtained from the electronic spectra of the N, N'-(aryl)benzaldimine ligands in ethanol solution was non-linear (except for the  $\pi \rightarrow \pi^*$  transition of the benzene ring fig 4.4.5), no further studies were made for these absorption bands using correlation analysis and the non-linearity of the experimental data for CT and  $n \rightarrow \pi^*$  transition are shown in figures 4.4.6 and 4.4.7. The figures show that the benzene ring (fig 4.4.5) is behaving as expected. There is a difference of about 12 wave-numbers between the most electron donating and the most electron withdrawing group. The  $\pi \rightarrow \pi^*$  transition of benzene ring is not significantly affected by the substituents and they behave as expected (figure 4.4.5).

The plot of charge transfer transitions (fig 4.4.6) shows that there is a difference of about 75 wavenumbers between the most electron donating and most electron withdrawing group, while the plot of  $n \rightarrow \pi^*$  transition shows a red shift for both the most electron donating and the most electron withdrawing substituent (fig 4.4.7). The red shift of the  $n \rightarrow \pi^*$  transition might be related to the behaviour of the charge transfer for the imines in ethanol.

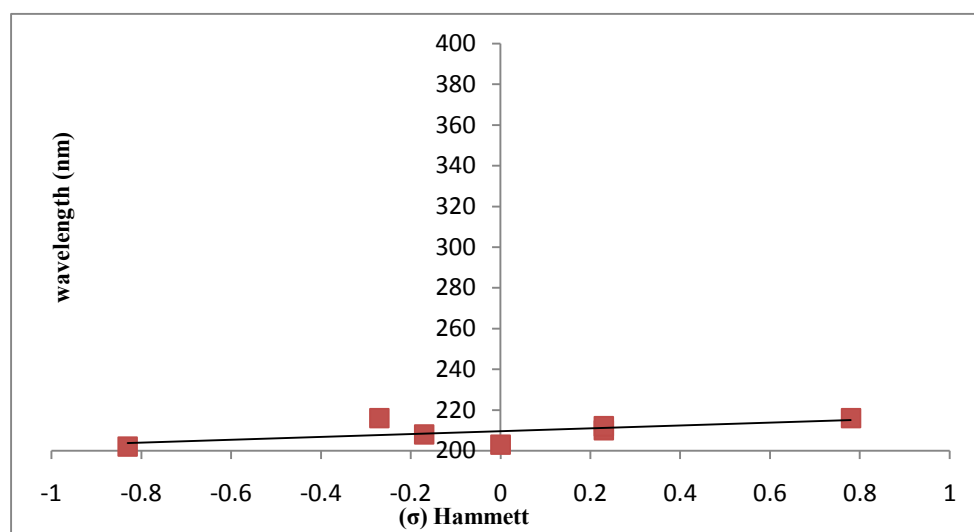


**Figure 4.4.5 Plot of wavelength (nm) versus Hammett  $\sigma$  values for  $\pi \rightarrow \pi^*$  transition of benzene ring for Schiff bases in EtOH solution**

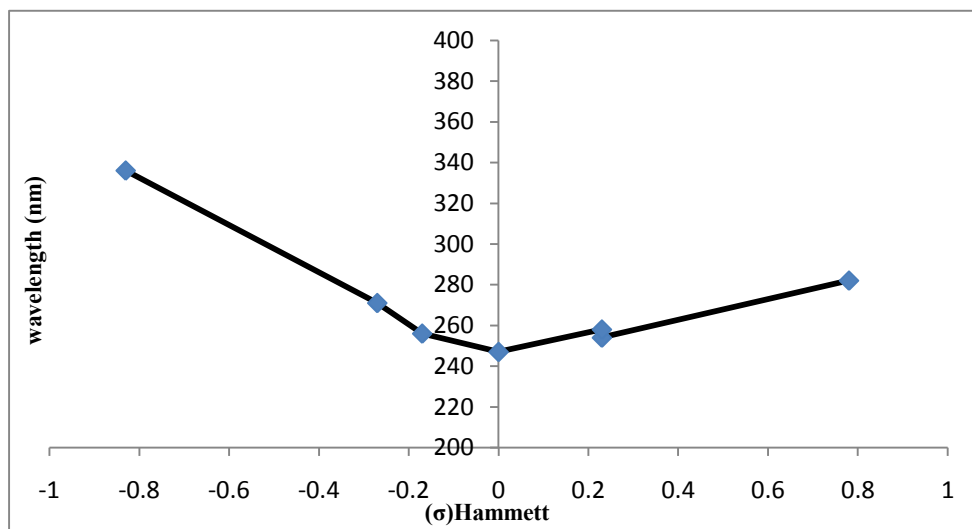


**Figure 4.4.6 Plot of wavelength (nm) versus Hammett  $\sigma$  values for charge transfer transitions for Schiff bases in EtOH solution**

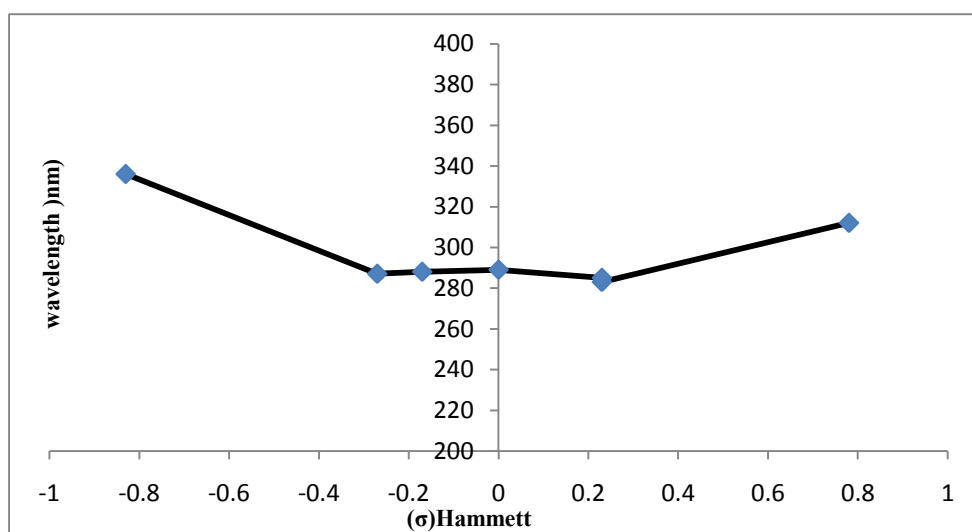


**Figure 4.4.7 Plot of wavelength (nm) versus Hammett  $\sigma$  values for  $n \rightarrow \pi^*$  transition for Schiff bases in EtOH solution**

#### 4.4.1.2 The electronic spectra of the N, N'-(aryl)benzaldiamine ligands and their copper(II) halide complexes

This section focuses on the interpretation of the electronic spectra, and the effect of the substituents on the spectra. The results obtained are then used to determine the likely geometry of the complexes. This was done by comparing the spectra of the free ligands with the spectra of the copper(II) complexes. The discussion has been restricted to those complexes whose composition have been confirmed by microanalyses.

The electronic spectral studies of the ligands (R-BENH) and their copper(II) dihalide complexes  $\{(Cu(R-BENH)X_2)\}$  were recorded in the 200 nm - 900 nm range in ethanol and chloroform solutions respectively. The corresponding electronic spectroscopic data including the molar absorption coefficients ( $\epsilon$ ) for ligands and copper(II)-halide complexes are summarized in tables 3.16 and 3.17. The abbreviation g.c.i stands for grating change in the instrument. This is the point where the instrument changes grating, resulting in a change in the absorbance intensity readings. For all the complexes this point was observed between 350 nm to 353 nm.

The UV-vis spectra of amine ligands and their copper(II)-halide complexes show few absorption bands in the visible and ultraviolet region. For the amine ligands, three absorption bands are expected. The  $\pi \rightarrow \pi^*$  (benzene),  $n \rightarrow \sigma^*$  and  $\sigma \rightarrow \sigma^*$  transitions and all the bands should appear in the ultraviolet region. Since the  $\sigma \rightarrow \sigma^*$  transition absorbs at the far ultraviolet region which is masked by the solvent, for this study only two absorption bands will be focused on; the  $\pi \rightarrow \pi^*$  and  $n \rightarrow \sigma^*$  transitions.

The  $\pi \rightarrow \pi^*$  transition is due to the  $\pi$ -electrons of the benzene ring and the  $n \rightarrow \sigma^*$  transition is the results of the excitation of the lone pair of electrons of the free primary amine<sup>13, 19</sup>. The electronic spectra of the ligands, in ethanol and chloroform, showed two absorption bands at about 212 and 440 nm respectively<sup>8</sup>. Furthermore in all the electronic spectra of the N, N'-(aryl)benzaldiamine ligands in both ethanol and chloroform solutions, the  $\pi \rightarrow \pi^*$  transition due to the azomethine group disappears when compared to the N, N'-

(aryl)benzaldimine ligand. This confirms the formation of the amine bond to all the N, N'- (aryl)benzaldimine ligands.

In the electronic spectra of the amine ligands, the absorption bands below 240 nm have high extinction coefficients in ethanol solutions, and are associated with  $n \rightarrow \sigma^*$  transitions<sup>19</sup>, because the  $n \rightarrow \sigma^*$  transitions require a greater deal of energy than  $\pi \rightarrow \pi^*$  transition and they can only absorb in the ultraviolet region. The absorption bands observed within the range of 260 – 272 nm in ethanol is corresponds to the  $\pi \rightarrow \pi^*$  transition.

In chloroform these two absorption bands are shifted towards the longer wavelength, with the absorption band between 262 nm and 313 nm attributed to the  $n \rightarrow \sigma^*$  transition of the amine group. The band between 332 nm and 448 nm corresponds to the  $\pi \rightarrow \pi^*$  transition.

From the values obtained in the electronic spectra of all the ligands, it can be concluded that the energy required for each transition within the ligands is substituent depended and is affected by the nature of solvent used. As can be seen in electronic spectra of chloroform solutions, the absorption bands were even shifted to the near visible region.

#### 4.4.1.2.1 Bromo complexes

For a copper(II) complex in a distorted tetrahedral environment there is the possibility of three types of electronic transitions,  $d \rightarrow d$  transitions; internal ligand transitions and charge transfer transitions (both metal to ligand and ligand to metal).

The UV-vis spectra of N, N'-bis(benzyl)-1, 2-diaminoethanedibromocopper(II) complexes in ethanol and chloroform solutions, showed five absorption bands between 231 – 852 nm. The  $d \rightarrow d$  transitions are La Porte forbidden transitions (they occur within the d orbitals of the metal ion and are not allowed by the selection rules) and so are very weak and difficult to identify. These transitions are expected below 900 nm; for these copper complexes they are

found between 686 nm and 872 nm. The internal ligand charge transfer and transitions are observed below 550 nm.

In the spectra of the bromo complexes the bands observed within the range 213 - 279 nm in ethanol and chloroform solutions are ascribed to the  $n \rightarrow \sigma^*$  and  $\pi \rightarrow \pi^*$  transitions. Since the ligands, N, N'-(aryl)benzaldimine ligands are transparent in the visible spectrum, the new absorption bands in the visible region are due to formation of the coordination compound.

The spectra of the bromo complexes show a similar pattern in the visible region of all the complexes; they consist of the absorption band at the near ultraviolet region within the range of 301 – 314 nm. Based on the facts above, the absorption bands correspond to the  $N \rightarrow Cu(II)$  LMCT<sup>20,21</sup>. These absorption bands are the results of a single orbitally allowed charge transfer transition, arising from the amine group<sup>22</sup>.

The absorption bands in the range 461 – 485 nm in both ethanol and chloroform solutions they may be assigned to  $Br \rightarrow Cu(II)$  LMCT, as result of the movement of non-bonding  $\pi$  electrons of the bromine atom from the bonding orbital of the bromide to the antibonding orbital of the copper metal<sup>23</sup>.

The stereochemistry of the bromide complexes is suspected to be predominately distorted tetrahedral, because tetrahedral copper(II) absorbs primarily in the red and near infrared. The tetrahedral  $CuN_4$  chromophores absorption occurs below 1000 nm, and they exhibit a single transition ( ${}^2E \rightarrow {}^2T_2$ ) at relative low energy between 625 to 769 nm<sup>24-27</sup>. The influence of the solvent and the substituent on the likely structure are discussed in more details below.

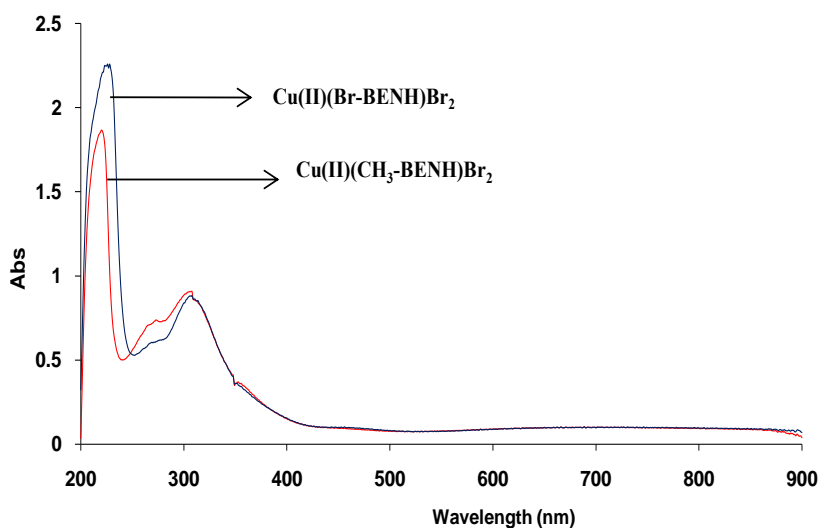


Figure 4.4.8 Uv-vis spectra of  $\text{Cu(II)(CH}_3\text{-BENH)Br}_2$  and  $\text{Cu(II)(Br-BENH)Br}_2$  in EtOH

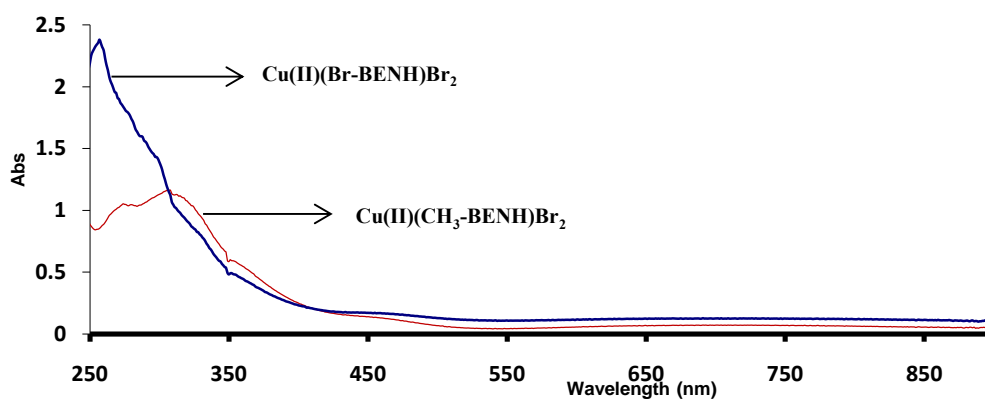


Figure 4.4.9 Uv-vis spectra of complexes,  $\text{Cu(II)(CH}_3\text{-BENH)Br}_2$  &  $\text{Cu(II)(Br-BEN)Br}_2$  in  $\text{CHCl}_3$

#### 4.4.1.2.2 Chloro complexes

According to the data from the electronic spectra of the chloro complexes in ethanol and chloroform solutions in table 3.18 and the overlap electronic spectra as given in figure 4.4.10 four bands were observed between 211 – 874 nm. The spectra showed absorption bands

between 211 - 232 nm, 265 - 281 nm, 306 - 308 nm and 621 - 874 nm, respectively corresponding to the  $n \rightarrow \sigma^*$  transition,  $\pi \rightarrow \pi^*$  transition,  $N \rightarrow Cu(II)$  LMCT and  $d \rightarrow d$  transitions. The stereochemistry of the complexes is suspected to be predominately tetrahedral, with only one absorption band observed in the visible region<sup>24-27</sup>. The influence of the solvent and the substituent on the likely structure are discussed in more detail below.

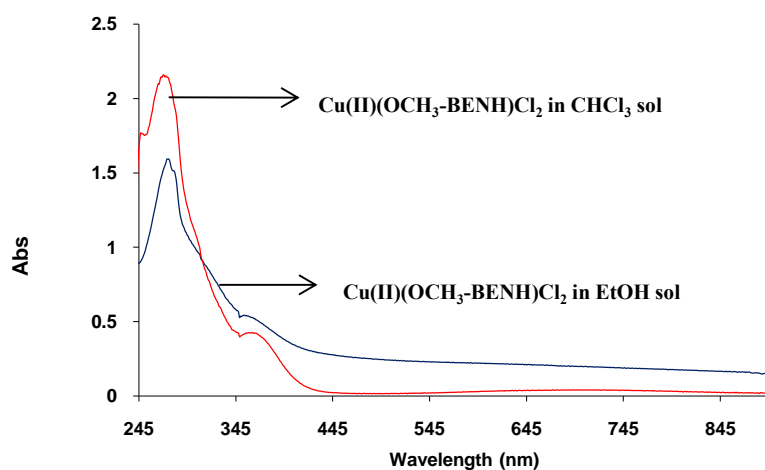


Figure 4.4.10 Uv-vis spectra of  $Cu(II)(OCH_3-BENH)Cl_2$  in EtOH and  $CHCl_3$

#### 4.4.2 Correlation analysis studies for the UV-vis data of the $N, N'$ -(aryl)benzaldimine ligands, $N, N'$ -(aryl)benzaldiamine ligands and their copper(II)-halide complexes

This section will focus on the correlation analysis of the imines, amine ligands and copper(II)-halide complexes whose composition have been confirmed by microanalyses. For the imine ligands the analysis will be conducted by correlating the  $\pi \rightarrow \pi^*$  transition of the benzene ring with the three substituent parameters. While for the amine ligands and their copper(II)-halide complexes Hammett parameters will be used, because this model gave a better correlation for the analysis of the amines and the copper(II)-halide complexes.

#### 4.4.2.1 N, N'-(aryl)benzaldimine ligands

Table 4.9 Correlation of  $\pi \rightarrow \pi^*$  transition for N, N'-(aryl)benzaldimine ligands with various substituent parameters in ethanol solution

Parameters	$\pi \rightarrow \pi^*$ transition In EtOH
Hammett ( $\zeta_\rho$ )	-0.54140
Swain ( $\zeta_I$ )	0.43527
Swain ( $\zeta_R$ )	-0.76523
Williams & Norrington ( $\zeta_I$ )	-0.11070
Williams & Norrington ( $\zeta_R$ )	-0.73340

The correlation analysis (table 4.9) between the three substituent parameters and  $\pi \rightarrow \pi^*$  transitions of the benzene ring for Schiff bases in ethanol solution, suggest that there is a negative resonance effect within the  $\pi \rightarrow \pi^*$  transitions of the benzene ring for the N, N'-(aryl)benzaldimine ligands. This was described better using Swain ( $\zeta_R$ ) and Williams & Norrington ( $\zeta_R$ ) parameters. This is in agreement with proton and carbon NMR studies of the free N, N'-(aryl)benzaldimine ligands, whereby the resonance effect is highly dominating in the benzene ring of the free imine ligands.

#### 4.4.2.2 N, N'-(aryl)benzaldiamine ligands

From the UV-vis experimental data of the amine ligands, both in ethanol and chloroform solutions two absorption bands were found in the ultraviolet region. The band in the lower energy region ( $\pi \rightarrow \pi^*$  transition) was found to be more sensitive to the electronic properties

of the substituent (table 3.16), with these bands shifting towards or away from the lower energy region.

The electron donor and the electron withdrawing substituents in ethanol solutions both seem to exhibit similar effects on the  $\pi \rightarrow \pi^*$  transition of the N, N'-(aryl)benzaldiamine ligands when compared to unsubstituted analogue (H-BEN), see figure 4.4.11. In ethanol these substituents increase the electron density of the benzene ring and decrease the  $\pi \rightarrow \pi^*$  transition energy gap resulting in a red shift. This destabilizes the HOMO of the  $\pi$  – orbitals of the benzene ring relative to the LUMO.

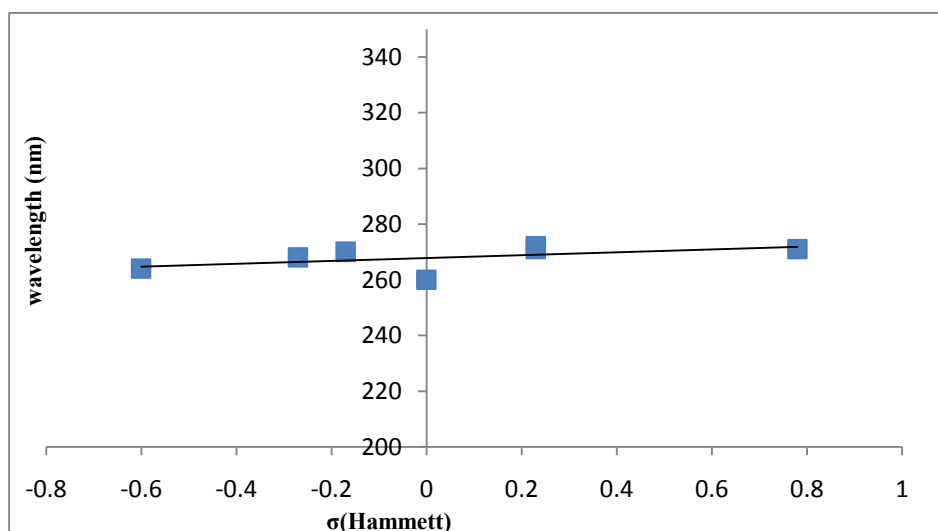


**Figure 4.4.11 Plot of wavelength (nm) versus Hammett  $\sigma$  values for  $\pi \rightarrow \pi^*$  transition of N, N'-(aryl)benzaldiamine ligands in EtOH solution**

Since the spectroscopic data for the  $\pi \rightarrow \pi^*$  transition of the N, N'-(aryl)benzaldiamine ligands in chloroform solution was non-linear (see figure 4.4.12), no correlation analyses were conducted. The absence of correlation within the data is expected, because chloroform is an aprotic solvent. Aprotic solvents have lone pairs and they possess  $n \rightarrow \zeta^*$  transitions which result in large frequency shifts in the electronic spectra.

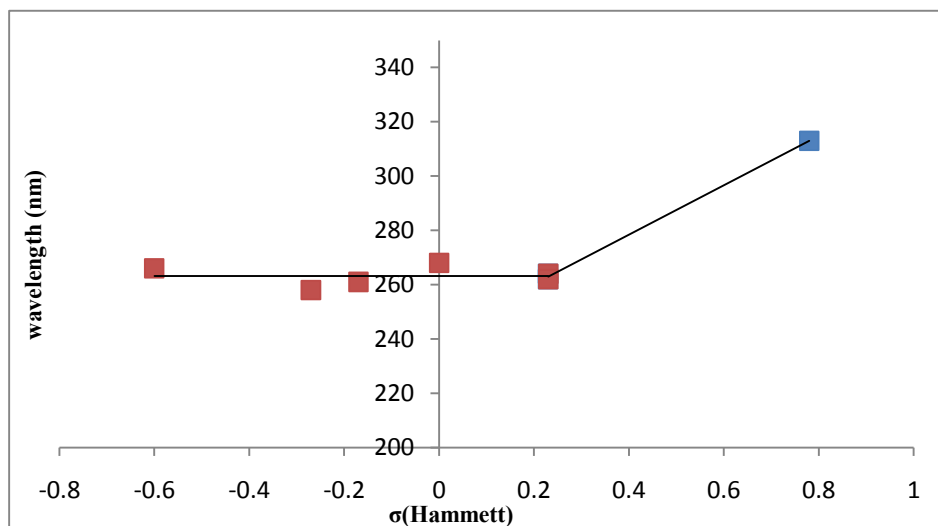


**Figure 4.4.12** Plot of wavelength (nm) versus Hammett  $\sigma$  values for  $\pi \rightarrow \pi^*$  transition of N, N'-(aryl)benzaldiamine ligands in  $\text{CHCl}_3$  solution

In chloroform solution, both the electron donating and electron withdrawing substituents (except for 4- $\text{NO}_2$ ) appear to decrease the electron density at the benzene ring, thereby increasing the  $\pi \rightarrow \pi^*$  transition energy gap, resulting in a blue shift, (this is presented in figure 4.4.12). The figure shows some similarity for both the electron donor and electron withdrawing substituents, in the manner in which the substituents influence the spectroscopic data. The blue shift stabilizes the HOMO relative to the LUMO. The nitro group often has an anomalous value using the Hammett substituent parameter<sup>28</sup>. The anomalous behaviour of the nitro group substituent may reflect a coupling of the  $\pi \rightarrow \pi^*$  benzene, with either the  $\pi \rightarrow \pi^*$  or the CT of the  $\text{NO}_2$  group<sup>15</sup>, or it may reflect coupling with the  $n \rightarrow \zeta^*$  transitions of the solvent. The contrast to the spectra of ethanol and chloroform shows a solvent effect is most likely responsible.

Since the behaviour of the  $\pi \rightarrow \pi^*$  transition in  $\text{CHCl}_3$  is non-linear, correlation analysis has been done only for EtOH. The analysis shows poor correlation with the Hammett parameter and opposing behaviour for the inductive and resonance parameters of the other two (see figure 4.4.11 and table 4.9). Swain parameters show a better correlation in EtOH when ( $\zeta_I$ ) is used rather than ( $\zeta_R$ ).

Table 4.10 Correlation of  $\pi \rightarrow \pi^*$  transition for N, N'-(aryl)benzaldiamine ligands with various substituent parameters in ethanol and chloroform solutions

Parameters	$\pi \rightarrow \pi^*$ transition
	In EtOH
Hammett ( $\zeta_\rho$ )	-0.02377
Swain ( $\zeta_I$ )	0.60061
Swain ( $\zeta_R$ )	-0.46109
Williams & Norrington ( $\zeta_I$ )	0.49151
Williams & Norrington ( $\zeta_R$ )	-0.61013

The plot in figure 4.4.11 indicates a linear relationship with a small scatter, this suggest that there is no dramatic shift in the  $\pi \rightarrow \pi^*$  transitions of N, N'-(aryl)benzaldiamine ligands due to the nature of the substituent, while in chloroform (see figure 4.4.12) a non-linear relationship is observed. From both figures 4.4.11 and 4.4.12 it can be concluded that the bands are sensitive to the nature of the solvent as seen from the slopes. For the electron withdrawing groups the polar solvent, ethanol, stabilises the cationic charge in the benzene ring, resulting in the red shift for the  $\pi \rightarrow \pi^*$  transitions of N, N'-(aryl)benzaldiamine ligands, while in the chloroform these bands suffered a slight blue shift.

#### 4.4.2.3 Bromo complexes

For the bromo complexes the data for the 4-N(CH<sub>3</sub>)<sub>2</sub> analogue is missing in figure 4.4.13 and 4.4.14, due to the unsuccessful synthesis for the complex, Cu(II)(OCH<sub>3</sub>-BENH)Br<sub>2</sub>.

The presence of metal ion in N, N'-(aryl)benzaldiamine ligands causes a slight shift in the absorption bands of the  $\pi \rightarrow \pi^*$  transitions for the bromo complexes in ethanol and chloroform solutions. The red shift caused by the donor and acceptor substituents in ethanol

solution, indicate that the energy gap between the  $\pi$  – orbitals of the benzene is smaller and thus stabilize the LUMO relative to the HOMO.

The donor substituents in chloroform solution cause the  $\pi \rightarrow \pi^*$  transitions of the bromide complexes to shift towards longer wavelength (red shift) and the withdrawing substituents (except for 4-Br) results in a blue shift. This implies that the presence of the donating group at the para position of the complexes decrease the energy gap between the  $\pi$  – orbitals of the benzene ring and stabilize the LUMO relative to the HOMO. For the withdrawing substituent the opposite effect is observed. From the spectroscopic data of the  $\pi \rightarrow \pi^*$  transitions of the bromide complexes (see figure 4.4.14) a notable change in the  $\text{NO}_2$  analogue is observed, which is now linear with other substituents in chloroform, as opposed to the free ligand (see figure 4.4.12).

The trend of the effect of the substituent and solvent on the bromo complexes is reflected in figures 4.4.13 and 4.4.14. These figures show a straight line for both solvents (EtOH and  $\text{CHCl}_3$ ). This indicate that in both ethanol and chloroform solutions, substituents are producing a similar effects on the  $\pi \rightarrow \pi^*$  transitions of the benzene ring and that while there is a shift in the electronic spectra due to the substituents using Hammett parameters, it is not dramatic with the complexes.

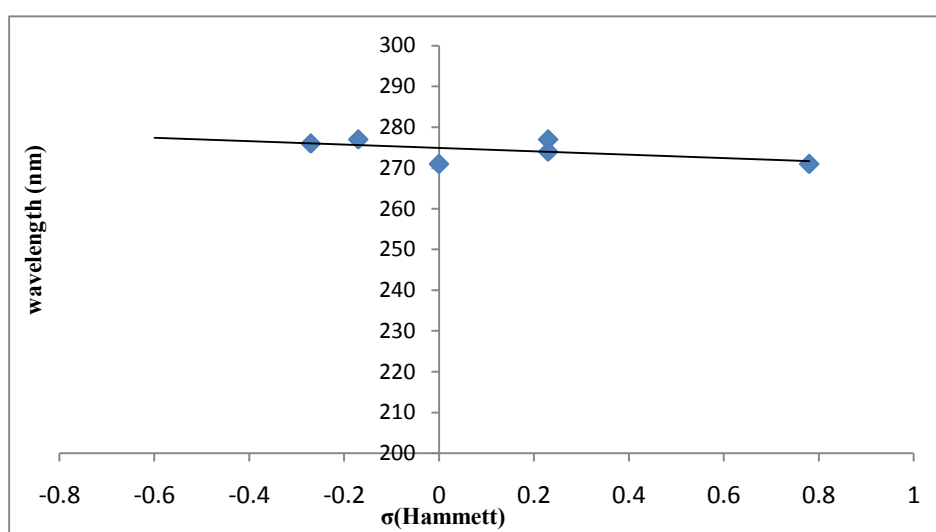


**Figure 4.4.13** Plot of wavelength (nm) versus Hammett  $\sigma$  values for  $\pi \rightarrow \pi^*$  transition of  $\text{Cu}(\text{R-BENH})\text{Br}_2$  in EtOH solution

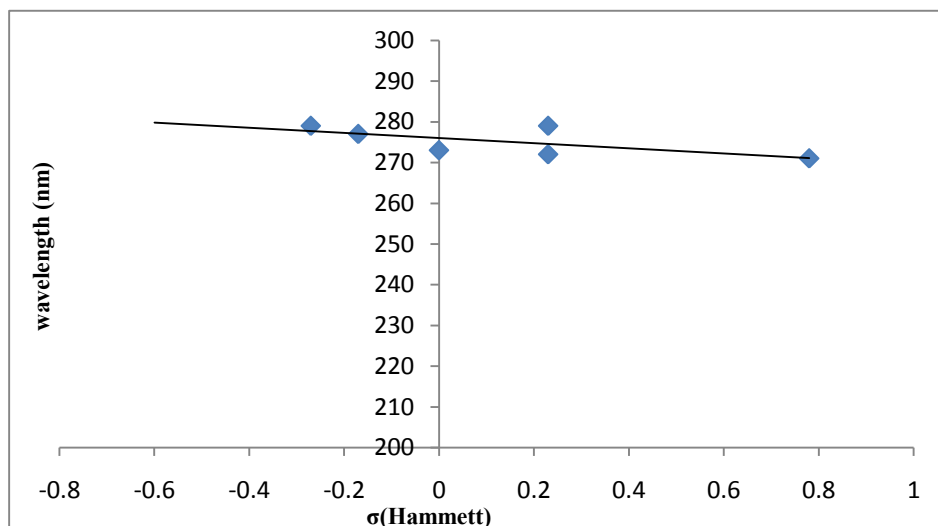


**Figure 4.4.14** Plot of wavelength (nm) versus Hammett  $\sigma$  values for  $\pi \rightarrow \pi^*$  transition of  $\text{Cu}(\text{R-BENH})\text{Br}_2$  in  $\text{CHCl}_3$  solution

The effect of the metal ion on the ligand orbitals compared with the free amines (ethanol solution) is shown in figure 4.4.15. The figure shows no parallelism between the plot of the free ligand and of the copper bromide complex in ethanol solution. This suggests that for the copper bromide complexes there is a slight metal contribution to the  $\pi \rightarrow \pi^*$  transition for the electron donating substituents in ethanol. In chloroform (figure 4.4.16) the mixing between the  $\pi$  – orbitals of the free ligand and of the metal orbitals is more influenced by the donor substituents, but the nitro substituent shows a significant blue shift. This suggests that there is a change, on complexation in the coupling experienced by the  $\text{NO}_2$  substituted ligand. This is identifiable by the behaviour of the d - d transitions discussed below.

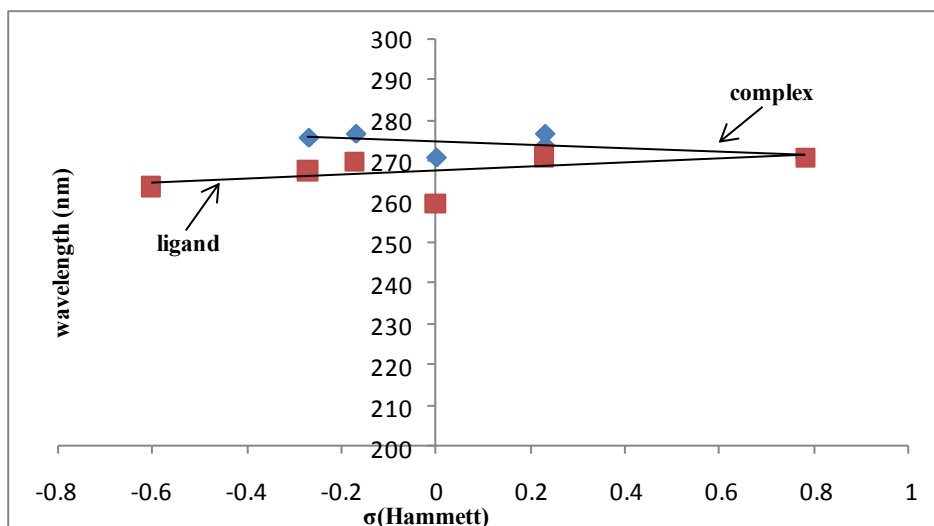


Figure 4.4.15 Plot of wavelength (nm) versus Hammett  $\sigma$  values for  $\pi \rightarrow \pi^*$  transition of  $\text{Cu}(\text{R-BENH})\text{Br}_2$  and of the free ligand in EtOH solution

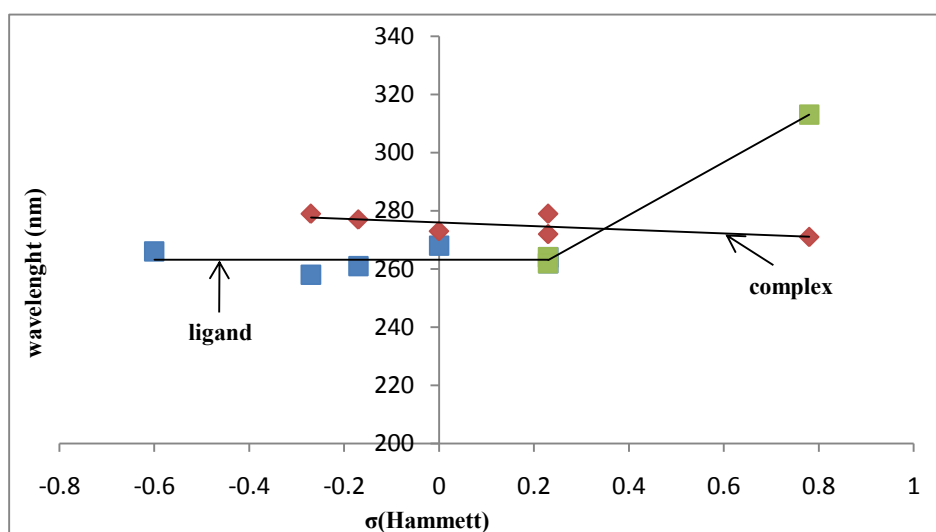
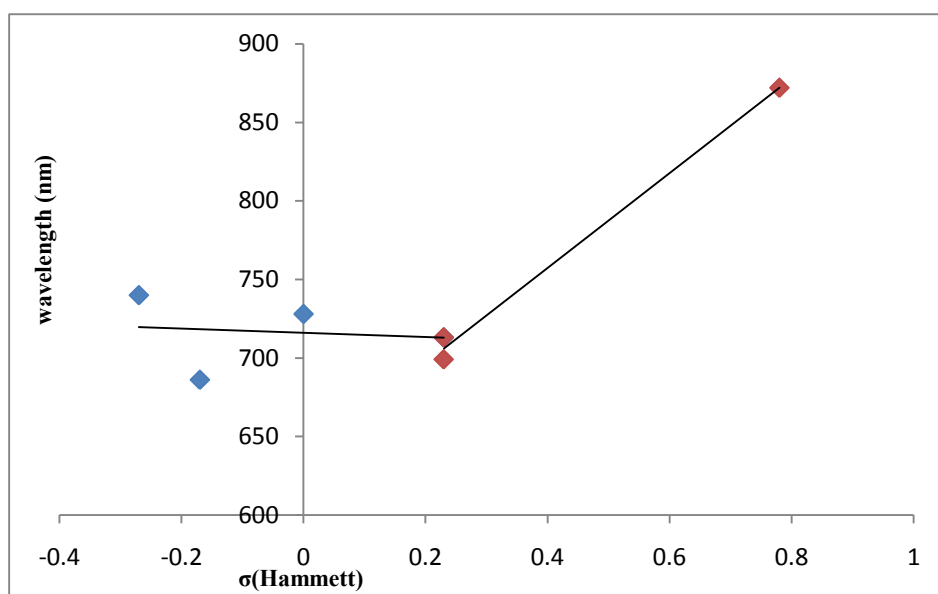


Figure 4.4.16 Plot of wavelength (nm) versus Hammett  $\sigma$  values for  $\pi \rightarrow \pi^*$  transitions of  $\text{Cu}(\text{R-BENH})\text{Br}_2$  and of the free ligand in  $\text{CHCl}_3$  solution

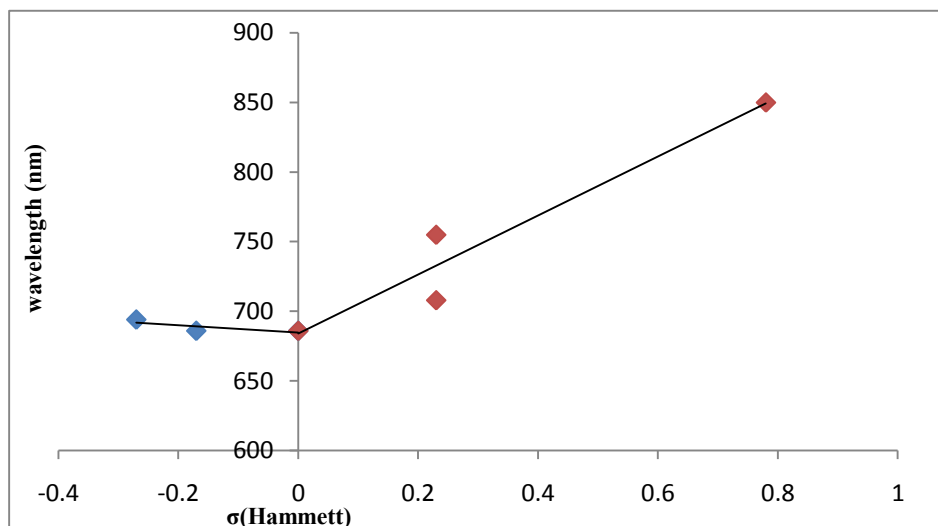
The plot (figure 4.4.17) of the Hammett parameters for the bromo complexes against the  $d \rightarrow d$  transitions show that there is a lack of linearity within the data of the  $d \rightarrow d$  transition, especially for the nitro analogue. The behaviour of the complex in ethanol is similar to that of the free ligand in chloroform. The lack of linearity within the data of the  $d \rightarrow d$  transition

of the complexes and nitro analogue might imply that the nitro group is not isostructural compared to the other bromo complexes or this may be due to a change in coupling within the electronic states. A possible explanation for the lack of linearity may be due to the strong resonance effect of the nitro group, which often results in the Hammett substituent constant having an anomalous value.



**Figure 4.4.17 Plot of wavelength (nm) versus Hammett  $\sigma$  values for  $d \rightarrow d$  transition of  $\text{Cu}(\text{R-BENH})\text{Br}_2$  in EtOH solution**

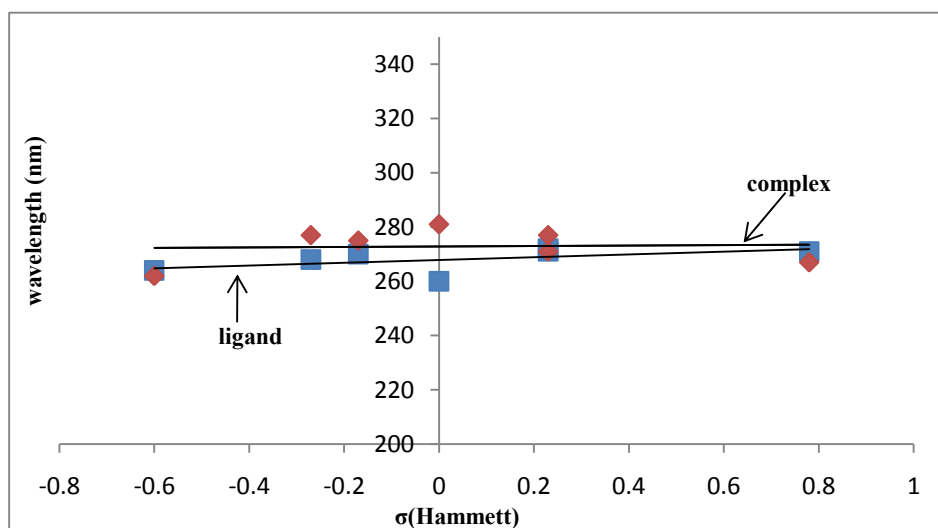
The effect of the electron donor and electron acceptor substituents on the  $d$  – orbitals of the bromide complexes in chloroform solution is illustrated in figure 4.4.18. The figure shows that the electron donor substituents cause a slight blue shift for the  $d \rightarrow d$  transition of the bromo complexes (compared with figure 4.4.17), while the electron withdrawing groups cause a clear blue shift on the  $d \rightarrow d$  transition. When contrasted with figure 4.4.17 this suggest that the polar solvents stabilise the electron withdrawing substituents more in ethanol resulting in a blue shift.



**Figure 4.4.18** Plot of wavelength (nm) versus Hammett  $\sigma$  values for  $d \rightarrow d$  transition of  $\text{Cu}(\text{R-BENH})\text{Br}_2$  in  $\text{CHCl}_3$  solution

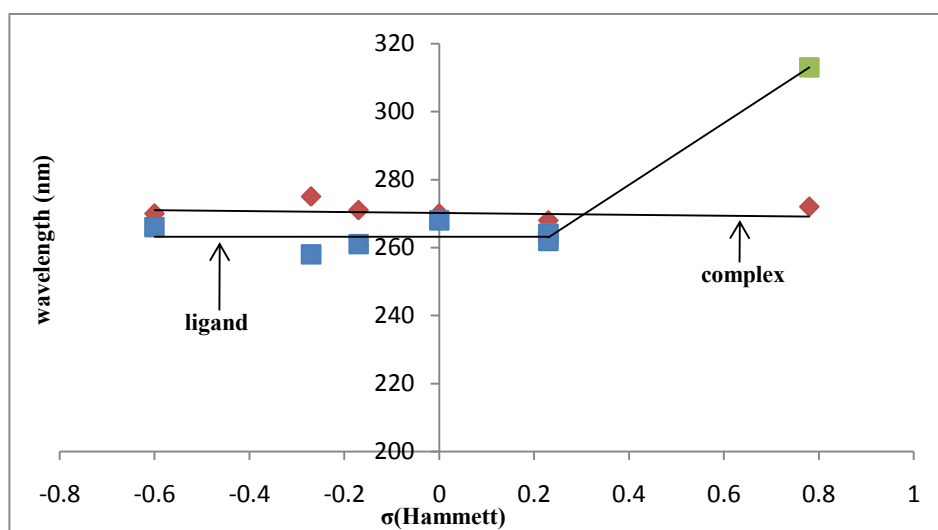
#### 4.4.2.4 Chloro complexes

The electronic effect transmitted (figure 4.4.19) by the donor substituents on the benzene ring of the chloro complexes in ethanol solution results in less mixing between the  $\pi$  orbitals of the free ligand and the metal orbitals compared to the bromo complexes.



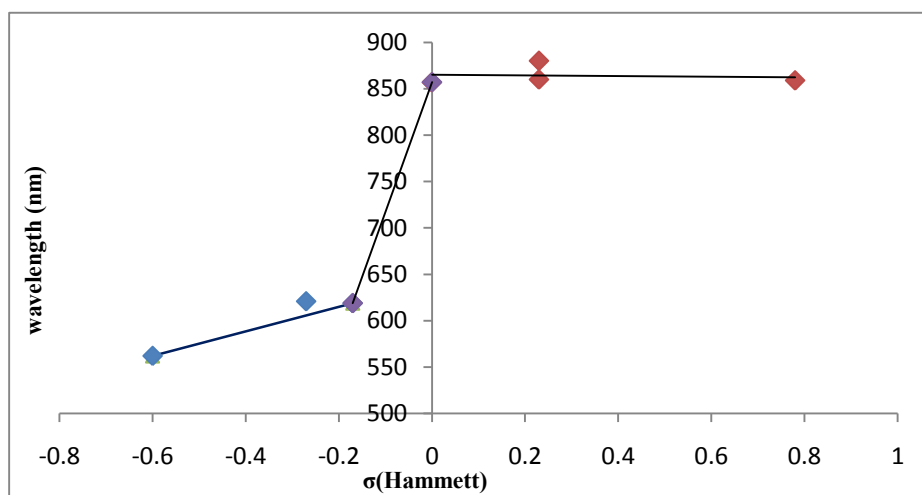
**Figure 4.4.19** Plot of wavelength (nm) versus Hammett  $\sigma$  values for  $\pi \rightarrow \pi^*$  transition of  $\text{Cu}(\text{R-BENH})\text{Cl}_2$  and of the free ligand in  $\text{EtOH}$  solution

In chloroform solution (figure 4.4.20) both the electron donor and the electron acceptor substituents contribute to the slight mixing of the  $\pi$  orbitals of the free amine ligand and the metal orbitals cause a bathochromic shift on the  $\pi \rightarrow \pi^*$  transition of the benzene ring, this suggests that the HOMO and the LUMO state of the benzene ring contain metal character. This is shown in figure 4.4.20. The experimental data obtained from the analysis of the  $\pi \rightarrow \pi^*$  transition of the benzene ring for chloride complexes indicates that the bands are slightly sensitive to the nature of the solvent and there is a minor shift in the electronic spectra due to the substituents.



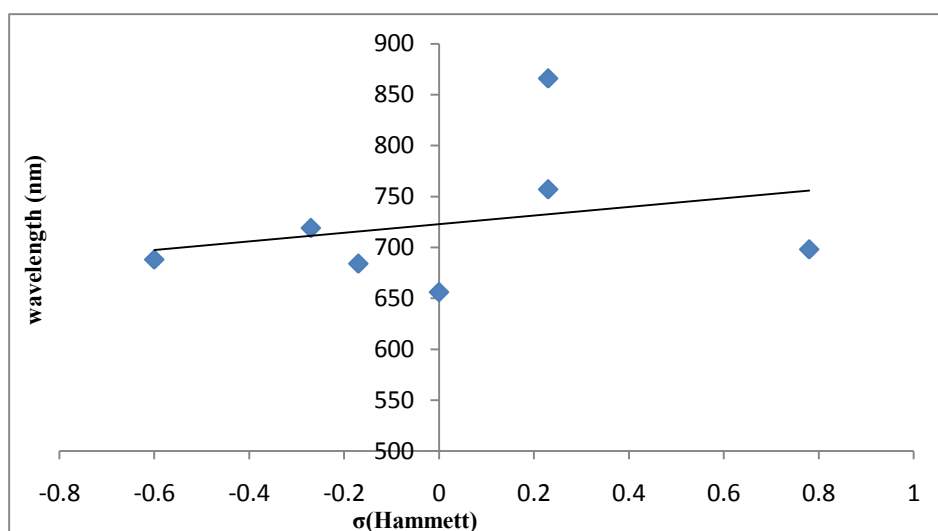
**Figure 4.4.20** Plot of wavelength (nm) versus Hammett  $\sigma$  values for  $\pi \rightarrow \pi^*$  transition of  $\text{Cu}(\text{R-BENH})\text{Cl}_2$  and of the free ligand in  $\text{CHCl}_3$  solution

Figure 4.4.21 represents the correlation of Hammett parameters with the  $d \rightarrow d$  transition of the chloro complexes in ethanol. As observed in the plot (figure 4.4.21) there is a difference of about 300 wavenumbers between the most electron donating and the most electron withdrawing substituent. This suggests a change in coordination sphere which means that the ethanol may be coordinated to the complex resulting in a tetragonal coordination for the donor analogues (with a larger crystal field splitting), while for the withdrawing groups a distorted tetrahedral geometry may be exist (yielding smaller crystal field splitting).



**Figure 4.4.21** Plot of wavelength (nm) versus Hammett  $\sigma$  values for  $d \rightarrow d$  transition of  $\text{Cu}(\text{R-BENH})\text{Cl}_2$  in EtOH solution

From the spectroscopic data obtained for the characterization of the chloro complexes in chloroform, in a noncoordinating solvent the plot, figure 4.4.22 shows a non perfect linear plot. But there is some degree of linearity between the Hammett substituent parameters and  $d-d$  transitions of the chloro complex in chloroform, with the exception for the bromo analogue. It is likely that all except the bromo analogue are probably distorted tetrahedral, while the bromo analogue (based of crystal field splitting consideration) is likely to be tetrahedral.



**Figure 4.4.22** Plot of wavelength (nm) versus Hammett  $\sigma$  values for  $d \rightarrow d$  transition of  $\text{Cu}(\text{R-BENH})\text{Cl}_2$  in  $\text{CHCl}_3$  solution

#### 4.4.3 The electronic spectra of the N, N'-bis(cinnamaldehyde)-1, 2-diiminoethane ligands and their copper(I)-halide and copper(II) halide complexes

The Ultraviolet-visible spectra of the N, N'-bis(cinnamaldehyde)-1, 2-diiminoethane ligands and their complexes were recorded in dichloromethane solution in the range of 200 nm to 900 nm region. This section will focus on the effect produced by the substituent  $\{(N(CH_3)_2)\}$  on the *para*-position of the N, N'-bis(cinnamaldehyde)-1, 2-diiminoethane ligand and the influence of the metal ion on the free ligand, CA<sub>2</sub>EN. The data obtained for the characterization of N, N'-bis(cinnamaldehyde)-1, 2-diiminoethane ligands and their metal complexes are listed in table 3.19. The electronic spectra obtained for CA<sub>2</sub>EN ligand in dichloromethane solution (figure 4.4.23), show extreme broadening of the absorption bands.

The absorption spectrum of CA<sub>2</sub>EN in dichloromethane solution shows one intense band at 311 nm, one broad band at 249 nm, one weak band at 339 nm, one very undistinguishable band between 262 nm and 308. All these bands are observed in the ultraviolet region<sup>29</sup>. The absorption at 249 nm ( $\epsilon = 3.50$ ) corresponds to a  $\pi \rightarrow \pi^*$  transition of the benzene ring. The absorption band observed at 339 nm in dichloromethane, solution is most probably due to the  $n \rightarrow \pi^*$  transition of imine group<sup>14</sup>, the broad band between 262 nm and 308 nm masked the  $\pi \rightarrow \pi^*$  transition of the imine group. The absorption band at 311 nm ( $\epsilon = 4.80$ ) corresponds to the CT band<sup>14</sup>.

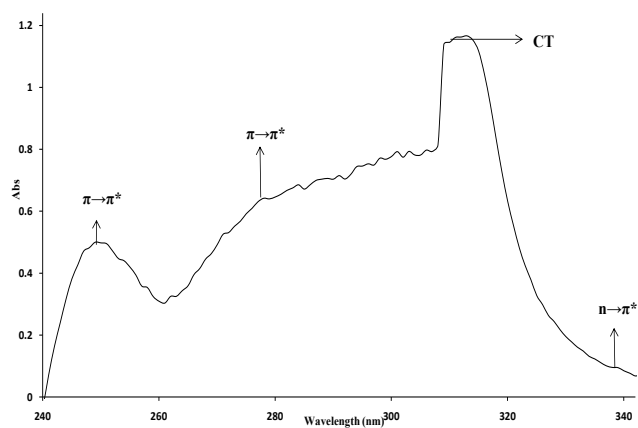


**Figure 4.4.23 Ultraviolet spectrum of CA<sub>2</sub>EN ligand in DCM**

The spectroscopic data obtained from the characterization of N, N'-bis(cinnamaldehyde)-1, 2-diiminoethane ligands (table 3.19 and figure 4.4.24) , show that the presence of the electron donor substituent {N(CH<sub>3</sub>)<sub>2</sub>} at the *para* position of N, N'-bis(cinnamaldehyde)-1, 2-diiminoethane shifts the  $\pi \rightarrow \pi^*$  transition of the benzene ring towards longer wavelength. This decreases the energy gap between the  $\pi^*$  and  $\pi$  of benzene ring, as a result the LUMO state of the  $\pi$  - orbitals is stabilized relative to the HOMO state. The same shift is observed for the charge transfer transition.

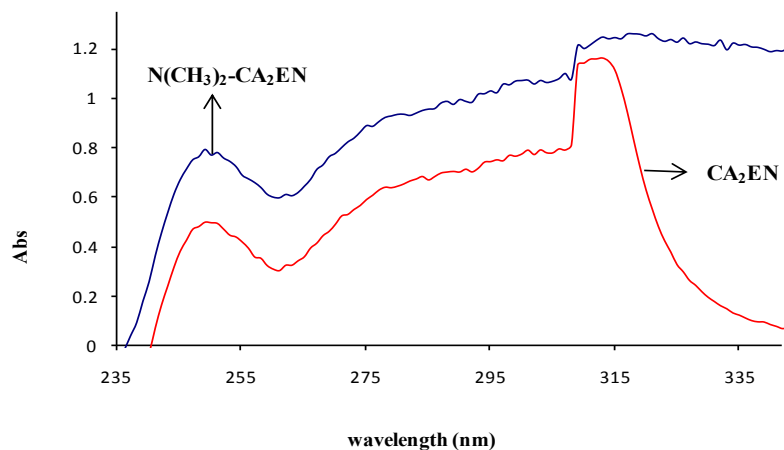


Figure 4.4.24 Ultraviolet spectra of  $\text{CA}_2\text{EN}$  and  $\text{N}(\text{CH}_3)_2\text{-CA}_2\text{EN}$  ligand in DCM

#### 4.4.3.1 Copper(I) and copper(II) halide complexes of *N, N'*-bis(cinnamaldehyde)-1, 2-diiminoethane ligand

The electronic spectra of the copper(I) and copper(II) complexes have been recorded in the 200 nm to 900 nm range in dichloromethane solution. The electronic spectra data are listed in table 3.19 and the electronic spectra are overlapped in figure 4.4.25 and 4.4.26.

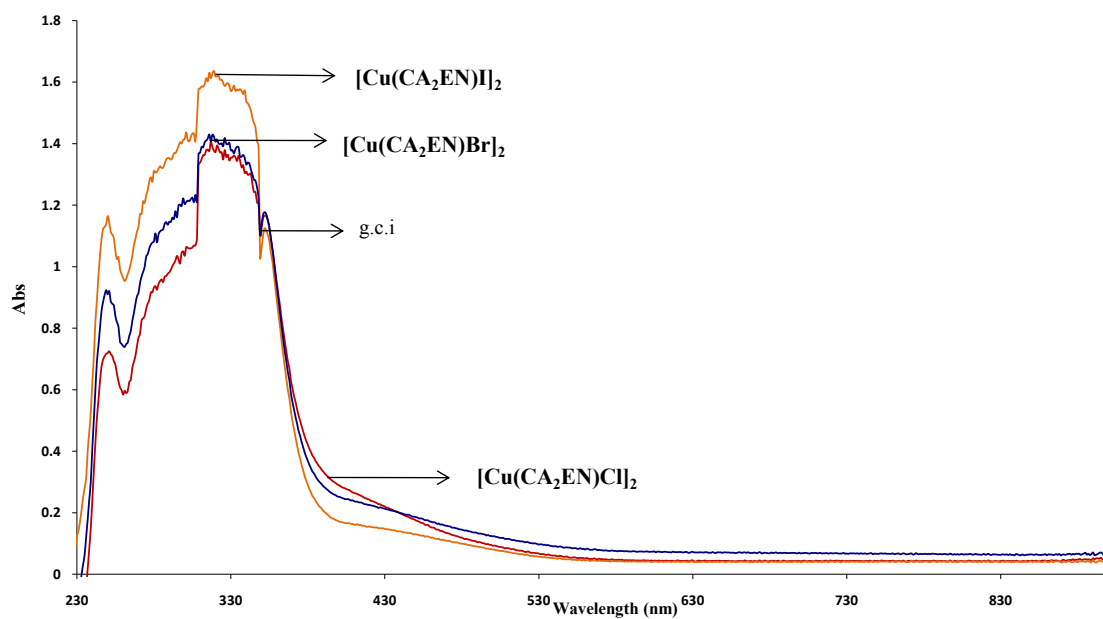
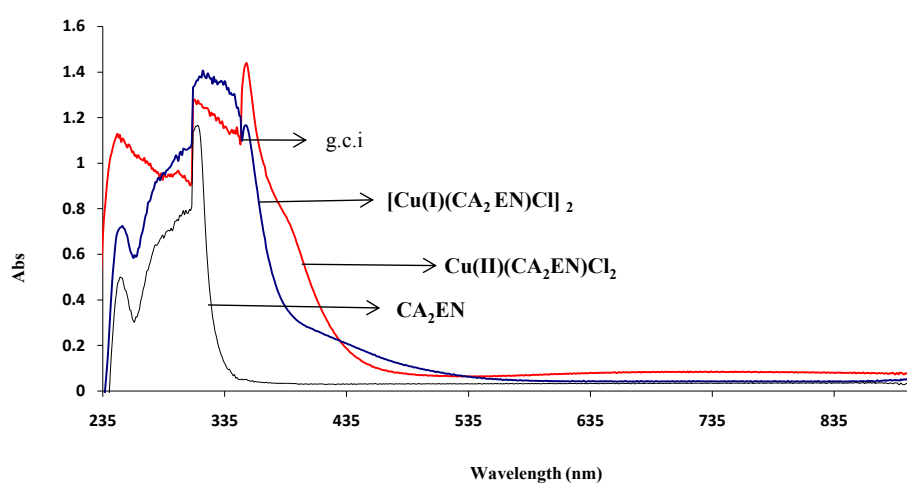


Figure 4.4.25 UV-vis spectra of  $[\text{Cu}(\text{CA}_2\text{EN})\text{X}]_2$  complexes in DCM

Since no  $d \rightarrow d$  transitions are expected for the  $d^{10}$  Cu(I) complexes, the UV-vis absorption bands are assigned to metal to ligand charge transfer (MLCT) or  $\pi \rightarrow \pi^*$  transition due to the ligand<sup>30</sup>. The absorption spectra of the complexes in dichloromethane feature one new shoulder in the visible region. This shoulder is observed within the range 432 nm and 449 nm. Since this shoulder is not observed in the electronic spectrum of the free ligand the band may be assigned to MLCT<sup>30</sup>. It shows slight halogen sensitivity.

While in electronic spectrum of  $\text{Cu}(\text{CA}_2\text{EN})\text{Cl}_2$ , figure 4.4.26 one extremely weak broad absorption band at 741 nm and one shoulder at 393 nm are observed. The broad band at 741 nm correspond to the  $d \rightarrow d$  transition within the orbitals of the copper(II) metal ion, since this band was not observed in  $[\text{Cu}(\text{I})(\text{CA}_2\text{EN})\text{Cl}]_2$ . Since copper(II)  $d \rightarrow d$  transitions typically have a molar extinction coefficient of 10 ( $\epsilon = 2$ ) the shoulder at 393 may be assigned to MLCT<sup>30</sup>.



**Figure 4.4.26** UV-vis spectra of  $[\text{Cu}(\text{I})(\text{CA}_2\text{EN})\text{Cl}]_2$ ,  $\text{Cu}(\text{II})(\text{CA}_2\text{EN})\text{Cl}_2$  and  $\text{CA}_2\text{EN}$  in DCM

From the experimental data, it can be concluded that on complexing with the  $\text{Cu}(\text{I})\text{Br}$  the  $N,N'$ -bis(cinnamaldehyde)-1, 2-diiminoethane ligand undergoes a slightly shift for the  $\pi \rightarrow \pi^*$  transition (benzene) towards longer wavelength. This decreases the energy gap of the  $\pi -$

orbitals of the benzene ring, this indicates less mixing between  $\pi$  – orbitals of the benzene ring and the metal orbitals and giving the  $\pi$  – orbitals slight metal character.

## 4.5 Infrared spectroscopy

Infrared spectroscopy is one of the most popular spectroscopic techniques used by chemists. This instrument deals only with molecules that have functional groups that only absorb light (photons) on low energy side (beyond red in the spectrum). The beam or photons associated with an infrared spectrum excite electrons due to the small energy these photons have, but the photons induce vibrational excitation of covalent bonded atoms and groups resulting in molecular vibrations.

The infrared region of the electromagnetic spectrum can be divided into three subsets, far-infrared, near-infrared and mid infrared. The mid-infrared region ( $4000\text{ cm}^{-1}$  to  $400\text{ cm}^{-1}$ ), is the region associated with the changes in vibrational energies within the molecule. The far-infrared region determines the vibrational modes for heavy metals such as inorganic molecules. The energy at near-infrared region is useful for the analysis of molecular overtone and combination vibrational modes.

### 4.5.1 Infrared spectral studies

The infrared spectrum of the N, N'-(aryl)benzaldimines are rich in fundamental vibrations. For the parent imine (X=H), as well as for the halogen substituents having 34 atoms, there are 96 modes of vibrations, which due to the two fold symmetry equates to 47 pairs of fundamentals, plus two for the C-C bond of the methylene bridge. For the polyatomic substituents, there are an additional  $3N$  fundamentals ( $N$ = the number of additional atoms). For the amine parent, there are an additional 12 modes (six for each reduced imine), and for the salts, a further 6 (three for each tertiary amine).

In the absence of a complete vibrational analysis of the molecules (beyond the scope of this work), the identification of suitable group frequencies to use in the characterisation of the

ligands was restricted to attempting to identify suitable C-N-H modes within the diimines, the diamines and their salts against a background of the substituted benzene moiety associated with the aromatic ring. The work by Varsányi and Szöke<sup>31</sup> is seminal in establishing the behaviour of the vibrational coupling within the benzene ring due to the substituent. According to the classification of Varsányi and Szöke<sup>31</sup>, given that the Ar-C of the methylene bridge is considered light, the substituents X= NO<sub>2</sub>, OH, Me, OMe, N(CH<sub>3</sub>)<sub>2</sub> are 1, 4 di-light substituents, while the substituents X=Cl, Br are 1-light -4- heavy substituents.

This causes profound differences in the vibrational coupling experienced by the different molecules<sup>31</sup>, for example the  $\nu$ C-X (Wilson mode 7a) which occurs between 1270-1100 cm<sup>-1</sup> (1, 4 di-light) or between 400-240 cm<sup>-1</sup> (1-light-4-heavy) strongly couples with the ring breathing mode (Wilson mode 1), which in turn occurs between 860-720 cm<sup>-1</sup> (1, 4 di-light) and between 1100-1050 cm<sup>-1</sup> (1-light-4-heavy). The other  $\nu$ C-X (Wilson mode 13) which occurs between 1300-1100 cm<sup>-1</sup> (for both 1, 4 di-light and 1-light -4- heavy substituents) couples with the Star of David ring breathing mode (Wilson mode 12) which in turn occurs between 860-760 cm<sup>-1</sup> (1, 4 di-light) and between 480-680 cm<sup>-1</sup> (1-light-4-heavy). The variation between the two sets of substituents is even more pronounced below 1000 cm<sup>-1</sup>, particularly those involving the out-of plane vibrations<sup>31</sup>. Not only is the frequency substituent sensitive, but so too is the intensity of the benzene vibrations, as well as the associated substituent internal vibrations. For example, with increasing Hammett  $\sigma$  function both the frequency and the intensity of the symmetric and asymmetric stretch NH<sub>2</sub> increases (with the symmetric having a steeper slope); but the behaviour of the OH stretch is opposite<sup>31</sup>. In solution this is further complicated in that these properties are solvent sensitive; polar solvents decrease the frequency, but increase the intensity of the  $\nu$ NH<sub>2</sub> vibrations<sup>31</sup>.

In addition to the aromatic ring, the vibrations of the methylene bridge needed to be considered, which was done by referring to the isotope labelled studies of metal complexes with ethylenediamine.

#### 4.5.2 Group frequencies of the N, N'-(aryl)benzaldimines

An ideal characteristic group frequency, the  $\nu\text{C}=\text{N}$  of an imine, occurring at about  $1645\text{ cm}^{-1}$ , is very prominent as it occurs in a region where there are few alternative assignments, and it is widely reported within the literature (and is also the reason why the Schiff base imines were initially considered for the present study). The in-plane bend  $\delta_{\text{ip}}\text{C}-\text{C}=\text{N}$  (about  $635\text{ cm}^{-1}$ <sup>30</sup>) and out-of-plane  $\delta_{\text{op}}\text{C}-\text{C}=\text{N}$  (about  $720\text{ cm}^{-1}$ <sup>31</sup>) occur in a region that is vibrationally rich, dependant on whether light or heavy. The former region includes both in-plane (modes 6b and 12) and out-of-plane (mode 4) benzene modes, the latter includes the in-plane benzene modes (modes 1, 12 and 6a), as well as a number of possible substituent internal vibrations<sup>31</sup>, and also the  $\text{CH}_2$  rock of the methylene bridge ( $\rho\text{CH}_2$ )<sup>32, 33</sup>.

Within the present study only the  $\nu\text{C}=\text{N}$  could be identified for all the substituents and a correlation analysis performed.

Table 4.11 Correlation of  $\nu\text{C}=\text{N}$  for N, N'-(aryl)benzaldimine ligands with various substituent parameters

Parameters	Correlation factor for $\nu\text{C}=\text{N}$
Hammett ( $\zeta_{\rho}$ )	0.4687
Swain ( $\zeta_{\text{I}}$ )	0.8897
Swain ( $\zeta_{\text{R}}$ )	0.1506
Williams & Norrington ( $\zeta_{\text{I}}$ )	0.7811
Williams & Norrington ( $\zeta_{\text{R}}$ )	0.1105

Correlation studies suggest that inductive effect is more pronounced at the  $\nu\text{C}=\text{N}$ , this effect is the results of the electrons being withdrawn with increasing value of  $\zeta$ , meaning more negative charge is drawn away from the N into the ring by the electron withdrawing substituents and  $\text{sp}^2$  hybrid state is more stable and  $\nu\text{C}=\text{N}$  is increased<sup>31</sup>.

The correlation analysis shows that the inductive effect is a better descriptor, this observation agrees with that found in the NMR studies, that there is no planarity of the imine bond with the benzene ring that the effect must be a field effect (through space rather than along the bonds).

The dual substituent parameters was able to explain and differentiate the (poorer) trend that Hammett has and conclusively show that conjugation is not the controlling factor within the imines.

Percy and Thornton <sup>34</sup> previously conducted an infrared study of *N*-arylsalicylaldimine complexes substituted in both aryl rings. Substitution on the aryl ring was found to relate to the Hammett parameter, and to Swain's field parameter, but not to any resonance capacity of the substituent <sup>34</sup>. They also observed that, with exception to the 3-methoxy substituent, on substitution of the salicylaldimine a correlation with the Taft resonance polar parameter was observed for the  $\nu$ C-N and  $\nu$ C-O, and an inverse correlation was observed for  $\nu$ C=N and  $\nu$ M-N <sup>34</sup>. They concluded that, on coordination, stabilization of the M-N and C=N bonds occurs at the expense of the C-N and C-O bonding, and they accounted for the anomalous 3-methoxy behaviour to steric effects of the bulky group *ortho* to the enol <sup>34</sup>. Clearly the presence of the 2-hydroxy group and the resultant chelate effect promotes aligning the imine double bond with that of the benzene ring.

The lack of correlation of  $\nu$ C=N for N, N'-(aryl)benzaldimine ligands with the resonance parameters may simply be due to the non co-planar of the imine  $\pi$  bond with that of the aromatic ring or may be because the system is not coordinated to a metal ion to allow for the delocalization of the electrons around the chelate of the ring. Regretably, because the copper is a strong enough Lewis acid to hydrolyse the Schiff base, it was not possible to determine whether on chelation the N, N'-(aryl)benzaldimine undergoes a similar alignment of the imine and benzene  $\pi$  bonds.

### 4.5.3 Group frequencies of the N, N'-(aryl)benzaldiamines

Secondary amines show a sharp single NH stretching absorption of variable intensity between 3450-3300  $\text{cm}^{-1}$ <sup>35</sup>. The vibration is known to be sensitive the nature of the surroundings<sup>30</sup>, and a broad second band below 3200  $\text{cm}^{-1}$  may also be observed if hydrogen bonded (with both free and hydrogen bonded forms often being simultaneously observed<sup>35</sup>). A weak bend ( $\delta\text{N-H}$ ) is expected between 1550-1650  $\text{cm}^{-1}$ <sup>35</sup> (easily masked by the bend for water), with the second bend of medium to weak intensity between 700-850  $\text{cm}^{-1}$ <sup>35</sup>. The former can be mistaken for the in-plane aromatic ring stretches (Wilson modes 8a and 8b); the latter can be either masked by or mistaken for the planar ring vibrations (modes 1,6a), and the out-of plane bends (modes 10a, 11, 17b)<sup>31</sup>, or the  $\text{CH}_2$  rock of the methylene bridge ( $\rho\text{CH}_2$ )<sup>32,33</sup>. The C-N stretch is a weak to medium band found between 970-960  $\text{cm}^{-1}$ <sup>32-35</sup>, and is considered of no practical significance<sup>35</sup> due to the abundance of the spectrum, while the weak C-C stretch between 860-850  $\text{cm}^{-1}$ <sup>32,33</sup> is an even poorer characteristic group.

Within the present study only the  $\nu\text{N-H}$  could confidently be identified for all the substituents and a correlation analysis performed.

Table 4.12 Correlation of  $\nu\text{N-H}$  for N, N'-(aryl)benzaldiamine ligands with various substituent parameters

Parameters	$\nu\text{N-H}$	$\nu\text{H-N}_{(\text{CuCl})}$	$\nu\text{H-N}_{(\text{CuBr})}$
Hammett ( $\zeta_\rho$ )	0.3164	0.7471	0.5400
Swain ( $\zeta_I$ )	0.6720	0.4583	0.8508
Swain ( $\zeta_R$ )	0.0563	0.6076	0.2232
Williams & Norrington ( $\zeta_I$ )	0.5955	0.6243	0.7897
Williams & Norrington ( $\zeta_R$ )	0.0259	0.6411	0.2100

The relative poor correlation between the substituent parameters and the  $\nu_{\text{N-H}}$  of N, N'-(aryl)benzaldiamine ligands suggest that a moderate inductive effect is observed among the  $\nu_{\text{N-H}}$ . The Swain parameters for the inductive effect provide a better correlation for free ligand and bromide complexes (In contrast, the chloride complexes appear more susceptible to the resonance effect). This is expected because as the  $\zeta$  value of the withdrawing substituent increase, then the more negative charge is being pulled away from the N into the ring, the  $\text{sp}^2$  hybrid state will be more stable and  $\nu_{\text{N-H}}$  will increase<sup>31</sup>. The proton NMR colleration studies show similar observations.

The lack of correlation of  $\nu_{\text{N-H}}$  for the coordinated N, N'-(aryl)benzaldiamines with the  $\zeta_{\text{R}}$ , resonance parameter for bromide complexes suggest that on coordination for N, N'-(aryl)benzaldiamine ligand system, unlike the salicylaldimes there is no delocalization around the coordinated ring. While the correlation for chloride complexes suggest there may be some alignment of the  $\pi$  system of the beznene ring on complex similar to the salicylaldimes. This suggests that the chloro and bromo complexes may not be isostructural in the solid state.

#### 4.5.4 Group frequencies of the N, N'-(aryl)benzaldiamine salts

For the secondary amine salts, the  $\text{NH}_2^+$  stretching absorption is expected to be broad and of medium intensity, with highly structured major maxima found between  $2700\text{-}2250\text{ cm}^{-1}$ <sup>35</sup> due to strong combination bands. The higher  $\delta_{\text{NH}_2^+}$  is found over a wider range ( $1600\text{-}1460\text{ cm}^{-1}$ )<sup>35</sup> than that of the uncharged primary amine, and the degeneracy may be removed to give two bands, with the aliphatic secondary amine salt being less intense<sup>34</sup> than the  $\delta_{\text{NH}_2}$  for ethylenediamine<sup>32, 33</sup>. The behaviour of the lower  $\delta_{\text{NH}_2^+}$ , the C-N stretch and the C-C stretch is not known, although for primary amines two medium to weak  $\delta_{\text{NH}_2}$  bands are expected between  $850\text{-}700\text{cm}^{-1}$ <sup>35</sup>.

Within the present study only the  $\nu_{\text{NH}_2^+}$  and the first  $\delta_{\text{NH}_2^+}$  could be identified for all the substituents and a correlation analysis performed. The low frequency, strong hydrogen bonding of the amine salt is clearly observed (figure 4.5.1).

Table 4.13 Correlation of  $\nu\text{NH}_2^+$  and  $\delta\text{NH}_2^+$  for N, N'-(aryl)benzaldiamine dihydrochloride salts with various substituent parameters

Parameters	$\nu\text{NH}_2^+$	$\delta\text{NH}_2^+$
Hammett ( $\zeta_\rho$ )	0.3046	0.0861
Swain ( $\zeta_I$ )	0.3134	0.1275
Swain ( $\zeta_R$ )	-0.6797	-0.1859
Williams & Norrington ( $\zeta_I$ )	0.1799	0.1054
Williams & Norrington ( $\zeta_R$ )	-0.7342	0.2650

The correlations (irrespective of the parameters employed) are poorer for the  $\delta\text{NH}_2^+$ . This is not unexpected as with the lower symmetry and the expected wavelength range (1600 – 1460  $\text{cm}^{-1}$ ) this fundamental vibration is expected to couple with the C–N–H bend and the H–C–N bend (the extent of which coupling would be very influenced by the nature of the molecule), hence substituent effects could be diluted out because of the variable coupling. The correlation of  $\nu\text{N–H}^+$  is unusual because, unlike the imine and amine, the stretch is inversely affected by the resonance parameters, whether employing the Swain or the Williams & Norrington parameter. This is agreement with the behaviour observed for the proton NMR.

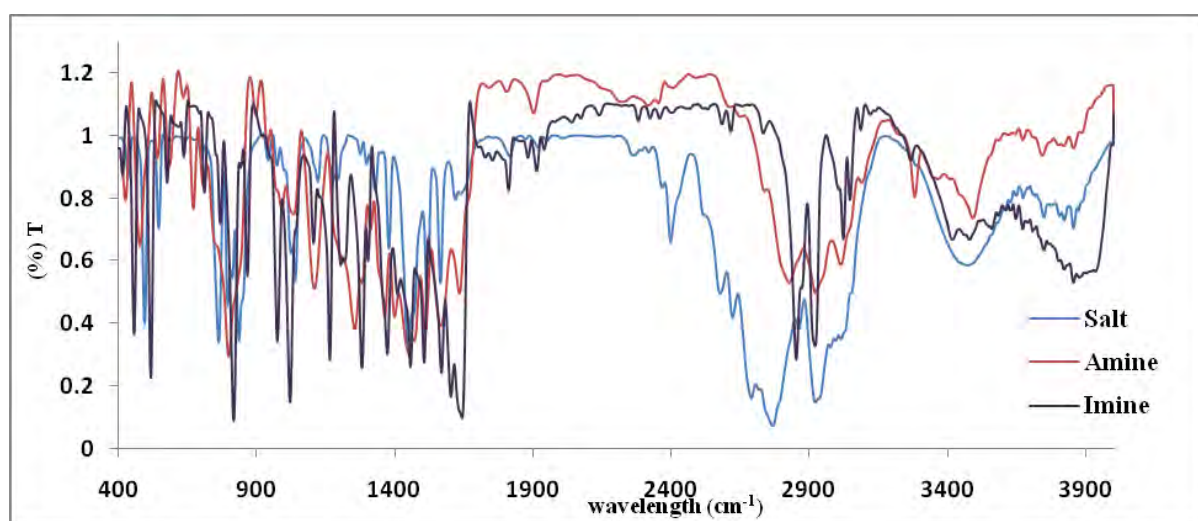


Figure 4.5.1 Mid-infrared spectra of 4-CH<sub>3</sub> analogues

#### 4.5.5 Group frequencies of the N, N'-bis(cinnamaldehyde)1, 2-diiminoethanes and their Cu(I) and Cu(II) complexes:

The very prominent  $\nu\text{C}=\text{N}$  of an imine, occurring at about  $1645\text{ cm}^{-1}$  where there are few alternate assignments, is an ideal characteristic group frequency to monitor metal binding. As mentioned above, the in-plane bend  $\delta_{\text{ip}}\text{C}-\text{C}=\text{N}$  (about  $635\text{ cm}^{-1}$ <sup>31</sup>) and out-of-plane  $\delta_{\text{op}}\text{C}-\text{C}=\text{N}$  (about  $720\text{ cm}^{-1}$ <sup>31</sup>) are not as suitable due to the additional benzene modes, possible substituent internal vibrations<sup>31</sup>, and also the CH<sub>2</sub> rock of the methylene bridge ( $\rho\text{CH}_2$ )<sup>31,32</sup>.

Table 4.14 Comparison between the  $\nu\text{C}=\text{N}$  stretches of the BEN and CA<sub>2</sub>EN ligands

R	BEN	CA <sub>2</sub> EN	
	$\nu\text{C}=\text{N}$	$\nu\text{C}=\text{N}$	$\Delta\nu\text{C}=\text{N}$
H	1614	1615	1
N(CH <sub>3</sub> ) <sub>2</sub>	1636	1620	16
$\Delta\nu\text{C}=\text{N}$	22	5	

In the current study only two N, N'-bis(cinnamaldehyde)-1, 2-diimineoethanes were investigated. The difference in the shift of  $\nu_{C=N}$  between the substituted Schiff bases  $\{N(CH_3)_2-CA_2EN$  and  $N(CH_3)_2BEN\}$  suggests that the two Schiff bases are not the same, there may be a presence of an extensive conjugation of the ethene and imine  $\pi$  bonds with that of the aromatic ring, and that on coordination, like the complexes of the salicylaldimes, there is possible delocalisation around the chelate ring.

The shifts of the  $\nu_{C=N}$  of the coordinated complexes indicate that the  $\nu_{C=N}$  of the free ligand,  $CA_2EN$  is metal sensitive. Since the presence of Cu(I) caused different shifts to the  $\nu_{C=N}$ , this suggests the presence of an extensive conjugation of the ethene and imine  $\pi$  bonds with that of the aromatic ring. The opposite is observed for Cu(II). These observations are in agreement with the UV/vis studies of the the N, N'-bis(cinnamaldehyde)-1, 2-diiminoethane ligands and their copper(I)-halide and copper(II) halide complexes.

Table 4.15 Comparison between the  $\nu_{C=N}$  stretches of the  $CA_2EN$  ligand and their copper Complexes

compound	$CA_2EN$	$[Cu(I)(CA_2EN)Cl]_2$	$[Cu(I)(CA_2EN)Br]_2$	$[Cu(I)(CA_2EN)I]_2$	$Cu(II)(CA_2EN)Cl_2$
$\nu_{C=N}$	1614	1624	1627	1627	1612
$\Delta\nu_{C=N}$		10	13	13	-2

#### 4.6 Conclusion

The NMR studies of the free N, N'-(aryl)benzaldimine ligands have confirmed that the presence of the electron withdrawing groups and the electron donating group at the *para*-position of the free N, N'-(aryl)benzaldimine ligands reduces the co-planarity of the imine group and the benzene ring but that through flexibility of the molecule, a through space field effect is induced on the protons of the bridge, an effect which is not observed in the carbon NMR studies of the free N, N'-(aryl)benzaldimine ligands. This is in agreement with the infrared studies of the free N, N'-(aryl)benzaldimine ligands, whereby the inductive effect is highly dominating in the  $\nu_{C=N}$  of the free imine ligands.

Both in the N, N'-(aryl)benzaldimine ligands and their dihydrochloride salts the benzene ring and the nitrogen atom are non-parallel to each other, the disappearance of the through space inductive effect in both ligands may be due to the reduction of the imine bond to an amine bond and because of the solvent effect.

The studies further show that the presence of the double bond within the N, N'-(aryl)benzaldimine ligand, N, N'-*bis*(benzyl)-1, 2-diiminoethane does not necessarily affect the chemical shifts of the aromatic protons, but stabilizing N, N'-*bis*(cinnamaldehyde)-1, 2-diiminoethane with a donor group at the *para*- position brings a change in the chemical shifts of the protons at the side chain of the N, N'-*bis*(benzyl)-1, 2-diiminoethane. This is supported by the infrared studies of the  $\nu_{C=N}$  of the N, N'-*bis*(cinnamaldehyde)-1, 2-diiminoethane.

The amine salt studies suggested that the electron withdrawing substituents were unable to withdraw the negative charge away from the positively charged N into the ring, this is supported by the correlation analysis of the three substituent parameters. This is expected, given the position in which the nitrogen atom is, relative to the *para*-position of the benzene ring.

The UV/vis studies of the N, N'-(aryl)benzaldimine ligands in ethanol solution indicated that the electronic effect produced by the substituents {electron donor or electron acceptor except for 4-N(CH<sub>3</sub>)<sub>2</sub>} onto the system affect is similar throughout the absorption bands of the imines. The effect of the solvent, ethanol enhances the bathochromic shift.

It can be concluded that, on the reduction of the iminic bond in N, N'-(aryl)benzaldimine ligands, the  $\pi \rightarrow \pi^*$  transitions of the benzene ring (amine ligands) both in ethanol and chloroform behave similarly (red shift). For both chloro and bromo complexes a slight mixing between the  $\pi$  – orbitals of the benzene ring of the free ligand and the  $\pi$  – orbitals of the benzene ring of the metal complex is observed. The mixing of these orbitals depends on the nature of the solvent. In chloroform a non-linear relationship is enhanced within the data of the complexes (both bromo and chloro), while in ethanol the opposite is favoured.

The stereochemistry of the Cu(R-BENH)Br<sub>2</sub> complexes was found to be predominately distorted tetrahedral, while for the chloro complexes tetragonal coordination involving the solvent was observed.

#### 4.7 References

1. T. Karanski, *J. Mass. Spectrom.*, 1999, **34**, 975–977.
2. D. L. Carroll, I. Dzidic, E. C. Horning, R. N. Stillwell, *Applied Spectro. Rev.*, 1981, **17**, 337–406.
3. E. Pretsch, J. Seibl, *Table of spectra data for structure determination of organic compounds*, 2<sup>nd</sup> ed., Springer-Verlag, New York, 1989, M55-M135.
4. D. F. Church, G. J. Gleicher, *J. Org. Chem.*, 1975, **40**, 536-537.
5. D. L. Johnston, W. L. Rohrbaugh, W. D. Horrocks, *Inorg. Chem.*, 1971, **10**, 547-552.
6. C. G. Swain, S. H. Unger, N. R. Rosenquist, M. S. Swain, *J. Am. Chem. Soc.*, 1983, **105**, 492-502.
7. S. G. Williams, F. E. Norrington, *J. Am. Chem. Soc.*, 1976, **98**, 508-516.
8. S. Ehrensons, R. T. C. Brownlee, R. W. Taft, *Prog. Phys. Org. Chem.*, 1973, **10**, 1-80.
9. Y. Dang, H. J. Geise, R. Dommissie, J. Gelan, J. Nouwen, *J. Chem. Soc. Perkin Trans*, **2**, 1990, 1785-1790.
10. G. C. Levy, R. L. Lichter, G. L. Nelson, *Carbon-13 nuclear magnetic resonance spectroscopy*, 2<sup>nd</sup> ed. Wiley-Interscience, New York, 1980, 102-103.
11. S. Patai, *The chemistry of carbon-nitrogen double bond*, ed. S. Patai, Wiley-Interscience, New York, 1970.
12. S. Basu, *Advances in quantum chemistry*, Vol. 1, ed. P. O. Lowdin, Academic Press, New York, 1964, 145.
13. R. T. Morrison, R. N. Boyd, *Organic chemistry*, 5<sup>th</sup> ed., ed. E. Ober, Allyn and Bacon, New York, 1987, 583-589.

14. S. Patai, *The chemistry of carbon-nitrogen double bond*, ed. S. Patai, Wiley-Interscience, New York, 1970, 184-201.
15. H. H. Hammud, A. G. Ghannoum, M. S. Masoud, *Spectrochim. Acta*, 2006, **63**, 255-265.
16. P. Brocklehurst, *Tetrahedron*, 1962, **18**, 299-304.
17. S. Millefiori, G. Favini, A. Millefiori, D. Grasso, *Spectrochim. Acta*, 1977, **33**, 21-26.
18. M. T. El-Haty, A. E. Mhamed, F. A. Adam, A. A. Gabr, *Spectrochim. Acta*, 1990, **46**, 1743-1749.
19. L. Sacconi, M. Ciampolini, F. Mffino, F. P. Cavasino, *J. Am. Chem. Soc.* 1962, **84**, 3245-3249.
20. B. P. Kennedy and A. B. P. Lever, *J. Am. Chem. Soc.*, 1973, **95**, 6907-6911.
21. V. M. Miskowski, J. A. Tich, R. Solomon, H. J. Schugar, *J. Am. Chem. Soc.*, 1976, **98**, 8344-8350.
22. P. S. Braterman, *Inorg. Chem.*, 1963, **2**, 448-452.
23. P. Cassidy, M. A. Hitchman, *Inorg. Chem.*, 1977, **16**, 1568-1570.
24. A. B. P. Lever, *Inorganic electronic spectroscopy*, 2<sup>nd</sup> ed., Elsevier, Amsterdam, 1984, 555-556.
25. B. N. Figgis, *Introduction to ligand fields*, John Wiley & Sons, New York, 1961, 237-238.
26. A. B. P. Lever, *Inorganic electronic spectroscopy*, Elsevier, London, 1980, 481.
27. D. M. Boghaei, S. J. S. Sabounchei, S. Rayti, *Synth. React. Inorg. Met.-Org. Chem.*, 2000, **30**, 1535-1540.

28. A. S. Ehrenson, R. T. Brownlee, R. W. Taft, *Prog. Phys. Org. Chem.*, 1973, **10**, 52-53.
29. M. Amirasr, k. J. Schenk, M. Salavati, S. Dehghanpour, B. Taeb, A. Tadjarodi, *J. Coord. Chem.*, 2003, **56**, 231-243.
30. A. A. Del Paggio, D. R. McMillin, *Inorg. Chem.*, 1983, **22**, 691-692.
31. G. Varsányi and S. Szöke “*Vibrational spectra of benzene derivatives*” 1969, Academic Press, New York.
32. A. M. A. Bennett, G. A. Foulds and D. A. Thornton, *Spectrochim. Acta*, 1989, **45A** 219-223.
33. A. M. A. Bennett, G. A. Foulds, D. A. Thornton and G. M. Watkins, *Spectrochim. Acta*, 1990, **46A**, 13-22.
34. G.C. Percy and D.A.Thornton, *J. Inorg. Nucl. Chem.*, 1973, **35**, 2319-2327.
35. E. Pretsch, P. Bühlmann, and C. Affolter „*Structure Determination of Organic Compounds: Tables of Spectroscopic Data*”, 3<sup>rd</sup>. ed, 2000, Springer, Berlin.